Dissecting the Molecular Mechanisms of Motor Neurone Disease in Yeast and Worms

By Amber Rose Peswani

A thesis submitted to the University of Kent for the degree of MSc in Cellular Biology

Abstract

Superoxide dismutase 1 (SOD1) is an enzyme responsible for intracellular breakdown of toxic reactive oxygen species in prokaryotes and eukaryotes. Mutations in SOD1 are linked to the motor neurone disease Amyotrophic lateral sclerosis (ALS), with around 20% of familial (fALS) cases and, it is proposed, a significant proportion of sporadic cases caused by SOD1 mutations, however the mechanism of neuronal death remains unknown. Misfolding and aggregation of SOD1 leading to a 'toxic gain of function' is the most widely accepted mechanism, but further work is needed. To gain new insights into the underlying mechanism of cell toxicity, I am using two model systems: the yeast *Saccharomyces cerevisiae* and the nematode worm *Caenorhabditis elegans*. One hypothesis being tested was proposed by Ghadge et al. (2006) who reported that truncated forms of SOD1 (both wild type and fALS–linked mutants) form toxic aggregates in spinal cords of chick embryos, hypothesising that proteolytic digestion of unstable mutant SOD1 creates these toxic fragments. My project aims to elucidate how fALS–linked SOD1 mutants and SOD1 truncations exert toxicity on *S. cerevisiae* and *C. elegans*. In *S. cerevisiae,* SOD1 truncations do not specifically localise to, or disrupt the functioning of, mitochondria nor reduce viability of yeast although cell growth is slowed. Conversely, a motor-defective phenotype is exhibited in transgenic fALS–linked SOD1 mutant (G85R) *C. elegans* accompanied by vulval defects, which lead to reduced lifespan. My findings suggest that amino acid supplementation of G85R *C. elegans* mutants improves their motor function and vulval defects, implicating a role of amino acid signalling in mutant SOD1-mediated toxicity.

Acknowledgements

Firstly, I would like to thank my supervisors, Prof. Mick Tuite and Dr. Campbell Gourlay, for their support and advice which allowed me to complete this research, and also for giving me the opportunity to work within the community that is the Kent Fungal Group (KFG). I am also grateful to the members of the KFG for their friendly and selfless approach to helping out other lab members, myself included. Many thanks also to Dr. Jennifer Tullet for her training, assistance and patience in teaching me how to work with *C. elegans.*

Next, I would like to thank our collaborators, Markus Ralser and Alan Morgan, for allowing me to present their findings as part of this project.

Lastly, I thank my family and friends for their encouragement, without which I could not have completed this project.

Contents

Abbreviations

ALS	Amyotrophic lateral sclerosis
CCS1	Copper chaperone for SOD1
C. elegans	*Caenorhabditis elegans*
E. coli	*Escherichia coli*
FALS	Familial ALS
IMS	Inter-membrane space
iPSC	Induced pluripotent stem cells
mTOR	Mammalian target of rapamycin
NADH	Nicotinamide adenine dinucleotide
OD	Optical density
ROS	Reactive oxygen species
SC	Synthetic Complete (minimal medium)
S. cerevisiae	*Saccharomyces cerevisiae*
SOD	Superoxide dismutase
TORC1	Target of rapamycin complex 1
VPC	Vulval precursor cell
YPD	Yeast extract peptone dextrose

Chapter 1

Introduction

1.1 Background of ALS

Amyotrophic lateral sclerosis (ALS) is a rapidly progressing and fatal motor neurone disease characterized by degeneration of motor neurones. Progression of ALS leads to muscle atrophy, fasciculations, loss of voluntary muscle control and eventual death, on average occurring 5 years after the presentation of symptoms.

In around 90% of cases, the disease manifests sporadically and with no apparent cause whereas in the other 10% of cases, the disease is inherited in an autosomal dominant manner; this inherited form is known as familial ALS (fALS). Approximately a third of familial ALS cases are caused by mutations in the gene C9orf72, and another 20% of cases are a result of mutation in the superoxide dismutase 1 gene, *SOD1*.

It was previously thought that mutations in the *SOD1* gene caused ALS due to the gene product losing its function or having an increased tendency to aggregate, thus resulting in neuronal cell death. More recent evidence suggests that the mutant *SOD1* gene product may cause cell death by exhibiting a toxic function not observed in the wild type (Bleackley et al., 2011).

1.2 Introduction to superoxide dismutases

In mammals and yeast alike, superoxide dismutase (SOD) enzymes are essential for catalysing the breakdown of toxic reactive oxygen species (ROS) into non-toxic substances within cells.

In eukaryotes, ROS are formed as by-products of the electron transport chain, released into the mitochondrial matrix and inter-membrane space (IMS) by NADH dehydrogenase enzyme and ubisemiquinone anion (Sturtz et al., 2001), and also from lack of regulation of intracellular metal pools. If not broken down, ROS can cause damage to essential cellular components leading to cell death.

Sod1p, the gene product of the *SOD1* gene, is a homodimer consisting of two identical polypeptide subunits, each containing both a copper and a zinc ion. Sod1p makes up 90% of the total superoxide dismutase within human cells (Noor et al., 2002). SOD are highly evolutionarily conserved, with yeast Sod1p being the orthologue of human Sod1p. The human and yeast orthologues are show similar mechanisms of maturation

and are structurally similar; the human protein consists of 154 amino acids and contains two cysteine residues required for protein stability, whereas the yeast orthologue consists of 153 amino acids and has two proline residues necessary for Ccs1p binding. Prokaryotes and eukaryotes both express a form of cytosolic SOD1 protein. Again, in prokaryotes and eukaryotes there exists another SOD enzyme known as Sod2p, which is a mitochondrial protein with a manganese ion in its active site; humans express a form of Sod2p which is orthologous to yeast Sod2p. However unlike yeast, mammalian cells express an additional SOD known as Sod3p, which consists of four subunits containing copper and zinc ions and is located extracellularly.

Sod1p is known as the Cu/Zn superoxide dismutase as it relies on the binding and incorporation of copper and zinc ions into its active site in order to form the mature and active SOD1 enzyme. The presence of transition metal ions in all superoxide dismutases is essential for their enzymatic ability to detoxify ROS due to the tendency of transition metals to readily exchange electrons with ROS by way of redox reactions (Askwith et al., 1998).

1.3 Interaction between Sod1p and Ccs1p

The activity of Sod1p relies heavily on the copper chaperone for SOD1, Ccs1p, a metallo-chaperone which mediates maturation of Sod1p and its correct folding (Sturtz et al., 2001).

Structurally, Ccs1p consists of three domains: the first domain contains a copper-binding motif and is utilised for binding copper when the availability of copper within the cell is scarce (Puig and Thiele, 2002). The second domain forms the majority of the protein and has a region of high homology (around 50% identity) to Sod1p's overall structure (Bleackley et al., 2011) – this region is responsible for the protein's interaction with Sod1p. The third domain contains a CxC motif which allows donation of the copper ion to Sod1p.

In *S. cerevisiae*, Ccs1p bound to a copper ion (Cu-Ccs1p) interacts specifically with immature Sod1p to insert the copper ion into its active site (Furukawa et al., 2004); interaction with Cu-Ccs1p also catalyses the reaction of Sod1p with oxygen to form an intra-molecular disulphide bond within Sod1p by facilitating oxidation of Sod1p

cysteine residues. Zinc binding to Sod1p stabilizes the incorporation of copper into the protein (Bleackley et al., 2011). When the interaction between immature Sod1p and Ccs1p is disrupted, improper formation of the disulphide bond results in a misfolded protein prone to aggregation. Alternatively, formation of the disulphide bond before incorporation of a copper ion results in Ccs1p no longer able to activate Sod1p, leaving it in an immature form. Immature SOD1 proteins are more susceptible to oxidative damage so it is important that they correctly undergo copper and zinc acquisition in addition to disulphide bond formation and dimerization to form the mature SOD1 protein, which is much more stable. Sod1p is considered a cytosolic protein but around 1-5% of cellular Sod1p localizes to mitochondrial IMS to reduce oxidative damage caused by ROS (Sturtz et al., 2001). Sod1p also localizes to various other organelles in small amounts to perform its function.

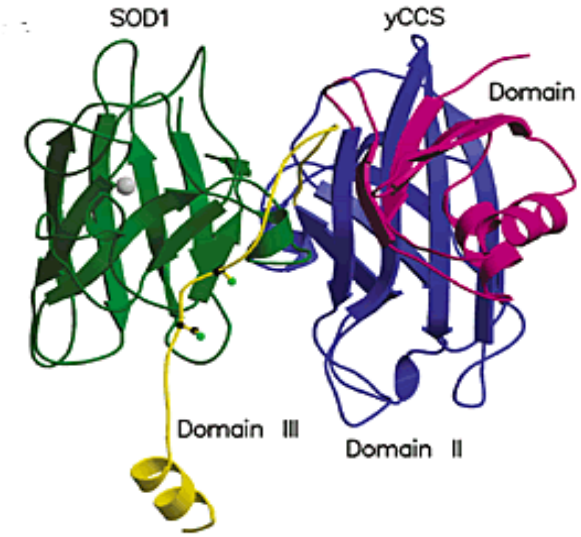

Figure 1.1: Interaction between yeast Sod1p and Ccs1p. The Sod1p monomer is shown in green, while Ccs1p domains 1, 2 and 3 are shown in pink, blue and yellow respectively. Ball-and-stick representations indicate cysteine residues, the gray sphere indicating a zinc ion (Lamb et al., 2001).

Generally, the human and yeast forms of Sod1p function similarly yet an important difference is that yeast Sod1p activation is dependent on Ccs1p whereas human Sod1p can be activated by other mechanisms (Bastow et al., 2011). Activation of SOD1 is suggested to be regulated by glutathionylation, performed by GSH in both yeast Ccs1p-dependent and human Ccs1p-independent processes (Mannarino et al., 2011; Brasil et al., 2013).

1.4 Intra-cellular copper transport facilitates maturation of Sod1p

Multiple studies by other authors have demonstrated that Sod1p transport into mitochondria is optimal while still in its immature 'apo' form, prior to disulphide bond

formation which is essential for the enzyme's activity. In its apo form, Sod1p transport through the mitochondrial outer membrane is facilitated by Ccs1p (Furukawa et al., 2004). However, it is hypothesised that once inside the mitochondrial IMS, maturation of SOD1 by the acquisition of metal ions, mediated by Ccs1p, causes Sod1p to be unable to pass through the mitochondrial outer membrane thus preventing translocation of Sod1p back into the cytoplasm. Equally, incorporation of metal ions into Sod1p while still in the cytoplasm may prevent its translocation into the mitochondria (Sturtz et al., 2001).

In order for Sod1p to mature inside the mitochondrial IMS, copper ions must be present within mitochondria; subsequently, delivery of copper to the mitochondria is essential. In *S. cerevisiae*, a copper pool exists in the cell's cytoplasm which serves as the source of copper for processes occurring both in the cytoplasm and in organelles as required (Cobine et al., 2006). Since copper has high redox potential and could therefore be toxic to the cell, its concentration and transport must be tightly regulated (Kawamata and Manfredi, 2010). Metallo-thioneines Cup1p and Crs5p located in the cytoplasm are responsible for regulating this pool of free copper ions.

Metallo-chaperones such as Ccs1p and Atx1p transport copper ions from the cytoplasmic copper pool to their required areas by protein-mediated transfer, Ccs1p carrying it to Sod1p and Atx1p carrying it to the Ccc2p transporter in post-Golgi vesicles for generation of cell membrane proteins.

It had been suggested that metallo-chaperones Ccs1p and Cox17p were able to transport copper from the cytoplasm to the mitochondria since these proteins exist in both areas of the cell (Puig and Thiele, 2002). The idea of copper transport by Cox17p arose from research relating to cytochrome oxidase (COX), a mitochondrial transmembrane protein whose catalytic subunits Cox1p and Cox2p both require copper as a cofactor. Their acquisition of copper is facilitated by copper chaperone Cox17p which delivers copper specifically to these COX subunits, located in the mitochondrial IMS, for their assembly. Research by other authors has demonstrated that Cox17p is present in the cytosol as well as the mitochondrial IMS; since metallation of Cox1p and Cox2p occurs only within the mitochondrial IMS, this suggests that the cytosolic Cox17p is also able to deliver copper to COX subunits in the

mitochondrial IMS. However, this theory was dispelled by the finding that in yeast *CCS1* and *COX17* deletion mutants, mitochondrial copper concentrations were no different to that of the wild type.

More recent research has elucidated that in both yeast and mouse cells, a separate copper pool is located in the mitochondrial matrix, which supplies copper to the IMS. Copper in the matrix pool is bound to non-proteinaceous ligands which may be accountable for the translocation of copper from the cytoplasm to the mitochondrial matrix pool. It is also believed that various additional transporters transfer copper from the matrix pool to other areas of the mitochondria (Cobine et al., 2006).

This evidence suggests that once inside the mitochondrial IMS, apo-Sod1p is metallated by Ccs1p using copper supplied by the mitochondrial matrix copper pool and undergoes disulphide bond formation, giving rise to mature Sod1p.

1.5 Mechanisms of SOD1-mediated toxicity

1.5.1 Mitochondrial dysfunction and oxidative damage.

Null mutations in *SOD1*, which produce either a non-functional protein or no gene product at all, display significant negative effects on yeast cells, with increased sensitivity to oxidative stress causing the mutant-expressing cells unable to grow well under aerobic conditions. Defects in mitochondrial function are demonstrated by the mutant's impaired ability to grow on non-fermentable carbons sources, as a result of a defect in the electron transport chain. Low viability of null mutants growing in the stationary phase can be attributed to their inability to synthesize mitochondrial proteins such as mitochondrial aconitase, an enzyme involved in the citric acid cycle. *SOD1* null mutant strains exhibit a deficiency in mitochondrial aconitase, rendering them unable to generate enough energy and nutrients to survive in the aerobic environment during the stationary phase (Longo et al., 1996; Cherry et al., 2012).

In addition, *SOD1* null mutants are auxotrophic for a number of amino acids; auxotrophy defines the inability of an organism to synthesize organic compounds essential for its growth. In particular, *SOD1* mutants are strongly auxotrophic for methionine and lysine and show variable auxotrophy for leucine. Some attribute these effects due to oxidative damage to metabolic enzymes involved in amino acid

biosynthesis (Cherry et al., 2012), however it has also been suggested that mutations Sod1p may directly affect metabolic signalling (Bastow, 2013). Furthermore, other evidence suggests that Sod1p mutation may alter metal ion homeostasis, due to the finding that over-expression of *ATX1* or *ATX2* genes encoding metallo-chaperones can suppress the oxidative damage observed in *SOD1* mutants (Cherry et al., 2012). The subsequent result of mutant Sod1p expression is a range of mitochondrial pathologies including damage to mitochondrial DNA and enzymes of the electron transport chain in addition to atypical mitochondrial morphology. These mitochondrial defects affecting overall cellular function, combined with the oxidative damage resulting from ROS, contribute to ALS (Sturtz et al., 2001).

Furthermore, Wong et al. (1995) found that in mice, mitochondrial abnormalities resulting from mutant Sod1p expression lead to unexpected formation of vacuoles, in a phenomenon known as vacuolation. These abnormalities also had profound effects on the nervous system overall, since distribution and accumulation of SOD1 G37R mutant protein, a fALS-associated mutation, occurred in the same tissues as the wild type Sod1p. Mice expressing the mutant SOD1 protein showed progressive degeneration of motor neurons in the brain stem and lumbar, thoracic and cervical regions of the spinal cord. At a cellular level, mutant *SOD1* mice showed noticeable vacuolation particularly in dendrites of the spinal cord and some in the motor neurone cell bodies, leading to a significantly reduced number of motor neurones in the lumbar of the spinal cord. The degree of vacuolation in dendrites and axons was sufficient to disrupt the cellular cytoskeleton and some axonal swelling was observed. The authors hypothesised that the vacuolation observed was in fact from degenerated mitochondria, damaged by mutant Sod1p. It was again noted that the Sodp1 mutant still retained the function of the wild type protein, suggesting this mitochondrial degeneration was due to the Sod1p mutant having a gain of function and that mutant Sod1p may target mitochondria.

1.5.2 Mutant SOD1 aggregation.

Studies have demonstrated that in mice, mutant SOD1 proteins associated with familial ALS is also shown to have a higher tendency to oligomerize than the wild type protein, causing accumulation and formation of intracellular protein aggregates

(Seetharaman et al., 2011). Evidence from these studies suggests that it is immature Sod1p mutants that form such aggregates, a result of disrupted interaction between Sod1p and Ccs1p which prevents Sod1p maturation. Further evidence has discovered that in mouse models expressing both fALS-associated mutant and wild type Sod1p, wild type Sod1p was not sufficient to overcome the pathologies exerted by its mutant counterpart, leading to the conclusion that the mutant Sod1p had in fact gained a toxic function rather than simply losing its protective function (Bleackley and MacGillivray, 2011; Wang et al., 2003).

Other studies have shown that it is only insoluble Sod1p mutants that form protein aggregates within cells (Wang et al., 2005). In mice, multiple different insoluble Sod1p mutants showed aggregation in somatodendritic compartments of the spinal cord motor neurons in particular, whereas the presence of soluble Sod1p mutants in these areas was 'virtually undetectable'. Importantly, there was no evidence of the insoluble mutant's presence in distal nerve fibres, showing that direct interaction between the mutant protein and the nerve axon is not necessary for toxicity to be observed.

1.5.3 Mutant SOD1 affects amino acid regulation.

SOD1 mutants in yeast display up-regulated translation of general amino acid control (GAAC) pathway signalling molecule, Gcn4, supporting the hypothesis that *SOD1* mutation causes metabolic defects (Bastow, 2013). GAAC is an evolutionarily conserved pathway that occurs in eukaryotic cells when they are under amino acid starvation conditions. Activation of GAAC facilitates specific translation of amino acids to restore homeostasis within the cell.

Gcn2 is the initiator of GAAC, and is activated in response to two factors: amino acid starvation and oxidative stress. In both cases, the cellular response is the activation of Gcn2 which phosphorylates eIF2α resulting in inhibition of mRNA translation initiation. In the case of amino acid starvation, eIF2α phosphorylation leads to increased expression of transcription factor, Gcn4. Gcn4 activates various genes required for amino acid biosynthesis pathways in order to increase the cell's synthesis of amino acids. By this mechanism, the cell decreases general protein synthesis and specifically increases amino acid biosynthesis, a process observed not only in yeast but also mammalian cells.

Under oxidative stress conditions, phosphorylation of eIF2α leads to dose-dependent inhibition of protein synthesis (Mascarenhas et al., 2008). Up-regulation of Gnc4 only occurs in response to oxidative stress induced by hydrogen peroxide and provides specific resistance against hydroperoxides, thus would not be affected by accumulation of ROS seen in mutant *SOD1* strains. This suggests that the up-regulated Gcn4 expression observed in *SOD1* mutant strains must be due to amino acid starvation and not oxidative stress, since ROS-induced oxidative stress does not affect Gcn4 expression. From this, it can be deduced that *SOD1* mutations lead to defects in amino acid biosynthesis. This evidence accompanied by the finding that SOD1 mutants demonstrate auxotrophy for multiple amino acids (Cherry et al., 2012) also supports the hypothesis that amino acid biosynthesis is disrupted in *SOD1* mutant strains.

GAAC integrates with the TOR pathway to facilitate nitrogen assimilation for synthesis of organic nitrogen compounds such as amino acids (Staschke et al., 2010), suggesting the TOR pathway may also be affected by *SOD1* mutation.

1.5.4 Mutant SOD1 disrupts TOR signalling

Target of rapamycin (TOR) pathway is responsible for sensing nitrogen and nutrient availability within the cell and regulates transcription accordingly by transcription factors including Gln3.

Mammalian TOR complex 1 (mTORC1) is an oligomer consisting of mTOR protein kinases in mammals. mTORC1 is regulated predominantly by Rheb, a ras-like GTPase, in its GTP-charged form known as Rheb-GTP. This regulation occurs through Rheb binding to mTOR which is essential for mTORC1 activation. The availability of nutrients, such as amino acids and particularly leucine in the cell determines Rheb-GTP's ability to bind to mTOR; thus, nutrient availability indirectly regulates mTORC1 activation through Rheb-GTP. In turn, activated mTORC1 is responsible for controlling mammalian cell growth as appropriate. TOR signalling also exists in simpler eukaryotes such as yeast.

Bastow (2013) discovered growth defects in *S. cerevisiae* expressing mutant Sod1p which could be rectified by addition of leucine to the growth medium. This is supported by the findings of Avruch et al. (2009) who discovered that the amino acid

regulation of TOR is a reversible process, most likely mediated by inhibition of Rheb-GTP where amino acids are scarce, leading to no TOR activation and no cell growth, and removal of this inhibition upon readdition of amino acids, leading to TOR activation and cell growth. Avruch et al. (2009) also discovered that removal of different amino acids had varying effects on TORC1 signalling but that leucine or arginine starvation showed the greatest TORC1 down-regulation.

The culmination of this evidence suggests that mutations in Sod1p may exert some interference on the integration of the GAAC and the TOR pathways in nitrogen assimilation which would account for the reduced amino acid biosynthesis observed in mutant-expressing cells. As a result of this, both GAAC and TOR pathways individually would be down-regulated due to this amino acid starvation, leading to defective cell growth.

1.5.5 SOD1 and the vacuole

The vacuole in yeast cells shows many similarities to the mammalian lysosome in terms of its function. Yeast vacuoles are an important storage compartment for amino acids and also provide an intracellular zinc pool which may be used for Sod1p maturation. Vacuolar zinc transport is mediated by vacuolar membrane protein Zrc1 and to prevent zinc toxicity to the cell, zinc levels are regulated by Zap1 (Ellis et al., 2004).

Michaillat et al. (2012) showed that *S. cerevisiae* vacuole fusion and fragmentation were regulated by nutrient availability through TORC1. Under nutrient starved conditions when TORC1 is inactive, vacuolar fusion was increased producing a single large vacuolar compartment; this suggested that when vacuole-associated TORC1 is active, it is able to stimulate vacuolar fragmentation. Conversely, vacuolar fragmentation occurs under stress conditions such as osmotic stress caused by a hypertonic environment (Baars et al., 2007). Thus, the regulation of mTOR signalling is closely linked to vacuolar function.

The vacuole also functions to degrade and recycle amino acids to facilitate protein synthesis. Evidence suggests mutant SOD1 expression may cause amino acid biosynthesis defects (Bastow, 2013), in addition to the finding that deletion of *PEP4*

from yeast SOD1 mutants resulted in growth defects. Pep4 protein in yeast is required for activation of vacuolar proteases that degrade proteins in the vacuole into their amino acid components, for use in protein synthesis (Jones, Zubenko, and Parker 1982). Bastow (2013) concluded that mutant SOD1 may be exerting a toxic effect through accumulation in the vacuole or impairment of vacuolar functions. This finding, in addition to the implication of mutant SOD1 in TOR signalling disruption, suggests a potential role of mutant SOD1 in vacuolar amino acid transport in yeast.

1.6 Modelling human neurodegenerative diseases

Many varieties of model organism are regularly used in research of neurodegenerative diseases. These include animal models, ranging from rodents to worms, in addition to the modest yeast model.

Arguably the most physiologically relevant, but not widely utilised, model in observing cellular effects of neurodegenerative diseases is human cells such as induced pluripotent stem cells (iPSCs). Spinal motor neurone neurofilaments, components of neuronal cell cytoskeletons, derived from iPSCs exhibit protein aggregate formation and neurite swelling when expressing mutant A4V and D90A SOD1 in early stages of the disease in this model (Chen et al., 2014). The same was also observed in human embryonic stem cell models expressing D90A mutant. Aggregates in these models resemble those seen in spinal cords of ALS patients, contributing to ALS research by showing that neurofilament aggregation occurs in early stages of ALS.

Transgenic animal models, particularly rodents, are commonly used in neurodegenerative research; similarly to that observed in ALS patients, many animal models show neurofilament aggregation (Chen et al., 2014). Some SOD1 and ubiquitin aggregates in animal models present impaired axonal transportation causing muscle denervation and subsequent death of neuronal cell bodies. Rodent models recapitulate characteristic features of ALS such as axonal and mitochondria function, neuromuscular degeneration and death of motor neurones (Gurney et al., 1994) and more recently have indicated that over-expression of human wild type SOD1 can also cause symptoms of ALS including motor neuronal degeneration and reduced lifespan (McGoldrick et al., 2013). Animal SOD1 ALS models often also show aggregate

formation in mitochondria, particularly in the mitochondrial IMS, causing mitochondrial swelling and vacuolation (Gurney et al., 1994, Wong et al., 1995).

Although non-human primate models are scarcely used in research due to ethical considerations, they can provide very useful insight into neurodegeneration. One non-human primate model has been used to investigate effects of ALS-associated TDP-43. It was discovered that injection of TDP-43 into cervical spinal cords of monkeys via a viral vector caused progressive muscle weakness, atrophy and eventual paralysis around the site of injection (Uchida et al., 2012). At a later stage of disease progression, TDP-43 was shown to aggregate in the cytoplasm of motor neurones along with abnormal accumulation of phosphorylated neurofilaments, similar to that seen in ALS patients.

Due to the ease of genetic manipulation and short lifespan of worms, *C. elegans* are now widely used in modelling protein misfolding disorders. In fact, the toxic mechanisms exhibited by non-coding mutations in worms show resemblance to those observed in mammalian cells (Therrien and Parker, 2014). Expression of human mutant SOD1 throughout the body of worms gives rise to impaired oxidative stress response and formation of protein aggregates (Oeda et al., 2011) in addition to disrupted neuronal transmission and movement defects (Wang et al., 2009). Similarly, pan neuronal human TDP-43 expression also leads to reduced worm motility and uncoordinated movement (Ash et al., 2010). Despite the differences that exist between mammals and worms, *C. elegans* ALS-associated neurodegeneration actually provides a good representation of the disease occurring in primate and rodent models.

A model organism the most relatively different from human cells but by far one of the most widely used in research of human diseases is yeast. Despite their differences, the unicellular eukaryote *S. cerevisiae* retains many of the same basic functions as mammalian cells. One of the many contributions of yeast models to neurodegenerative research is the finding that mutant human SOD1 expression disrupts mitochondrial function and decreases electron transport, suggesting mutant SOD1 may impair assembly of the electron transport chain complex (Bastow et al., 2011). In addition to this, protein misfolding and aggregation and well as many other

cellular dysfunctions can be monitored in yeast, representing human neurodegenerative diseases.

1.7 Aims of the project

Continuing from the findings obtained by Bastow (2013), this project intended to gain insight into a number of research questions:

1. **To investigate the toxicity of truncated SOD1 proteins in yeast** as originally put forward by Ghadge et al. (2006) who discovered truncated SOD1 proteins to cause disease in chick embryo spinal cord neural cells. Growth and viability of cells expressing various truncations of wild type SOD1 were measured to determine whether the truncations were toxic to yeast and whether protein length or GFP-tagging affected toxicity.
2. **To investigate the effect of toxic SOD1 on mitochondria** and identify whether the gain-of-function demonstrated in toxic Sod1p targets mitochondria directly. Localisation of truncated SOD1 proteins in mitochondria was analysed in addition to analysis of mitochondrial function by testing the capability of yeast SOD1 mutants' to respire.
3. **To elucidate the metabolic dysfunction observed in SOD1 mutants in relation to vacuolar amino acid transport.**

   Growth analysis and viability of vacuolar amino acid transporter deletion strains expressing truncated SOD1 proteins were performed to investigate synthetic effects. Free amino acids concentrations in gene deletion strains were also analysed to determine whether gene deletion caused amino acid auxotrophies.
4. **To determine the effects of mutant SOD1 on *C. elegans*.**

   Mutant SOD1 and wild type SOD1 were over-expressed in *C. elegans* to observe their toxic effects on the nervous system and organism as a whole. Lifespan and motility assays were used to assess their toxicity.

Chapter 2

Material and Methods

2.1 Growth media and conditions for *Saccharomyces cerevisiae*, *Escherichia coli* and *Caenorhabditis elegans*

For all *S. cerevisiae* and *E. coli* solid media, 2% w/v granulated agar (Difco) was added to the media before autoclaving. Media were sterilised in a Prestige Medical bench-top autoclave at 121°C.

S. cerevisiae and *E. coli* were grown on either solid or liquid media, with *S. cerevisiae* grown at 30°C and *E. coli* grown at 37°C. All liquid cultures subjected to continuous shaking at 200rpm. *C. elegans* were grown only on solid media, at 15°C, 20°C or 25°C as required.

2.1.1 Yeast extract, peptone, dextrose (YEPD) medium for *S. cerevisiae.*

2% w/v glucose, 1% w/v yeast extract, 2% w/v bactopeptone.

2.1.2 Synthetic Complete (SC) drop-out medium for *S. cerevisiae.*

2% w/v glucose, 0.67% w/v Yeast Nitrogen Base (Difco), 0.164% w/v synthetic complete leucine drop-out supplement (Formedium).

Standard SC drop-out leucine medium.

Yeast Nitrogen Base (YNB) contains ammonium sulphate and no amino acids; amino acid supplement was added as required. Leucine drop-out supplement (Formedium) contained all amino acids except leucine and was used for the selective growth of successfully transformed yeast cells expressing the *LEU2* gene present on the plasmid.

Low fluorescence SC double drop-out leucine and uracil medium.

0.67% w/v low fluorescence Yeast Nitrogen Base (Formedium), 0.174% w/v synthetic complete leucine and uracil drop-out supplement (Formedium). 2% v/v sterile liquid glucose solution was added after autoclaving.

Low fluorescence SC double drop-out leucine and uracil media was used for cultures prepared for fluorescence microscopy to provide the same nutrients as standard SC double drop-out leucine and uracil media, but gives a colourless solution which causes less interference during imaging. Sterile liquid glucose was added after autoclaving,

from a 40% glucose stock solution, to avoid caramelisation and darkening of the glucose during autoclaving.

2% glycerol SC drop-out leucine medium.

0.67% Yeast Nitrogen Base (Difco), 0.164% synthetic complete leucine drop-out supplement (Formedium), with 2% w/v (final) glycerol added after autoclaving.

A solid version of this medium was used for mitochondrial function experiments of selectively grown transformed cells (Section 3.7.2)

2.1.3 Luria Broth (LB) medium for *E. coli.*

1% w/v bactotryptone, 0.5% w/v yeast extract, 1% w/v NaCl

To select for *E. coli* successfully transformed with plasmids encoding the Amp^R (ampicillin resistance) gene, 100µg/ml (final) of ampicillin was added to the media after autoclaving, from a 100mg/ml stock solution in water. The stock was kept at -20°C.

2.1.4 Nematode Growth Medium (NGM) for *C. elegans.*

Standard NGM.

0.3% w/v NaCl, 0.25% w/v bactopeptone, 1.7% w/v granulated agar.

Distilled water was added up to the total volume then autoclaved. Following autoclaving, the liquid medium was cooled to 55°C in a water bath then sterile salt solutions added as follows:

2.5% v/v KH_2PO_4 (pH6)
0.1% v/v $MgSO_4$ (1M)
0.1% v/v $CaCl_2$ (1M)
0.1% v/v cholesterol (5mg/ml dissolved in ethanol)

Salt solutions were added in the specified order to avoid a precipitate forming.

Amino acid-supplemented NGM.

Leucine-supplemented solid NGM was made by adding varying volumes of sterile filtered 50mM leucine stock solution of L-leucine (Sigma) dissolved in sterile water. This was added to the medium after autoclaving, up to the total volume. Media was supplemented with 1 mM, 2mM or 5mM leucine.

2.2 Strains

2.2.1 *S. cerevisiae* strains.

Yeast strains were obtained from the *MATa* Library, a gene deletion collection generated as part of the *Saccharomyces* Genome Deletion Project and were purchased from Open Biosystems. All strains were stored at -80°C.

Table 2.1. Genotypes of yeast strains used in this study.

Strain	Genotype	Collection
BY4741	MATa his3Δ1 leu2Δ0 met15Δ0 ura3Δ0	CWG424
BY4741 Δsod1	MATa his3Δ1 leu2Δ0 met15Δ0 ura3Δ0 sod1::HIS5	MFT
BY4741 Δavt1	MATα his3Δ 1 leu2Δ 0 lys2Δ 0 ura3Δ 0 avt1::KANMX	MATa
BY4741 Δavt2	MATα his3Δ 1 leu2Δ 0 lys2Δ 0 ura3Δ 0 avt2::KANMX	MATa
BY4741 Δavt3	MATα his3Δ 1 leu2Δ 0 lys2Δ 0 ura3Δ 0 avt3::KANMX	MATa
BY4741 Δavt4	MATα his3Δ 1 leu2Δ 0 lys2Δ 0 ura3Δ 0 avt4::KANMX	MATa
BY4741 Δavt5	MATα his3Δ 1 leu2Δ 0 lys2Δ 0 ura3Δ 0 avt5::KANMX	MATa
BY4741 Δavt6	MATα his3Δ 1 leu2Δ 0 lys2Δ 0 ura3Δ 0 avt6::KANMX	MATa
BY4741 Δavt7	MATα his3Δ 1 leu2Δ 0 lys2Δ 0 ura3Δ 0 avt7::KANMX	MATa
BY4741 Δvba1	MATα his3Δ 1 leu2Δ 0 lys2Δ 0 ura3Δ 0 vba1::KANMX	MATa
BY4741 Δvba2	MATα his3Δ 1 leu2Δ 0 lys2Δ 0 ura3Δ 0 vba2::KANMX	MATa
BY4741 Δvba3	MATα his3Δ 1 leu2Δ 0 lys2Δ 0 ura3Δ 0 vba3::KANMX	MATa
BY4741 Δvba4	MATα his3Δ 1 leu2Δ 0 lys2Δ 0 ura3Δ 0 vba4::KANMX	MATa
BY4741 Δvba5	MATα his3Δ 1 leu2Δ 0 lys2Δ 0 ura3Δ 0 vba5::KANMX	MATa

2.2.2 *E. coli* strains.

For amplifying plasmids by transformation and purification, α-select chemically competent *E. coli* cells with the genotype F- *deo*R *end*A1 *rec*A1 *rel*A1 *gyr*A96 *hsd*R17(rk-, mk+) *sup*E44 *thi*-1 *pho*A Δ(*lac*ZYA-*arg*F)U169 Φ80*lac*ZΔM15 λ- were obtained from Bioline.

For *C. elegans* culture and maintenance, *E. coli* strain OP50, a uracil auxotroph, was obtained from Dr. Jennifer Tullet (University of Kent).

2.2.3 *C. elegans* strains.

N2 wild type strains were obtained from Dr. Jennifer Tullet, University of Kent.

Pnb-1::hSOD1-YFP and Pnb-1::hSOD1 G85R-YFP strains were created by Prof. Jiou Wang (John Hopkins Bloomberg School of Public Health), obtained through Prof. Alan Morgan (University of Liverpool). These strains contained integrated transgenes encoding human wild type SOD1 protein and the SOD1 G85R mutant protein, both C-terminally fused to YPF.

N2 strains were genetically out-crossed with the human *SOD1* transgenic strains to standardize their genetic backgrounds (see Section 2.6.5) for use in future work.

2.3 Plasmid use and analysis

2.3.1 Plasmids.

Table 2.2. Plasmids used in this study.

Plasmid Name	Backbone	Insert	Source
pUKC 2801	pAG425	n/a	Addgene
pUKC 2809	pAG425	Yeast SOD1	E.Bastow
pUKC 3216	pAG425	Yeast SOD1 fragment 1-36	E.Bastow
pUKC 3217	pAG425	Yeast SOD1 fragment 1-49	E.Bastow
pUKC 3218	pAG425	Yeast SOD1 fragment 1-84	E.Bastow
pUKC 3219	pAG425	Yeast SOD1 fragment 1-115	E.Bastow
pUKC 3220	pAG425	Yeast SOD1 fragment 1-125	E.Bastow

pUKC 3221	pAG425-EGFP	n/a	Addgene
pUKC 3222	pAG425-EGFP	Yeast SOD1	E.Bastow
pUKC 3228	pAG425-EGFP	Yeast SOD1 fragment 1-36	E.Bastow
pUKC 3229	pAG425-EGFP	Yeast SOD1 fragment 1-49	E.Bastow
pUKC 3230	pAG425-EGFP	Yeast SOD1 fragment 1-84	E.Bastow
pUKC 3231	pAG425-EGFP	Yeast SOD1 fragment 1-115	E.Bastow
pUKC 3232	pAG425-EGFP	Yeast SOD1 fragment 1-125	E.Bastow
B1468	pRS316	Cox4-RFP	G. Wang

All plasmids containing EGFP were N-terminally tagged. All pUKC plasmids contained the yeast *LEU2* selectable marker, the GPD promoter, the 2µ plasmid origin of replication and ampicillin resistance gene Amp^R as bacterial selectable marker. The B1468 Cox4-RFP plasmid was obtained from Dr. Geng Wang (Tsinghua University School of Life Science, China) and contained a *URA3* yeast selectable marker.

2.3.2 Transformation of *S. cerevisiae.*

Initially, one colony of the yeast strain BY4741 was inoculated into 10ml YPD in a sterile 50 ml falcon tube and incubated at 30˚C with shaking at 200rpm overnight. The next day, 2ml of the culture was transferred to a sterile 2ml microcentrifuge tube and pelleted using a bench-top microcentrifuge at 13,000 rpm for 20 seconds. The supernatant was discarded and following were added to the cell pellet:

240µl sterile 50% PEG-4000

36µl 1M LiAc

34µl sterile water

2.5µl β–mercaptoethanol,

10µl single stranded DNA (salmon sperm)

4µl plasmid DNA (~1 µg)

The mixture was vortexed for 1 minute to resuspend the cell pellet then incubated for 30 minutes at 30˚C. The mixture was incubated for a further 30 minutes at 42˚C then cells were pelleted by microcentrifugation at 2000rpm for 5 minutes. For temperature sensitive strains, a 45 minute - 1 hour incubation at 30˚C was followed by 15 minutes

of incubation at 42˚C. After this time, the supernatant was discarded and the pellet resuspended in 150µl of sterile water and spread onto SC-leu solid media which were then incubated at 30˚C overnight in a static incubator.

2.3.3 Transformation of *E. coli.*

50µl of competent cells and 1µl of plasmid DNA (~ 1µg DNA) were each thawed on ice before being mixed together in a 1ml microcentrifuge tube. The mixture was incubated on ice for 20 minutes then transferred to a water bath at 42˚C for 45 seconds. The mixture was incubated on ice for a further two minutes before adding 400µl of fresh LB medium. The LB-transformation mixture was incubated at 37˚C for 1 hour in a shaking incubator then 100µl was spread onto LB solid media containing ampicillin (100ug/ml) and incubated at 37˚C overnight in a static incubator.

2.3.4 Plasmid purification from *E. coli.*

Plasmids were isolated from *E. coli* grown overnight in LB medium with added ampicillin. Cells were harvested in a microcentrifuge at 8000rpm for 2 minutes and then plasmid DNA was isolated using the Thermoscientific GeneJET Plasmid Miniprep Kit K0503, according to Protocol A of the manufacturer. Centrifugation was carried out at 13,000rpm unless specified otherwise. Prior to use, RNase A was added to the resuspension buffer and ethanol added to the wash buffer, as specified in the protocol.

As high copy plasmids were being isolated, no more than 5ml of bacterial culture was processed per GeneJET spin column.

2.4 Protein analysis

2.4.1 Native protein extraction.

Native lysis buffer:

10mM NaPO4 pH 7.8 with NaOH

5mM EDTA

0.1% triton

50mM NaCl

1 protease inhibitor cocktail tablet (Roche)

60 OD units of overnight culture (yeast in stationary phase of growth) were harvested by centrifugation at 4000rpm for 5mins and 22°C. Harvested cells were then resuspended in 1ml of sterile ice cold water, transferred to a sterile 2ml Eppendorf tube and harvested in a Beckman benchtop centrifuge at 13000rpm for 15 seconds. The cells were then placed on ice. Supernatant was discarded and the cells resuspended in 400µl of ice cold native lysis buffer, centrifuged again as before and the supernatant discarded. Next, cells were resuspended in 200µl of native lysis buffer, whilst on ice, before adding 425-600µm acid-washed glass beads up to the meniscus. Cells were then lysed by vortexing for 1 minute followed by incubation on ice for 1 minute. This was repeated five times. After lysing, cells were harvested at 13000rpm for 5 minutes, placed on ice, then the cell lysates extracted and transferred to pre-chilled 2ml Eppendorf tubes. This was repeated to remove cell debris and the resulting native extracts were stored at 4°C for a few days prior to use.

2.4.2 Bradford assay.

To determine the concentration of protein in cell-free extracts, standards of known protein concentration were first prepared using bovine serum albumin (BSA) and concentrations of 100µg/ml, 250µg/ml, 500µg/ml, 750µg/ml, 1000µg/ml and 1500µg/ml. The unknown concentration protein extracts were then diluted in water to 1:4 ratio. To a cuvette containing 1.5ml of Bradford reagent, 50µl of protein sample (known standards and diluted unknown samples) was added, covered with parafilm, then inverted and left for 5-15 minutes to react. After this time, samples were measured in an Eppendorf BioPhotometer™ Plus at OD_{595} using a blank of Bradford reagent. Unknown protein concentrations were calculated by constructing a standard curve of protein concentration against absorbance at 595nm using the known BSA standards and plotting the unknown proteins.

2.4.3 Protein separation by native PAGE and visualisation by SOD activity assay.

The native protein extracts were diluted appropriately and 5X native sample buffer added in preparation for native PAGE.

5X native sample buffer:

0.31M Tris pH 6.8

0.05% v/v bromophenol blue

50% v/v glycerol

Native 12% polyacrylamide gels were made in plastic cassettes, first filling the cassette approximately ¾ full with resolving gel and covering with 100% ethanol to ensure even solidification. Once set, the ethanol was poured off and rinsed 2-3 times with distilled water before adding the stacking gel to the top of the cassette and placing an appropriate comb to form wells.

Table 2.3. Composition of stacking and resolving gels for native PAGE.

12% Stacking gel	Resolving gel
41.3% deionized water	60% deionized water
33% acrylamide/bisacrylamide (30% solution)	14% acrylamide/biscrylamide (30% solution)
25% 1.5M Tris-HCl pH8.8	25% 0.5M Tris-HCl pH6.8
0.06% APS	0.05% APS
0.13% TEMED	0.4% TEMED

Native PAGE was run using 1x Tris-glycine native running buffer at 144 volts for approximately 1.5 hours, then the gel was stained in nitroblue tetrazolium (NBT) solution for 45 – 60 minutes on a shaker and shielded from light by covering the container with tin foil.

NBT solution (double concentration):

50% v/v KPO4 pH7.8

0.2mg/ml w/v riboflavin

0.265mg/ml w/v NBT (1 NBT tablet (Sigma) dissolved in 10ml water, to 1mg/ml concentration)

0.2% v/v TEMED

After staining, the NBT solution was removed then the gel rinsed 2-3 times with dH_2O and developed under a lamp in a small amount of dH_2O. Development begun as soon as the gel was exposed to bright light, with the stained gel turning from yellow to dark blue in colour and with clear bands appearing where active SOD was present. Optimal signal was observable within the first hour after exposure but was usually left to develop overnight under the lamp.

2.5 Analysis of *S. cerevisiae*

2.5.1 Growth analysis.

Colonies of yeast were inoculated into appropriate liquid media and grown overnight (as specified in section 2.1). The next day, the density of the cultures was determined by absorbance at OD_{600} in an Eppendorf Biophotometer™ Plus then cultures diluted to OD_{600} 0.1 in 1ml of liquid media in a sterile 24-well microwell plate. Optical densities of the growing cultures were measured in a BMG LABTECH SPECTROstar Nano microwell plate reader with double-orbital shaking at 400rpm, with an excitation of 600 and 3 flashes per well. Cycle time was 1800 seconds (30 minutes).

After obtaining the absorbance data, growth analysis was done by calculating the log phase doubling time from the data using a Microsoft Excel template of semi-logarithmic graphs plotting time in hours against OD_{600} absorbance values to determine the R-squared values and line equations of exponential trend lines, with the smallest R-squared value indicating fastest exponential growth. Doubling time (hours) was calculated by dividing ln2 by the x value of the line with the smallest R-value.

The semi-logarithmic graph template used was created by Dr. Gemma Staniforth (University of Kent).

2.5.2 Viability assays.

Liquid cultures were prepared by inoculating colonies into SC drop-out leucine medium and incubating at 30°C shaking for 1-2 days as required. After this time, cultures were removed from the incubator and samples diluted by a factor of 1 in 80 in sterile distilled water in a 2ml Eppendorf tube.

100µl of the diluted culture was pipetted onto a haemocytometer next to the coverslip, next to the coverslip and the cell suspension drawn into the haemocytometer chamber by capillary action. Cells in each of the four large corner squares (each subdivided into 16 smaller squares – see **Figure 2.1**) of the grid were counted under a light microscope at 40X magnification.

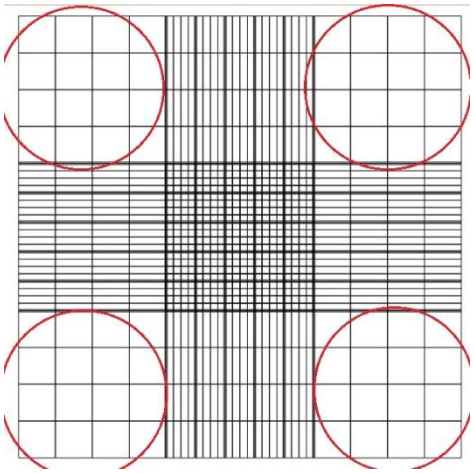

Figure 2.1: Diagram indicating four large corner squares of a haemocytometer used to count cells for a viability assay.

The average number of cells in the four corner squares was calculated as follows:

*Average number of cells in corner squares x dilution factor (80) x 10,000 (*standard for haemocytometer) *= number of cells per ml of undiluted culture*

Serial dilutions were carried out, first diluting each sample to ~10^6 cells/ml in sterile water; next, diluting by 1/10 to give ~10^5 cells/ml, then again by 1/10 to give ~10^4 cells/ml and lastly by diluting 2/10 to give ~2000 cells/ml (in total volume of 1ml). 100µl aliquots of this final dilution, containing 200 cells, were spread on SC drop-out leucine agar plates and incubated at 30°C for approximately 5 days until colonies grew. Colonies were then counted using a manual or automated cell counter, each colony indicating one viable colony forming unit. Percentage viability was then calculated.

2.5.3 Replica plating assays.

The optical density of overnight cultures grown in SC drop-out leucine liquid medium were determined and diluted to OD_{600} 1, 0.1, 0.001 and 0.0001 respectively in a 24-well microwell plate by serial dilution. 5µl of the diluted cultures were placed in parallel spots on 2% glycerol SC drop-out leucine agar plates and left to dry for at least

10 minutes. Spotted plates were then incubated at 30°C in a static incubator for 3-4 days.

2.5.4 Fluorescence microscopy.

Sample preparation.

The optical density (OD_{600}) of a yeast culture grown overnight in low fluorescence liquid medium (see Section 2.x) , was determined then diluted in the same liquid media to OD_{600} 0.3 and grown for a further 3-4 hours in a shaking incubator until exponential growth phase was reached, identified by an OD_{600} between 0.6 and 0.8. 150µl of the log phase cells were pipetted onto a glass microscope slide and covered with a coverslip. A drop of immersion oil was then added to the coverslip prior to viewing.

Microscope set-up and use.

An Olympus IX81 motorised inverted research microscope with attached Hamamatsu Orca AG cooled CCD camera were used to acquire fluorescent images. An Olympus MT20 advanced fluorescence illumination system was used as the light source, using 1 ms on/off time shutter speed setting. The Olympus cell^R imaging software was used to adjust camera settings and obtain and edit images. Cells were viewed at 100X magnification on the GFP-RFP setting and photographs captured on pixel size setting 'binning 1x1'.

2.6 *C. elegans* preparation and analysis

2.6.1 Bleaching.

After obtaining the *C. elegans* Pnb-1::hSOD1-YFP and Pnb-1::hSOD1 G85R-YFP strains, the plates required cleaning before use. Firstly, 2ml of M9 buffer was added to plates of gravid adult worms, swirled to remove all worms from the surface of the plate and then transferred to a 1.5ml Eppendorf tube. Centrifugation of the suspension was performed to pellet the worms and the supernatant was carefully removed by pipetting. A 7:8 mixture of household bleach containing 5% sodium hypochlorite to 4M NaOH was added to the worm pellet and vortexed for 3-5 minutes to kill all hatched worms and contaminants. The NaOH and bleach solution should not be left on for more than 5 minutes for risk of killing the *C. elegans* eggs. After bleaching, the mixture

was centrifuged at 3000rpm to pellet the remaining eggs, then the pellet resuspended in 1ml M9 buffer. Centrifugation and resuspension was repeated twice more to wash off all bleach solution. The final suspension of eggs in M9 was pipetted onto a seeded NGM plate and incubated at 15-25°C.

Stocks of clean, hatched worms were maintained in 50% osmotically-balanced M9 buffer and 50% freezing buffer and stored at -80°C.

Table 2.4: Compositions of M9 and freezing buffers.

Freezing buffer:	M9 buffer:
0.59% w/v NaCl	0.3% w/v KH_2PO_4
0.68% w/v KH_2PO_4	0.7% w/v Na_2HPO_4
30% v/v glycerol	0.5% w/v NaCl
0.3% v/v 1M $MgSO_4$ (added after autoclaving)	0.025% w/v $MgSO_4$

2.6.2 Lifespan assays.

In preparation for the lifespan assay, NGM agar plates were seeded with 200µl of OP50 strain of *E. coli* grown overnight at 37°C. These were used as the *C. elegans* food source. Once the bacteria had dried overnight, 200µl 5-fluoro-2'-deoxyuridine (FUDR) from a 100µM stock solution in water was inoculated on to the dried OP50 cells to give a final concentration of 10µM, and left to soak into the agar for at least 2 hours.

Once the plates had fully dried, 20 L4 larval stage hermaphrodite worms were placed onto each plate, with 5 plates of 20 worms per strain to give a total of 100 specimens per strain. L4 stage hermaphrodites can be identified by the prominent crescent shape in their abdomen. This particular stage of worm is used in order to age synchronize the population used in the assay, thus day 1 of the assay begins on day 1 of adult life for all specimens. FUDR was used to inhibit hatching and growth of *C. elegans* progeny, to avoid counting of young worms that are not age synchronized.

Throughout the assay, worms were observed every 2-3 days and scored on whether they were alive, dead or censored (lost or died of unnatural causes). Worms were

deemed to be dead if they did not move at all after being gently poked with a 'worm pick' composed of platinum wire attached to a glass pipette.

2.6.3 Motility assays with leucine supplementation.

First, leucine-supplemented NGM agar plates were prepared by seeding with cooled heat-killed OP50, killed by heating for 1 hour at 75°C in a water bath. Heat-killed bacteria were used to prevent metabolism of the supplemented amino acids by live bacteria. Once the bacterial cells were dry, 200µl 5-fluoro-2'-deoxyuridine (FUDR) from a 100µM stock was added to the plates and left to dry.

In preparation for the assay, L4 stage worms were picked onto a clean NGM agar plate without bacteria and left for approximately 1 hour to remove the majority of live bacteria from their bodies and fully digest any consumed bacteria. After cleaning, 10 L4 worms were placed onto 3 leucine-supplemented NGM plates for each strain and each concentration of leucine, giving 30 worms per strain per concentration. Worms were placed on control plates without leucine or experimental plates with leucine concentrations of 1mM, 2mM or 5mM and categorised and scored as either A, B or C every 2 days based on their motility. The scoring was determined by:

A: Worm moves freely without touching it or moves freely when the plate is tapped.

B: Worm moves freely once it is touched.

C: Worm only moves slightly when touched (moves head or tail but cannot move freely).

Worms were censored if they died during the assay or were lost on the plate. Any hatched progeny were removed from the plates and worms were transferred onto new plates if contamination occurred or there was live bacterial growth.

2.6.4 Genetic out-crossing.

In order to standardize the genetic backgrounds of the strains used, for valid comparisons to be made, male N2 worms from Dr. Jennifer Tullet (the same strain as the N2 hermaphrodites used in lifespan and motility assays) (T/T genotype) were bred with Psnb-1::SOD1 and Psnb-1::SOD1 G85R hermaphrodites obtained from Prof. Alan Morgan (University of Liverpool) (+/+ genotypes).

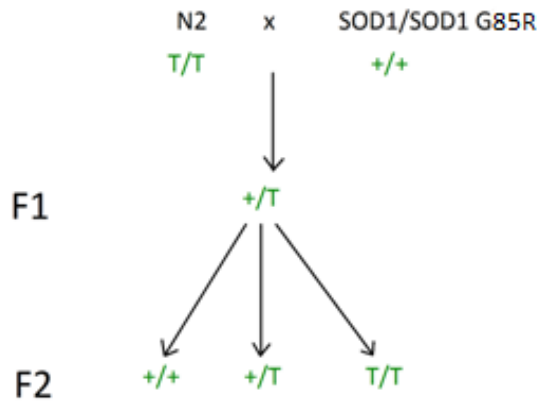

Figure 2.2: Genotypes of *C. elegans* parents and progeny in genetic out-crosses.

The success of breeding was monitored by the fluorescent phenotypes exhibited by the progeny; a successful cross would give approximately 50% +/T genotypes, consisting of half fluorescent worms and half not fluorescent, 25% +/+ genotypes in which all worms were fluorescent and 25% T/T genotype showing no fluorescence (table 2.5).

Table 2.5: Genotypes of F2 generation genetically out-crossed *C. elegans* and corresponding fluorescent phenotypes.

	+	T
+	+/+ 100% fluorescent	+/T 50% fluorescent
T	+/T 50% fluorescent	T/T 0% fluorescent

On a bacteria-free NGM agar plate, a small area of OP50 was spread onto the centre, with 6 N2 males and 3 hermaphrodites of either SOD1 wild type or SOD1 G85R mutant strains placed onto the bacteria. These worms were incubated at 15-25°C for around 3-4 days to breed and progeny to grow. Once F1 generation progeny had reached L4 stage, 5 L4 stage hermaphrodites were isolated onto a new OP50-seeded NGM plate and incubated for another 3-4 days to self-fertilize. When F2 generation progeny had grown to L4 stage, 15 L4 stage cloned hermaphrodites were separated onto one

seeded NGM plate per individual worm and incubated for another 3-4 days. After growth of sufficient progeny, the worms were screened using a Leica MZFLIII Fluorescence Stereomicroscope on GFP2 setting. Plates containing all fluorescent worms (T+/T+ genotype) were kept while those containing some (T+/T) or no fluorescent worms (T/T) were discarded. Breeding was repeated five more times each time using 3 hermaphrodites from the T+/T+ plates. After six full crosses, the out-crossed worms stored at -80°C in a 1:1 solution of freezing buffer and M9 buffer (for compositions, see Table 2.4).

Chapter 3

Investigating toxicity exerted by expressing truncated wild type yeast SOD1 proteins in *S. cerevisiae*

3.1 Introduction

3.1.1 Using yeast as a model to study neurodegeneration.

Yeast has been used extensively in modelling and understanding human diseases, neurodegenerative diseases. Although clear differences exist between yeast and complex higher eukaryotes like humans, basic processes including the cell cycle, intracellular transport and protein quality control systems are highly conserved between yeast and human cells. Disruption of protein quality control systems leads to mitochondrial defects, transcriptional deregulation and impaired trafficking in both species (Tenreiro and Outeiro, 2010); for example, neurodegenerative diseases Alzheimer's and Parkinson's are characterised by protein misfolding and formation of amyloidogenic aggregates, which is mirrored by yeast prion diseases that exhibit similar characteristics and biochemical properties. Furthermore, cell death by apoptotic and non-apoptotic mechanisms is a process observed in neurodegenerative diseases, as a result of mitochondrial oxidative damage. This also appears to be conserved in yeast (Braun, 2012), which may undergo programmed cell death after sustaining oxidative damage in order to facilitate survival of the clonal population by decreasing nutrient usage (Cheng et al., 2008). It is suggested that approximately half of the genes involved in human heritable diseases also have homologues in yeast (Hartwell, 2004).

A number of features observed in Parkinson's disease can also be modelled in yeast; specifically, expression of heterologous α-synuclein inhibits yeast growth and over-expression can cause cell death, characteristics also observed in higher eukaryotic models such as *Drosophila*, *C. elegans* and mice (Feany and Bender, 2000; Masliah et al., 2000, Lakso et al., 2003). Yeast has also been utilized in identifying therapeutic agents for α-synuclein toxicity by reducing formation of cytoplasmic aggregates, improving protein trafficking and reducing mitochondrial damage. These therapeutic agents were found to also reduce α-synuclein induced toxicity in *C. elegans* and rat neuronal midbrain cultures (Su et al., 2010).

In addition, similarities are shown between yeast and transgenic mouse models of Huntington's disease, particularly in relation to the regulation of polyQ expression and toxicity by the kynurenine pathway (Campesan et al., 2011; Giorgini et al., 2008;

Zwilling et al., 2011). Murine and mammalian cell models expressing Huntington's Disease-associated huntingtin protein also showed traits of mitochondrial dysfunction and oxidative stress reproduced in yeast models (Bossy-Wetzel et al., 2008; Ross and Tabrizi, 2011; Correia et al., 2012).

3.1.2 Yeast as a model to study the role of SOD1 in ALS.

Yeast models have also been used in understanding the mechanisms by which mutant SOD1 causes toxicity in diseases such as familial ALS. Growing evidence suggests that SOD1, despite being a primarily cytosolic protein, is essential in regulating mitochondrial function and preventing oxidative damage. Sturtz and Culotta (2001) reported that *Δsod1* strains of *S. cerevisiae* exhibited metabolic defects including defective methionine and lysine biosynthesis when grown aerobically in media containing glucose; they also reported rapid death of stationary phase that correlated with increased production of reactive oxygen species, while other evidence shows an increase in protein carbonyls in *Δsod1* cells, products of metal-catalyzed oxidation indicative of oxidative stress even in the presence of mitochondrial SOD2 (Weisiger and Fridovich, 1973). Investigation into the role of anti-apoptotic mitochondrial protein, Bcl-2, in SOD1-mediated toxicity also showed Bcl-2 expression in a *Δsod1* strain of *S. cerevisiae* to improve survival of stationary phase cells by providing an antioxidant and anti-apoptotic role (Longo et al., 1997). Pedrini et al. (2010) indicated that fALS-associated SOD1 mutants interact with Bcl-2, causing a toxic effect in mice and human spinal cord cells.

However, Nishida et al. (1994) studied mutations in yeast *SOD1* that correspond to the human disease-causing mutants, showing defects in metal incorporation and enzymatic activity, suggesting fALS was not solely caused by oxidative damage. Further research has found that expression of yeast SOD1 encoding ALS-associated mutations leads to increased mitochondrial respiration in addition to increased amino acid biosynthesis and trehalose biosynthesis, which are linked to leucine signalling, portraying a potential effect of mutant SOD1 on amino acid signalling (Bastow, 2013).

3.1.3 Truncated wild type SOD1 proteins in neural death.

Zu et al. (1997) reported that some fALS genotypes show truncations in exon 5 of wild type SOD1 encoding amino acids 119 to 153 at the carboxyl end of the human SOD1 protein. One such truncation, L126Z, is caused by a substitution resulting in a stop codon at amino acid residue 126 of the protein (Zu et al. 1997); while another, FS126, has two base pairs deleted leading to a frameshift and stops translation at residue 131 (Pramatarova et al. 1994). These truncated SOD1 proteins have shown a tendency to form aggregates in human embryonic kidney cells (Wang et al. 2003).

Ghadge et al. (2006) first investigated truncated SOD1-mediated toxicity. When expressing wild type SOD1-YFP in chick embryo spinal cord cells, it was discovered that the protein was distributed throughout the cells' cytoplasm, whereas mutant A4V SOD1-YFP formed intracellular aggregates and caused apoptosis. However, when truncated 1-125 amino acid SOD1-YFP was electroporated and expressed in the same cell type, cells exhibited aggregate formation and showed increased DNA fragmentation indicative of apoptotic signalling cascades (shown by TUNEL assays) compared to wild type SOD1-YFP expression. Further truncated SOD1-YFP proteins 36, 49, 84 and 115 amino acids in length (truncated from the carboxyl end) were also electroporated and expressed in chick embryo spinal cord neural cells and showed aggregate formation and signs of apoptotic signalling by TUNEL. Further to this, to mimic the genotype of individuals carrying one mutant *SOD1* allele and one normal *SOD1* allele, truncated 1-36 amino acid SOD1 was co-electroporated with wild type SOD1; this still showed a significant increase in apoptosis compared to wild type SOD1, even in the presence of functional Sod1p, indicating a toxic gain of function in the truncated Sod1p.

In this chapter, the effects of expressing truncated wild type SOD1 proteins in baker's yeast, *S. cerevisiae*, will be investigated and the mechanisms by which they cause toxicity will be explored.

3.2 Expression of truncated SOD1 proteins causes defective cell growth

Growth analyses are a useful tool in investigating the effects of genetic or epigenetic changes on the growth rate and viability of cells. When grown at optimal conditions of 30°C in rich media such as YPD, *S. cerevisiae* have a doubling time of approximately 1.5 hours, however they are sensitive to nutritional deprivation, thus growth in minimal

media increases doubling time to around 2 hours. Changes in growth pattern or doubling time can be an indicator of impairment or enhancement of cellular function as a result of genetic manipulation or response to stress. Growth of cells following gene deletion is commonly used as a method of assessing the importance of a gene under changing growth conditions.

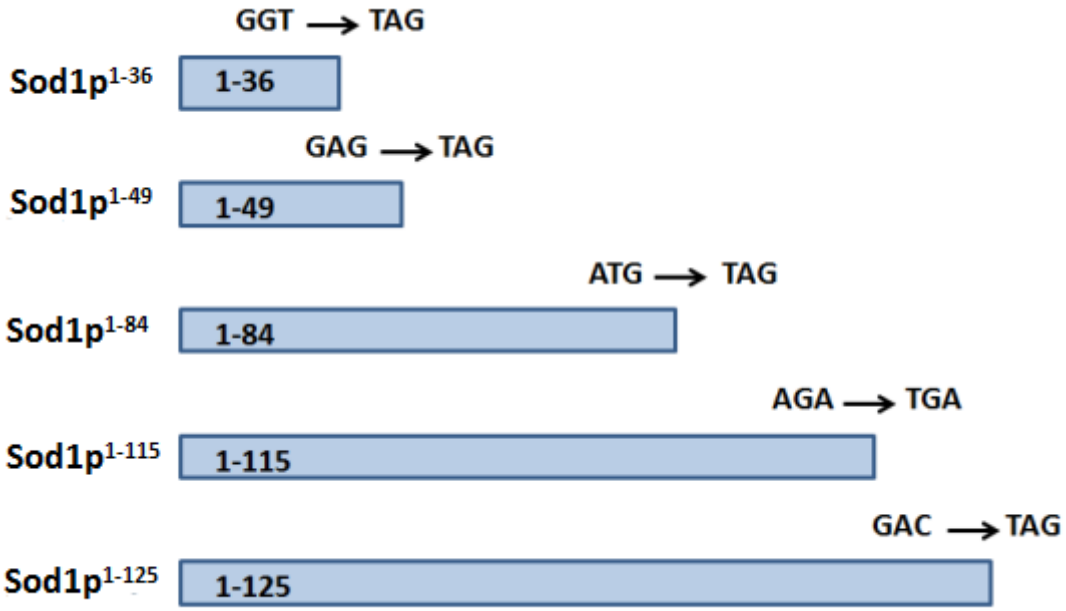

Figure 3.1: Truncated wild type yeast SOD1 proteins. Truncated proteins were created by site-directed mutagenesis and insertion of a stop codon leading to production of truncated SOD1 proteins 36, 49, 84, 115 and 125 amino acids in length (Bastow, 2013). Image adapted from (Bastow, 2013).

For these experiments, *S. cerevisiae SOD1* deletion strains were a transformed with plasmids encoding truncated forms of yeast SOD1 described in Figure 3.1.

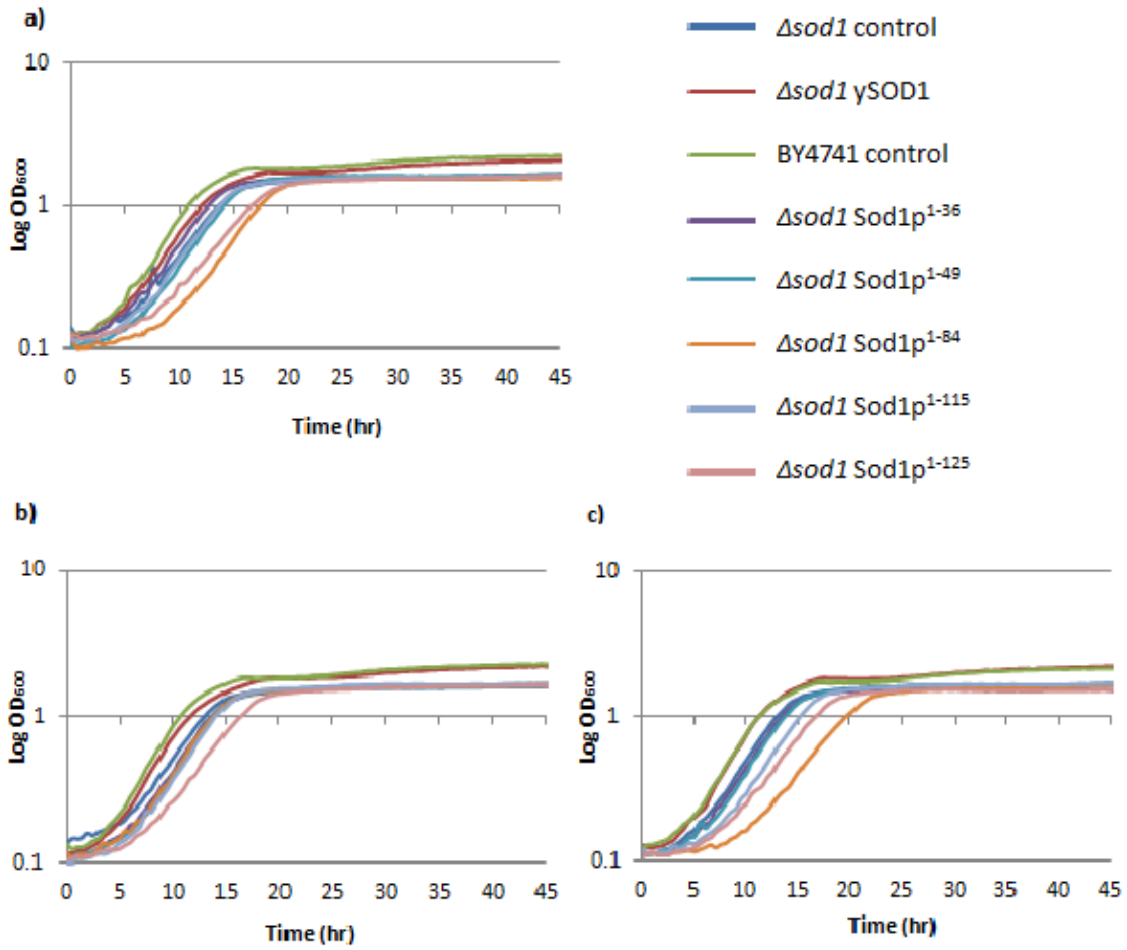

Figure 3.2: Expression of truncated SOD1 proteins causes defective growth in yeast. The five truncated isoforms of Sod1p, Sod1p$^{1-36}$, Sod1p$^{1-49}$, Sod1p$^{1-84}$, Sod1p$^{1-115}$ and Sod1p$^{1-125}$were expressed in a Δ*sod1* strain. Cells were grown for 48 hours in SC-leu media at 30°C. The three growth curves **a)**, **b)**, and **c)** represent three biological repeats of this experiment.

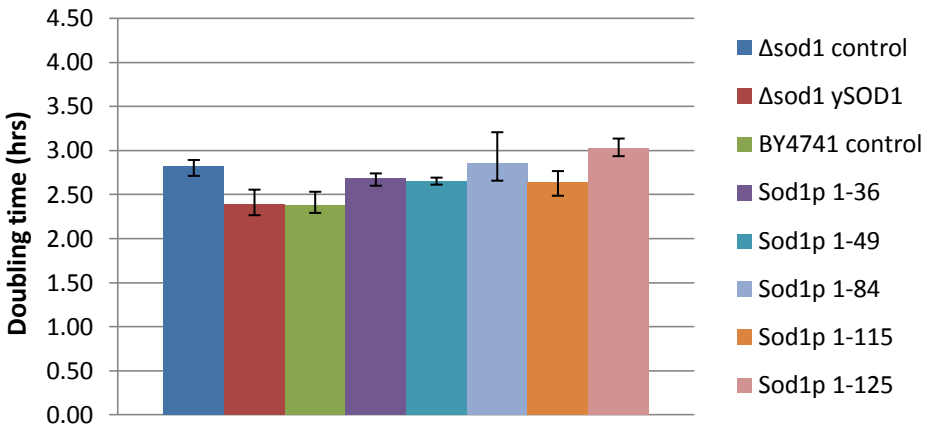

Figure 3.3: Sod1p$^{1-84}$ and Sod1p$^{1-125}$ protein fragments are most toxic to cells. The three biological repeats of growth data were used to calculate an average doubling time for each strain. Error bars indicate variability between the three repeats. On average, no truncated

proteins gave a doubling time equal to that of the wild type control suggesting they are not fully functional, although Sod1p$^{1-36}$, Sod1p$^{1-49}$ and Sod1p$^{1-115}$ truncations grew marginally better than the *Δsod1* control expressing no SOD1. Sod1p$^{1-84}$ and Sod1p$^{1-125}$ truncations grew slower than the negative control.

The growth curves (Figure 3.2) created from plotting the obtained data on a logarithmic scale indicated that the Δ*sod1* positive control expressing full-length ySOD1 was able to reach the same final OD_{600} as the BY4741 positive control expressing the empty plasmid, with no significant decrease in growth rate. However the *Δsod1* negative control expressing no Sod1p, along with all five Sod1p truncations, reached a lower final OD_{600} than the positive controls; while the two positive controls also show a slight growth increase after diauxic shift occurs, the growth of cells expressing truncated proteins or negative control plateaus soon after diauxic shift, indicating these cells may be less able to metabolise non-fermentable carbon sources.

Exponential phase growth also appears to be slowed in cells expressing Sod1p$^{1-84}$ protein fragment in two of three growth curve repeats whereas Sod1p$^{1-125}$ fragments appears slowed in all three. This is reflected in the average doubling times (Figure 3.3), where the two fragments have the slowest doubling times, indicating they may be toxic to cells. To determine whether the differences observed in doubling times were significant, statistical analysis was performed by means of t-testing.

	BY4741 control	***Δsod1* control**
***Δsod1* control**	0.012	-
***Δsod1* ySOD1**	0.974	0.018
BY4741 control	-	0.012
Sod1p $^{1-36}$	0.035	0.140
Sod1p $^{1-49}$	0.060	0.080
Sod1p $^{1-84}$	0.097	0.432
Sod1p $^{1-115}$	0.086	0.146
Sod1p $^{1-125}$	0.003	0.032

Figure 3.4: T-tests indicating significance of differences in doubling time between truncated SOD1 proteins and controls. T-tests performed using a two-tailed hypothesis and a critical P-value of 0.05 to test whether there was a significant difference in doubling time between cells expressing each truncated SOD1 protein against either a positive (BY4741 strain) or negative

(Δ*sod1* strain) control. P-values >0.05 are deemed insignificantly different and those <0.05 indicate significance and are highlighted yellow.

In a two-tailed t-test with a P-value of 0.05, the BY4741 control was significantly different to the *Δsod1* control but not *Δsod1* ySOD1, as expected. Similarly, the *Δsod1* control was significantly different to both positive controls. The t-test indicates that of the truncated proteins tested, only Sod1p$^{1-36}$ and Sod1p$^{1-125}$ have growth rates significantly different to the BY4741 control whereas only Sod1p$^{1-125}$ is significantly different to the *Δsod1* control. However, an important observation is that the third biological repeat conducted for Sod1p$^{1-84}$ appeared anomalous compared to the results of the first two repeats. The doubling time for repeats 1 and 2 were 2.72 and 2.65 hours but for repeat 3, was 3.2 hours. When including all three results in the t-test, this gave a P-value of 0.097, which indicates insignificant difference to the control, despite Sod1p$^{1-36}$ having a mean doubling time closer to that of the control and being shown significant in the t-test; since the t-test also takes variability in the dataset into account when calculating a significance value, the presence of this anomaly likely affected the t-test and inaccurately calculated the significance value. In order to accurately calculate the significance, further repeats would need to be done to allow exclusion of the anomaly. Nevertheless, it can be concluded that Sod1p$^{1-36}$ may exhibit toxicity that slows cell growth somewhat, but cells still grow faster than when *SOD1* is deleted. Sod1p$^{1-125}$ is the only truncated protein shown to be significantly different, and in this case slower, than both positive and negative controls, so it can be concluded that Sod1p$^{1-125}$ protein fragment is actively exhibiting a toxic effect.

3.3 SOD1 truncation leads to loss of enzymatic activity

To determine whether the Sod1p$^{1-36}$, Sod1p$^{1-49}$ and Sod1p$^{1-115}$ truncated proteins identified as non-toxic in growth experiments were providing any enzymatic functionality, native protein extracts isolated from overnight yeast cultures were diluted appropriately with native sample buffer then loaded into a 12% polyacrylamide gel and separated by native PAGE for approximately 1.5 hours. The gel was then stained with nitroblue tetrazolium (NBT) chloride solution and developed under a bright light. NBT is a photogenic substrate and when exposed to bright light, changes

the stained gel from yellow to dark blue/purple in colour. This process relies on the reactivity of the solution components riboflavin and TEMED, which form superoxide radicals upon light exposure. The reduction of NBT by superoxide radicals forms a blue-coloured product however active SOD1 enzyme breaks down the superoxide radicals and competitively inhibits NBT reduction, causing a clear band to form where active SOD1 is present.

The activity assay (Figure 3.5) shows no detoxification of superoxide radicals by any of the truncated SOD1 proteins indicating none of them possess enzymatic activity, due to the lack of signal for Sod1p in any of the lanes containing Sod1p fragments. This suggests that Sod1p$^{1-36}$, Sod1p$^{1-49}$ and Sod1p$^{1-115}$ truncated proteins are not active nor are they toxic under these conditions, whereas Sod1p$^{1-84}$ and Sod1p$^{1-125}$ truncations are also enzymatically inactive but have some acquired toxicity. The mechanism of this toxicity will be investigated in later sections.

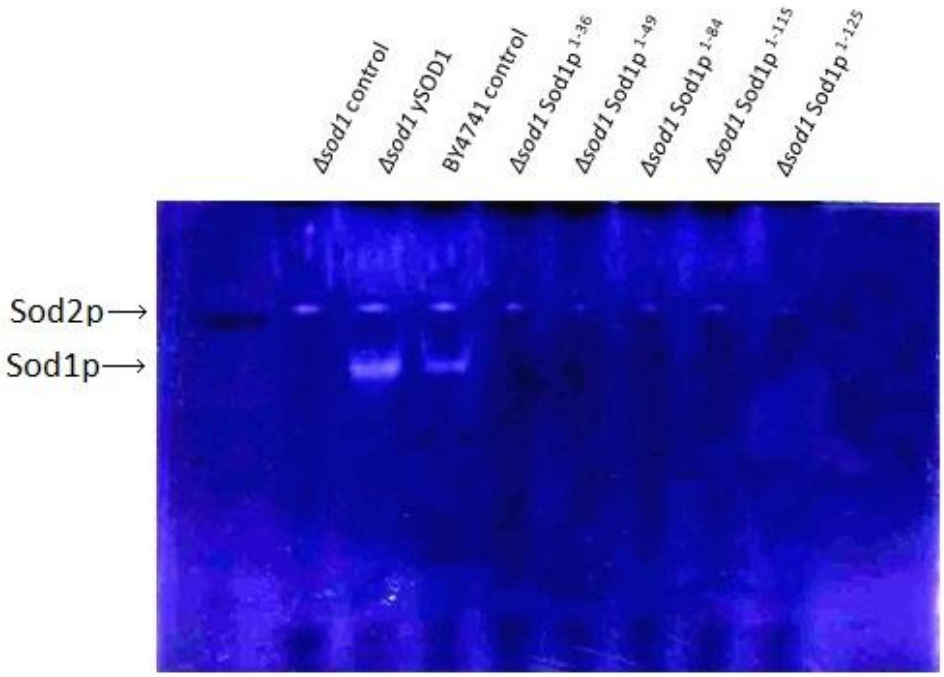

Figure 3.5: Truncated SOD1 proteins are unable to detoxify superoxide radicals produced in an NBT assay. Native proteins with native sample buffer added were loaded onto the polyacrylamide gel and assessed for SOD1 activity as described in Materials and Methods 2.4.3. Native proteins were loaded onto the gel at between 1000-3000ug/ml concentrations as determined by Bradford assays, to ensure a strong signal was produced. The top row of clear bands indicates Sod2p, which shows clear bands in the controls but weak bands in cells

expressing truncated SOD1 proteins. The lower row of bands indicates active SOD1, and is only seen in the two positive controls.

3.4 Enzymatic activity of truncated SOD1-GFP fusion proteins

For the purpose of visualisation by fluorescence microscopy, cells were transformed with plasmids expressing N-terminal GFP tagged versions of the truncated SOD1 proteins made by Bastow (2013). Stevens and Chia (2010) found that tagging Sod1p with GFP may affect its enzymatic activity; when comparing GFP-tagged G93A human SOD1 mutant with its untagged version, the GFP-tagged version showed a 65% reduction in activity; however, no difference in their dimerization states was observed. To maintain the validity of the experiments using these GFP fusion proteins, cells expressing truncated SOD1-GFP fusion proteins were analysed.

3.4.1 GFP fusion to Sod1p$^{1-115}$ truncation increases its toxicity.

A *S. cerevisiae SOD1* deletion strain containing pAG425-EGFP plasmids encoding the truncated SOD1 proteins and controls were grown overnight in 5ml SC-leu liquid medium, then cultures diluted the next day to OD_{600} 0.1 in the same media in a 24-well microwell plate and their growth recorded. Surprisingly, it was discovered that the doubling time of Sod1p$^{1-115}$-GFP protein has greatly increased (Figure 3.6b), inferring a strong toxic effect acquired as a result of fusing GFP to this protein fragment. On the contrary, the doubling time of Sod1p$^{1-125}$-GFP fragment compared to its non GFP-tagged counterpart is reduced to the extent that it appears to exceed the rate of the wild type control, indicating GFP fusion may have reduced or eliminated the toxicity of this protein fragment. Statistical analysis was performed to determine whether these differences could be deemed significant.

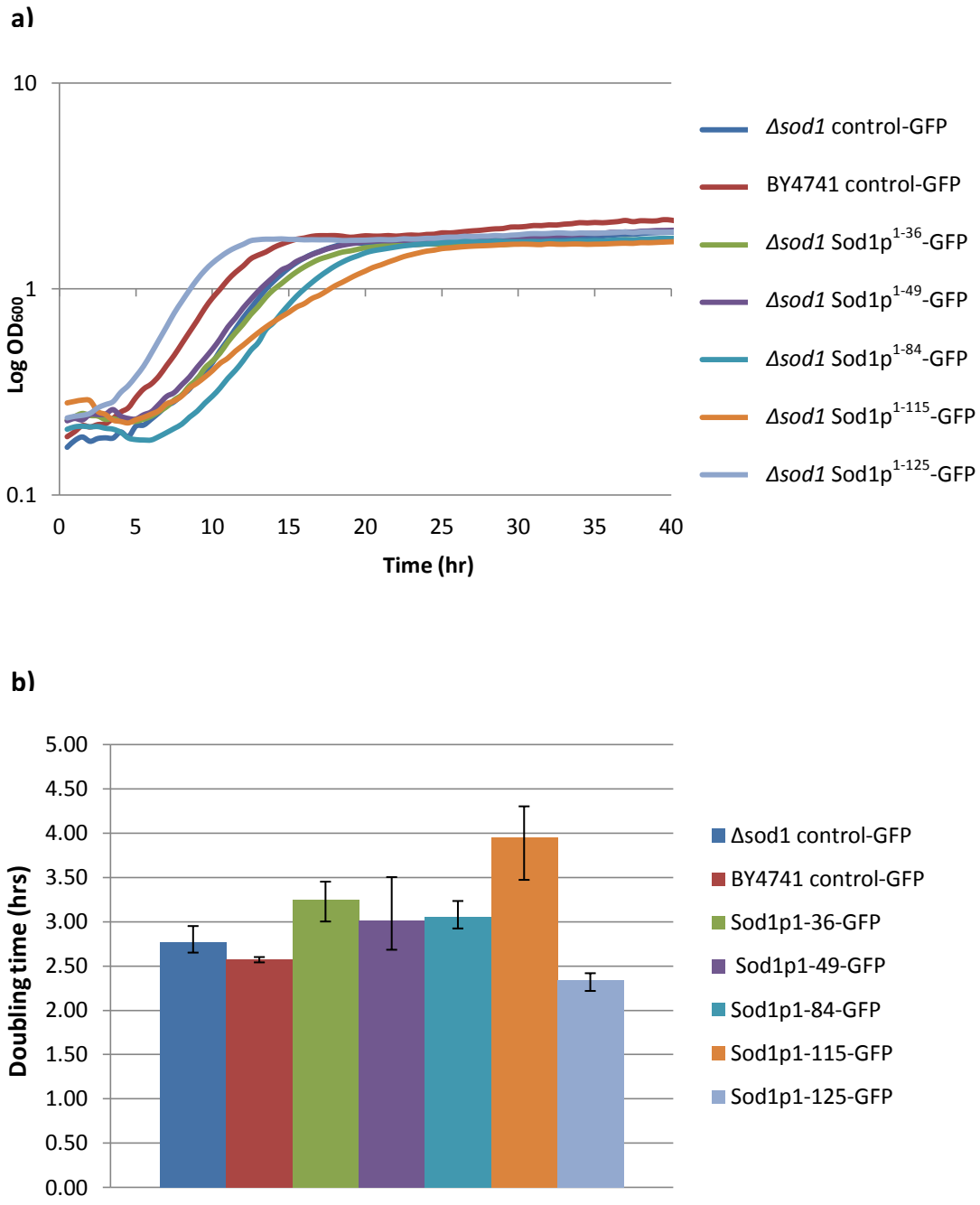

Figure 3.6: GFP fusion affects the growth of cells expressing truncated SOD1 proteins in a Δ*sod1* strain. a) Growth analysis shows cells expressing Sod1p$^{1-115}$-GFP fusion protein to have a significantly slowed exponential phase growth rate compared to all other fragments and controls, and reaching a lower final OD_{600}. **b)** The doubling time of cells expressing Sod1p$^{1-115}$-GFP fusion protein is significantly greater than other fragments, suggesting a toxic effect on cells. Conversely, the doubling time of cells expressing Sod1p$^{1-125}$-GFP is comparable to the controls, being the only experimental strain with a doubling time of < 3hrs. Doubling times were calculated from an average of three biological repeats, error bars indicating variability between the three repeats.

	BY4741 control-GFP	*Δsod1* control-GFP
***Δsod1* control-GFP**	0.17	-
BY4741 control-GFP	-	0.17
Sod1p $^{1-36}$ -GFP	0.03	0.048
Sod1p $^{1-49}$ –GFP	0.23	0.44
Sod1p $^{1-84}$ –GFP	0.03	0.10
Sod1p $^{1-115}$ –GFP	0.03	0.03
Sod1p $^{1-125}$-GFP	0.04	0.02

Figure 3.7: T-tests indicating significance of differences in doubling time between truncated SOD1-GFP fusion proteins and controls. T-tests performed using a two-tailed hypothesis and a p value of 0.05 to test whether there was a significant difference in doubling time between cells expressing each truncated SOD1-GFP fusion protein against either a positive (BY4741 strain) or negative (*Δsod1* strain) control. T-test values >0.05 are deemed insignificantly different and those <0.05 indicate significance. Values highlighted in yellow indicate significance.

To determine whether differences in doubling time were significant, t-tests were performed. Analysis showed that compared to the BY4741 wild type control, doubling times of cells expressing all truncated proteins except Sod1p$^{1-49}$-GFP differ significantly. However, only Sod1p$^{1-115}$-GFP and Sod1p$^{1-125}$-GFP differ significantly from the *Δsod1* control, implying any difference caused by expressing GFP-fused Sod1p$^{1-36}$ or Sod1p$^{1-84}$ are not due to acquired toxicity any more than simply deleting the functional *SOD1* gene. By looking at the mean doubling times of the three repeats (Figure 3.6b), it can be confirmed that expression of Sod1p$^{1-115}$-GFP significantly slows cell growth indicating a strong toxic effect, and also confirmed the growth rate of Sod1p$^{1-125}$-GFP significantly increases growth rate even compared to the wild type protein, leading to the hypothesis that GFP fusion may have provided structural stability to the truncated protein to allow Sod1p$^{1-125}$ to form a functional enzyme.

3.4.2 GFP fusion allows Sod1p$^{1-125}$ truncation to form a functional dimer.

The growth analysis of truncated SOD1-GFP fusion proteins suggested that GFP-tagging of truncated SOD1 proteins may affect their enzymatic activity. Native protein extracts were prepared from these strains and examined for SOD activity as described in Materials and Methods 2.4.3.

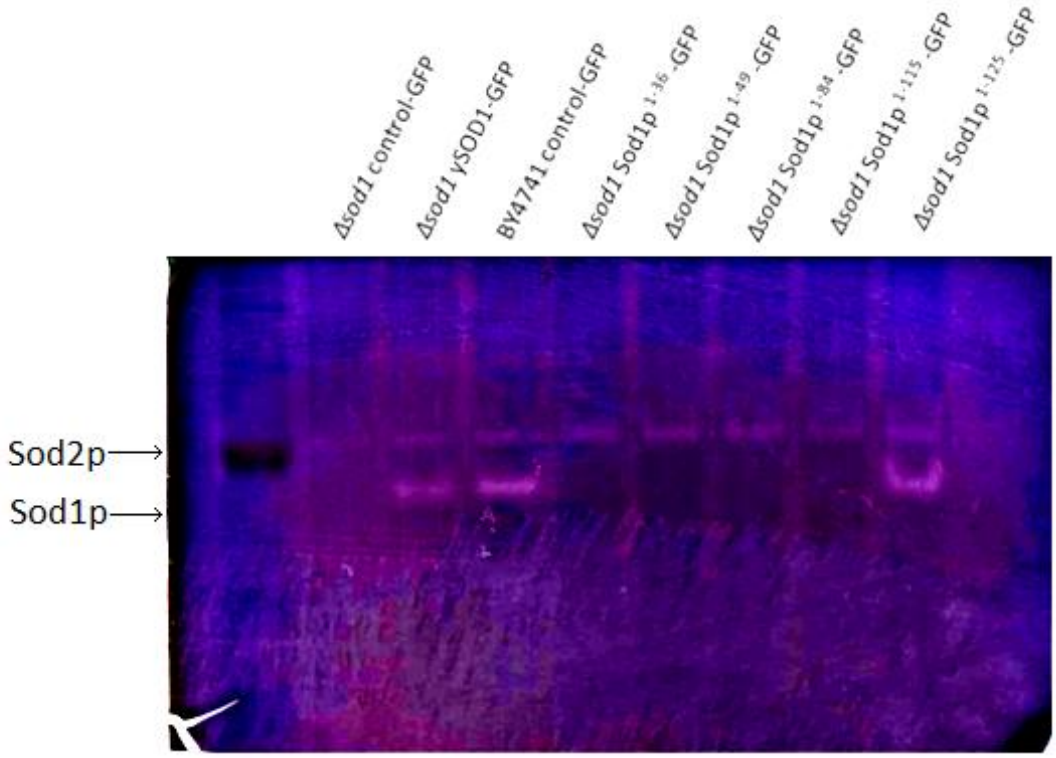

Figure 3.8: Truncated Sod1p$^{1-125}$ fused to GFP shows enzymatic functionality in an NBT assay. Native proteins were diluted to 1200µg/ml in water and appropriate volume of native sample buffer for loading onto a 10% polyacrylamide gel. The top row of clear bands indicates Sod2p clearly present in all samples. The lower row of bands indicates active SOD1, and is seen not only in the two positive controls but also very prominently in the Sod1p$^{1-125}$-GFP sample.

Contrary to the NBT assay of truncated SOD1 protein without GFP fusion, which showed none of the truncated proteins to have enzymatic activity, GFP fusion to Sod1p$^{1-125}$ appears to restore its function to that of full-length Sod1p; this suggests that similar to the findings of Stevens and Chia (2010), GFP fusion did indeed alter the activity of the truncated Sod1p$^{1-125}$ enzyme, perhaps by altering its stability or to ability dimerize. This may indicate that Sod1p$^{1-125}$ retains some structural component that the

other protein fragments do not due to their truncation, or that Sod1p$^{1-125}$ is the only truncation long enough in length to form a stable protein.

3.5 Viability is largely unaffected by expression of truncated SOD1 proteins

Viability was determined by calculating the number of cells in an overnight culture then diluting the cultures by serial dilution and finally spreading a known number of colony forming units onto solid SC-leu media. Colony growth was counted, with one colony indicating one viable colony forming unit, and percentage viability was calculated. Assessing cell viability can highlight incidences of premature cell death or senescence within the culture.

Truncated SOD1 proteins were expressed in a *Δsod1* strain in order to investigate whether they reduced viability after 24 hours of growth in SC-leu media.

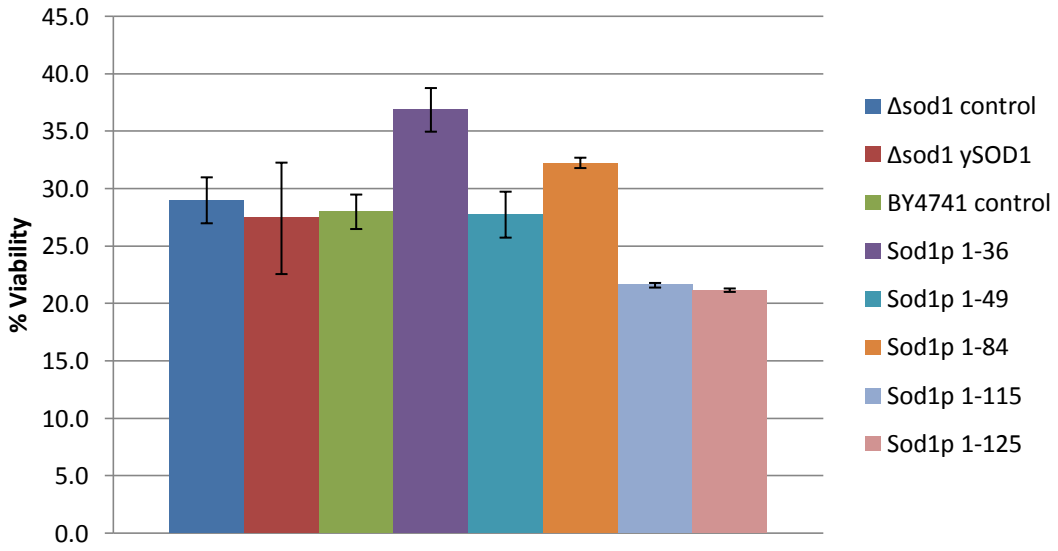

Figure 3.9: Average viability of cells expressing truncated yeast *SOD1* is largely unaffected by protein fragment length in a *Δsod1* strain. Representative of an average of two biological repeats of the same experiment, each an average of 3-4 technical repeats. Error bars represent variability between biological repeats. Viability of controls particularly *Δsod1* ySOD1 appears very variable between biological repeats but was less so between technical repeats. In all three repeats, the longest Sod1p fragments, Sod1p$^{1-115}$ and Sod1p$^{1-125}$, give the lowest viability of all fragments but do not show significant reduction compared to the BY4741 control, which expresses an empty pAG425 plasmid in a wild type strain.

Although there was some visible pattern in viability of cells expressing Sod1p fragments, with longer fragments Sod1p$^{1-115}$ and Sod1p$^{1-125}$ showing the lowest percentage viability in all experiments performed, the significance of differences in viability between fragments are difficult to assess due to the variability of controls, where the differences in viability between fragments were generally 20-25% in all experiments, whilst the ySOD1 control varied up to around 20% between experiments. Statistical analysis by means of t-testing showed the differences in viability between cells expressing truncated SOD1 proteins and the negative control were not significant; the conclusion from this data is that the differences observed in viability when expressing truncated SOD1 proteins are due to natural variability rather than a significant life-reducing effect exerted by the Sod1p fragments.

3.6 Role of mitochondria in SOD1-mediated toxicity

Association with mitochondria has been strongly linked to mutant SOD1-mediated toxicity especially in ALS disease states. A significant body of evidence shows that high levels of mutant SOD1 are present in spinal cords of transgenic ALS mice (Jonsson et al., 2006; Karch et al., 2009; Zetterström et al., 2013) while Wong et al. (1995) showed that expression of SOD1 mutants lead to mitochondrial abnormalities. Further studies in motor neuronal cell lines found that expression of mutant SOD1 in the IMS leads to formation of insoluble oligomers inside mitochondria, resulting in toxicity and cell death (Cozzolino et al., 2009; Magrané et al., 2009). Most previous research has hypothesised that mitochondrial toxicity by mutant SOD1 is caused by accumulation of these insoluble protein aggregates, with multiple mouse models showing correlation between occurrence of insoluble mutant SOD1 aggregates and manifestation of ALS symptoms (Johnston et al., 2000; Wang et al., 2002). In the following experiments, truncated SOD1 proteins were expressed in yeast to investigate their localisation.

Fluorescence microscopy was used to determine whether truncated SOD1 proteins localised to the mitochondria of *S. cerevisiae*, by fusing the Sod1p fragments to green fluorescent protein (GFP) and expressing them in yeast along with red fluorescent protein (RFP) fused to mitochondrial inner membrane protein, Cox4. Cultures were grown overnight in low fluorescence media were diluted the next day to OD_{600} 0.3 in the same media then grown for a further 3-4 hours to reach exponential phase before

observation using a fluorescence microscope with beamsplitter attached. A beamsplitter allows two paths of light at different wavelengths to be directed at the sample, illuminating GFP and RFP simultaneously. The captured images are then overlaid to observe co-localisation (Figure 3.11).

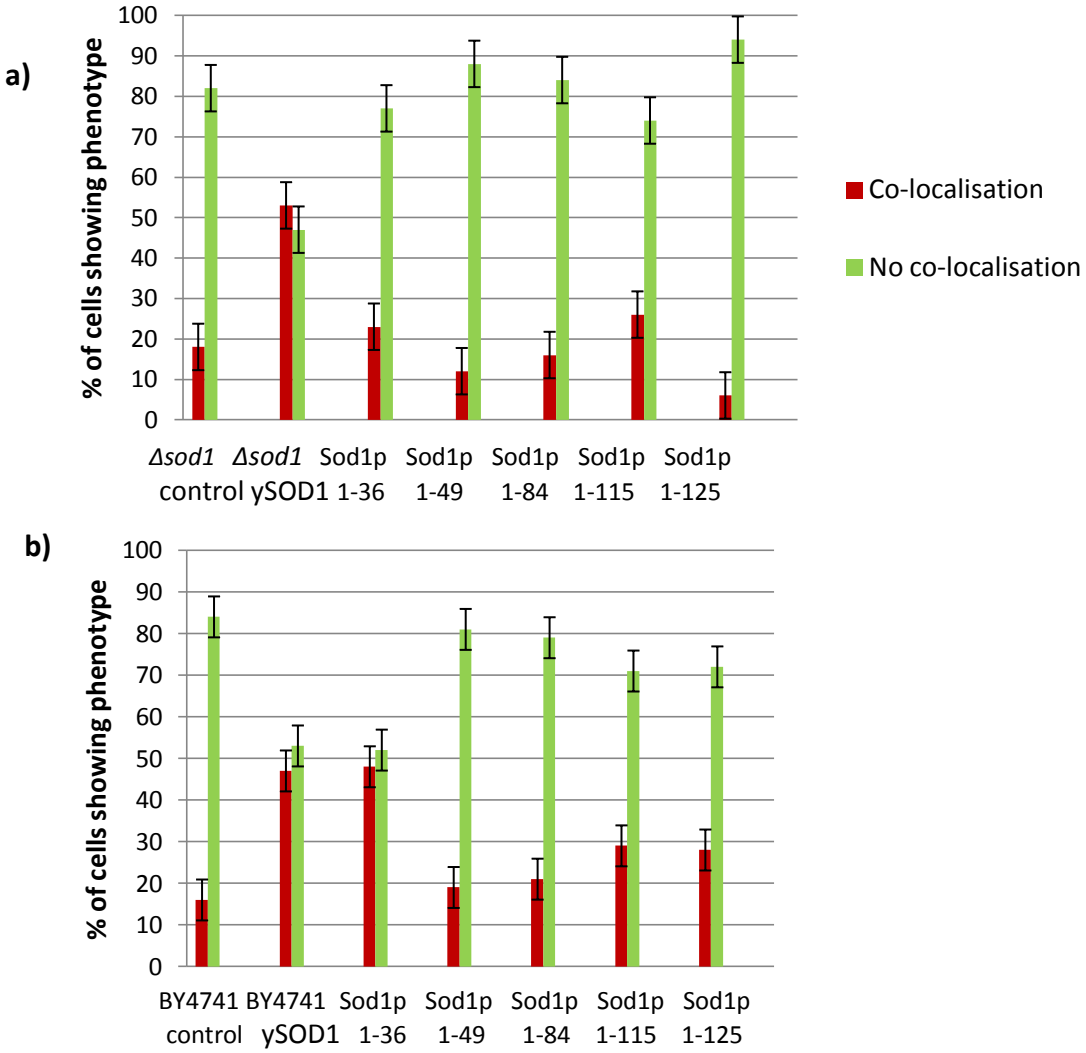

Figure 3.10: Incidence of co-localisation of truncated Sod1p with mitochondria. Co-expression of GFP-fused truncated SOD1 proteins along with Cox4-RFP fusion protein was used to identify mitochondrial localisation **a)** in a *SOD1* deletion strain and **b)** in a wild type BY4741 strain. One hundred cells were observed for each sample and cells scored positively for co-localisation if there was any GFP and RFP co-localisation within the cell, indicating GFP localisation to mitochondria. Error bars indicate standard error.

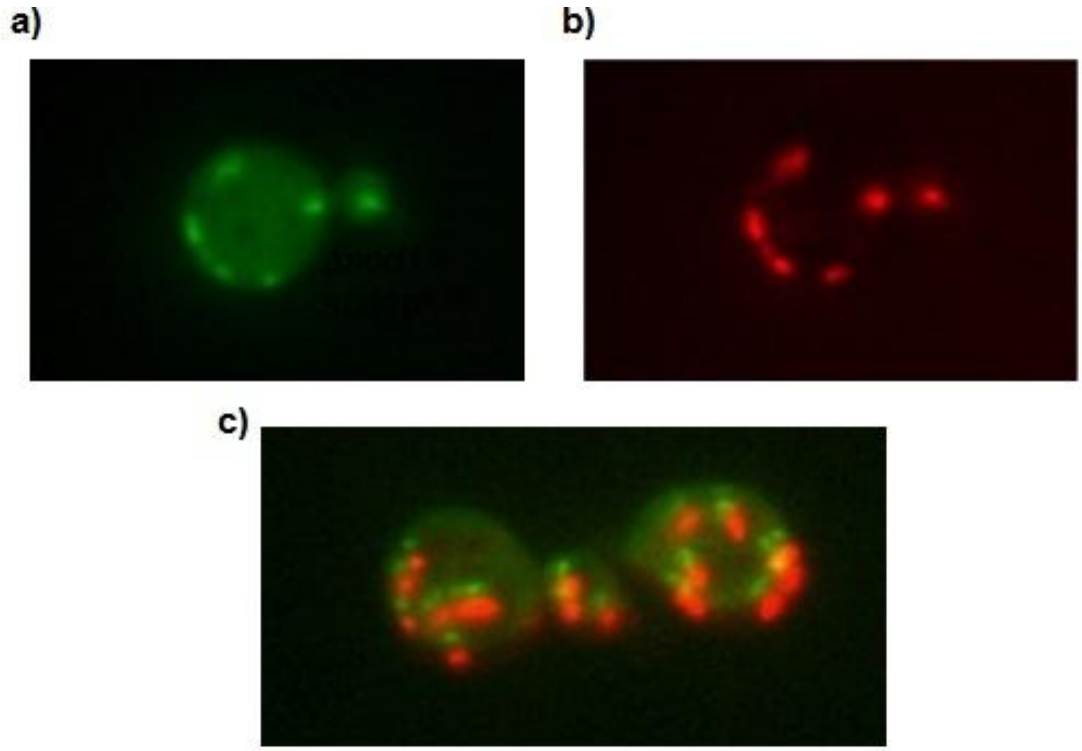

Figure 3.11: GFP and RFP localisation and co-localisation. Images taken from an exponential phase sample of Δ*sod1* strain expressing truncated Sod1p$^{1-36}$-GFP fusion protein with Cox4-RFP showing **a)** Sod1p$^{1-36}$-GFP localisation **b)** Cox4-RFP mitochondrial localisation and **c)** visualisation of both fluorescent proteins using a beamsplitter.

Co-localisation of GFP-tagged truncated SOD1 proteins with Cox4-RFP in the wild type strain was found to be significantly higher in the positive control expressing full-length Sod1p than in cells expressing any of the truncated SOD1-GFP proteins (Figure 3.10b) with the exception of Sod1p$^{1-36}$ in which 50% of cells showed mitochondrial localisation; This finding was not reproduced when Sod1p$^{1-36}$ was expressed in a *SOD1* deletion strain (Figure 3.10a) where ySOD1 still showed approximately the same degree of co-localisation but all Sod1p fragments exhibit less that 30% co-localisation.

3.7 Effects of vacuolar amino acid transporter deletion

Earlier in this chapter, it was shown that expression of toxic Sod1p fragments in a *SOD1* deletion strain caused cell growth to slow but did not reduce viability. Evidence supporting this study (Bastow, 2013) suggests that mutations in SOD1 may lead to metabolic defects that can result in amino acid auxotrophy.

The yeast vacuole acts as a storage compartment for amino acids where they remain inert, until they are transported to the cytosolic amino acid pool when required for metabolism and protein synthesis (Sekito et al., 2008). The majority of the vacuolar amino acid pool consists of basic and neutral amino acids whereas acidic amino acids glutamate and aspartate are almost solely localised to the cytosolic pool. AVT and VBA are two types of vacuolar amino acid transporters existing in yeast. Most of these transporters, including AVT and VBA classes, actively transport amino acids across the membrane by utilizing a proton electrochemical gradient generated by Vacuolar-type H^+-ATPase (V-ATPase) enzyme (Nelson et al., 2000). AVT transporters are all members of the amino acid/auxin permease family and are related to neuronal vesicular GABA-glycine transporters found in higher eukaryotes, and have known orthologues in plants, invertebrates like *C. elegans* as well as mammals such as rats and mice (Sekito et al., 2008; Young et al., 1999). While VBA transporters belong to the major facilitator superfamily (MFS), a large group of membrane transporters found ubiquitously in prokaryotes and eukaryotes (Pao et al., 1998; Shimazu et al., 2005; Sekito et al., 2008).

Null mutant	**Transporter type**	**Competitive fitness**	**Starvation resistance**	**Abnormal vacuolar morphology**	**Other features of mutant**
AVT1/ YJR001W	Large, neutral amino acids vacuole importer	-	-	abnormal	
AVT2/ YEL064C	Unknown	-/+	normal	abnormal	
AVT3/ YKL146W	Large, neutral amino acids vacuole exporter	-	normal	abnormal	
AVT4/ YNL101W	Large, neutral amino acids vacuole exporter	normal	normal	abnormal	
AVT5/ YBL089W	Unknown	-	normal	abnormal	+ toxin resistance
AVT6/ YER119C	Aspartate and glutamate	-	normal	normal	+ accumula-tion of

	vacuole exporter. Involved in nitrogen starvation response				glutamate and aspartate
AVT7/ YIL088C	Unknown	+	-	abnormal	
VBA1/ YMR088C	Basic amino acid permease	-	normal	normal	- nutrient uptake
VBA2/ YBR293W	Basic amino acid permease	normal/+	normal	abnormal	
VBA3/ YCL069W	Basic amino acid permease	-	-	abnormal	
VBA4/ YDR119W	Proposed basic amino acid permease	-	normal	normal	- utilization of nitrogen sources
VBA5/ YKR105C	Plasma membrane transporter, roles in amino acid uptake and drug sensitivity	+	normal	normal	+ replicative lifespan

Figure 3.12: Roles of yeast AVT and VBA amino acid transporter and phenotypes of null mutants. Ubiquitous vacuolar transporters involved in influx and efflux of amino acids. The majority of null mutants show abnormal vacuolar morphology and reduced competitive fitness, while some also show decreased stress resistance and tolerance to drugs such as caffeine and cyclohexamide. + indicates an increase in a characteristic while – indicates a decrease.

Emerging evidence has implicated a link between mutant SOD1 and the yeast vacuole. Corson et al. (1999) found that *SOD1* deletion caused a significant increase in vacuolar fragmentation, whereas Wong et al. (1995) and Bastow (2013) showed mutant SOD1 expression also led to increased vacuole formation. Deletion of *SOD1* results in amino acid auxotrophies, indicating a role of SOD1 in metabolic function. (Chang and Kosman, 1990; Kwon, Jeong, and Roe, 2006; Cozzolino et al., 2009). In this section, the potential interaction between Sod1p and vacuolar amino acid transport will be explored by using amino acid transporter deletion mutants to examine auxotrophies and growth effects.

3.7.1 Expressing truncated SOD1 causes growth defects in some vacuolar amino acid transporter deletion strains.

To examine whether there was an interaction between truncated Sod1p and any of the vacuolar amino acid transporters, AVT and VBA amino acid transporter deletion strains were transformed with a plasmid encoding the truncated SOD1 protein that proved most toxic to cells in earlier Chapter 3, the Sod1p$^{1-115}$-GFP fusion protein. Their growth was analysed and doubling times calculated and compared to those of the deletion strains expressing the control pAG425-EGFP plasmid.

Repeat 1

Strain	Dt when expressing plasmid: Sod1p $^{1-115}$ -GFP	Dt when expressing plasmid: GFP Control	% difference in doubling time
Δavt1	2.76	2.82	-2
Δavt2	2.98	2.99	0
Δavt3	2.49	2.40	4
Δavt4	2.82	2.72	3
Δavt5	2.95	3.18	-7
Δavt6	2.74	2.62	5
Δavt7	3.08	2.70	14
Δvba1	2.84	2.77	2
Δvba2	3.14	3.22	-2
Δvba3	3.05	2.70	13
Δvba4	2.95	2.35	25
Δvba5	2.92	2.57	14
BY4741	2.38	2.64	-10

Repeat 2

Strain	Dt when expressing plasmid: Sod1p $^{1-115}$ -GFP	Dt when expressing plasmid: GFP control	% difference in doubling time	Average % difference
Δavt1	3.14	2.81	12	5
Δavt2	3.07	2.13	44	22
Δavt3	3.08	3.15	-2	1
Δavt4	2.87	3.16	-9	-3
Δavt5	3.05	3.65	-17	-12
Δavt6	2.38	3.20	-26	-10
Δavt7	3.08	2.66	16	15
Δvba1	3.37	3.44	-2	0
Δvba2	3.33	2.86	17	7
Δvba3	3.73	2.86	31	22
Δvba4	3.32	2.85	17	21
Δvba5	3.34	2.71	23	19
BY4741	2.38	2.64	-10	-10

Figure 3.13: Growth is slowed by expression of Sod1p1^{-115}-GFP fusion protein in vacuolar amino acid transporter deletion strains. Percentage difference in doubling time (Dt) indicates the increase or decrease in doubling time when expressing Sod1p$^{1-115}$-GFP fusion protein compared to the control expressing only GFP. Average % difference gives an average of doubling time differences between the two biological repeats. A positive figure indicates growth being slowed by expression of Sod1p$^{1-115}$ –GFP compared to the control whereas a negative figure indicates a growth increase. Those with an average doubling time increase of >20% are highlighted in yellow and those with an increase of >5% in orange. Strains with an

increase in doubling time when expressing Sod1p$^{1-115}$ -GFP were deemed to be affected by its toxicity. BY4741 control data are from one repeat only.

Growth analysis showed that deletion of *AVT3, AVT4, AVT5, AVT6* and *VBA1* did not exhibit a synthetic effect with the truncated Sod1p$^{1-115}$-GFP fusion protein when compared to the GFP control (Figure 3.13). However a synthetic interaction was observed in strains lacking *AVT1, AVT2, AVT7, VBA2, VBA3, VBA4* or *VBA5* in at least one of the experiments (Figure 3.12, Repeat 2) The most prominent and reproducible effects were observed in cells lacking *AVT2, VBA3* or *VBA4* which all showed a >20% decrease in growth when expressing Sod1p$^{1-115}$-GFP.

3.7.2 Investigation of a synthetic effect by truncated SOD1 proteins on mitochondrial and vacuolar function.

Further investigation into the impact of truncated Sod1p expression on mitochondria looked at their effects on mitochondrial function rather than physical aggregate formation, this time in vacuolar amino acid transporter deletion strains. When investigating polyQ aggregation in disease, Solans et al. (2006) reported decreased mitochondrial respiration and an increase in ROS production, as a result of aggregate formation. Ferri et al. (2010) also suggested that toxicity of mutant SOD1 is a result of mitochondrial dysfunction but not by aggregate formation, since solubilisation of mutant Sod1p outside the mitochondrial matrix of human motor neurones by over-expression of glutaredoxin did not prevent mitochondrial toxicity; whereas glutaredoxin expression inside the mitochondrial matrix was able to inhibit mitochondrial dysfunction by restoring the correct redox environment. Results 3.2 also indicated that Δ*sod1* cells expressing Sod1p fragments may have a slight defect in non-fermentable metabolism as growth analyses showed growth appeared to plateau after diauxic shift.

To determine whether truncated SOD1 proteins cause mitochondrial dysfunction and indeed hindering the cells' ability to grow post-diauxic shift, they were expressed in yeast strains with deleted vacuolar amino acid transporter genes and grown on media containing non-fermentable carbon source glycerol instead of fermentable source glucose.

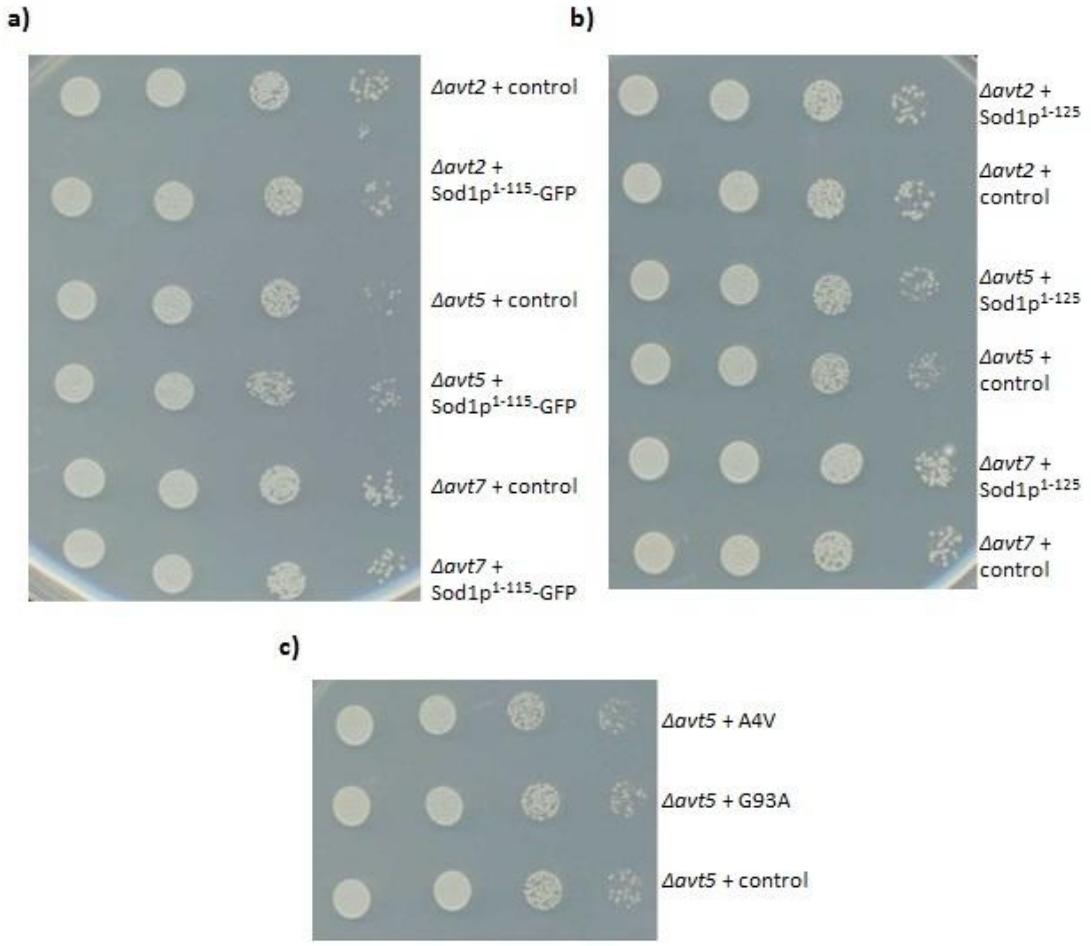

Figure 3.14: Amino acid transporter deletion strains expressing truncated and mutant *SOD1* are able to grow on non-fermentable carbon sources. From left to right (for each image): 5µl spot of culture with an OD_{600} of 1, measured in an Eppendorf Biophotometer™ Plus; spot with OD_{600} of 0.1; spot with OD_{600} of 0.01; spot with OD_{600} of 0.001, achieved by serial dilution. Controls in figures **a)** and **c)** contain empty pAG425 backbones while controls in **b)** contain pAG425-EGFP backbones.

All vacuolar amino acid transporter strains expressing either fALS-associated SOD1 mutants or toxic truncated proteins retained the ability to grow in the absence of glucose, reflecting their functional respiratory metabolism and suggesting oxidative phosphorylation defects are not part of the toxic mechanism exerted by these proteins.

These results did not elucidate any novel insight into the mechanism by which toxic Sod1p fragments or mutants may be causing mitochondrial dysfunction, so the focus of the next experiments explored alternative cellular targets for SOD1-mediated toxicity. Since it is thought that toxic SOD1 protein likely affect multiple cellular targets

to cause cell death and their mechanism has been notoriously difficult to elucidate, the role of mitochondria in SOD1-mediated toxicity has not been ruled out.

3.7.3 Effects of truncated SOD1 expression on the viability of vacuolar amino acid transporter deletion strains.

Vacuolar amino acid transporter deletion strains that exhibited a toxic effect as a result of Sod1p$^{1-115}$-GFP expression were also transformed with a plasmid expression different truncated SOD1 protein, non-GFP fused Sod1p$^{1-125}$. *AVT1, AVT2, AVT7, VBA2, VBA4* and *VBA5* deletion strains expressing either Sod1p$^{1-115}$-GFP, Sod1p$^{1-125}$ or a GFP only control plasmid were grown for 48 hours in SC-leu media, along with a wild type control, and assessed for culture viability.

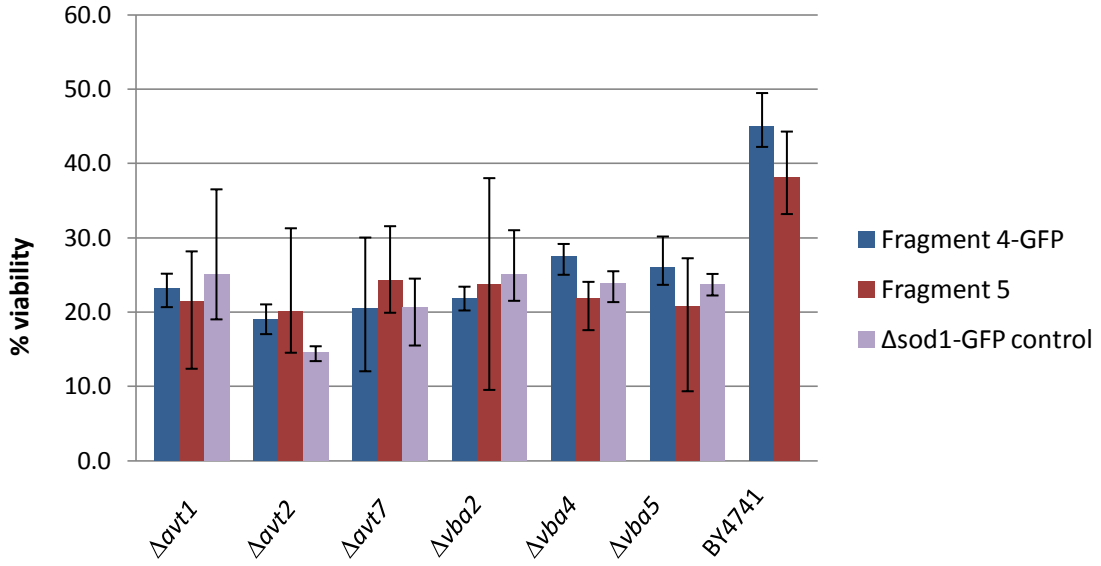

Figure 3.15: Viability of vacuolar amino acid transporter deletion strains expressing toxic SOD1 truncations are reduced compared to wild type control. Deletion strains expressing truncated SOD1 proteins were grown for 48 hours in SC-leu media then their percentage viability calculated according to Materials and Methods 2.5.2. Data representative of an average of 3 biological repeats, each an average of 4 technical repeats. Error bars indicate variability between biological repeats.

Of those tested, all vacuolar amino acid transporter deletion strains showed approximately halved viability in comparison to the wild type BY4741 strain. However the expression of neither Sod1p$^{1-115}$–GFP or Sod1p$^{1-125}$ truncations lead to significant reductions in viability when compared the GFP control, although strains expressing Sod1p$^{1-125}$ in particular showed a high degree of variability; this suggests the

expression of these truncated SOD1 proteins do not lead to a synthetic effect on amino acid transporter function, impacting on cell viability.

3.7.4 Deletion of *SOD1* and vacuolar amino acid transporter genes cause amino acid auxotrophies.

Bastow (2013) showed that deletion of the *SOD1* gene from yeast BY4741 strain caused lysine and leucine auxotrophies, suggesting there may be a link between amino acid biosynthesis and SOD1. Due to the synthetic effect observed on growth of vacuolar amino acid transporter strains expressing truncated SOD1 proteins, this lead to the question of whether vacuolar amino acid transport could also be regulated by SOD1, and whether deletion of amino acid transporters may also show imbalances in amino acid biosynthesis as described in *SOD1* deletion strains.

Analyses shown in this section use Mass Spectrometry data obtained from Markus Ralser's group in the Department of Biochemistry, University of Cambridge. The Ralser group has systematically assessed the total amino acid levels from all strains in the yeast deletion collection (Unpublished data). As part of an ongoing collaboration, the Ralser group provided data from the *SOD1* deletion and all of the vacuolar amino acid transporter deletion strains. Cell extracts for Mass Spectrometry analysis were prepared from cell extracts of strains harvested during exponential growth phase after culture in minimal media.

For each strain, their Mahalanobis Distance was also determined; Mahalanobis Distance gives an indication of outliers in a multivariate dataset, in this case showing which deletion strains' amino acid profiles are significantly different to the average obtained across the entire deletion collection data set (4686 strains). A Mahalanobis Distance value >30 indicates a significant difference from the average, values over 30 were observed in *AVT1*, *AVT3*, *AVT7*, *VBA5* and *SOD1* deletion strains. The amino acid profiles of outlier strains are represented in Figure 3.15, where amino acid levels measured in µmols refer to the concentration of each amino acid in the cell extract tested, whilst the 'average' amino acid level indicates the average concentration of amino acids across an entire data set of 4686 strains tested by the Ralser group.

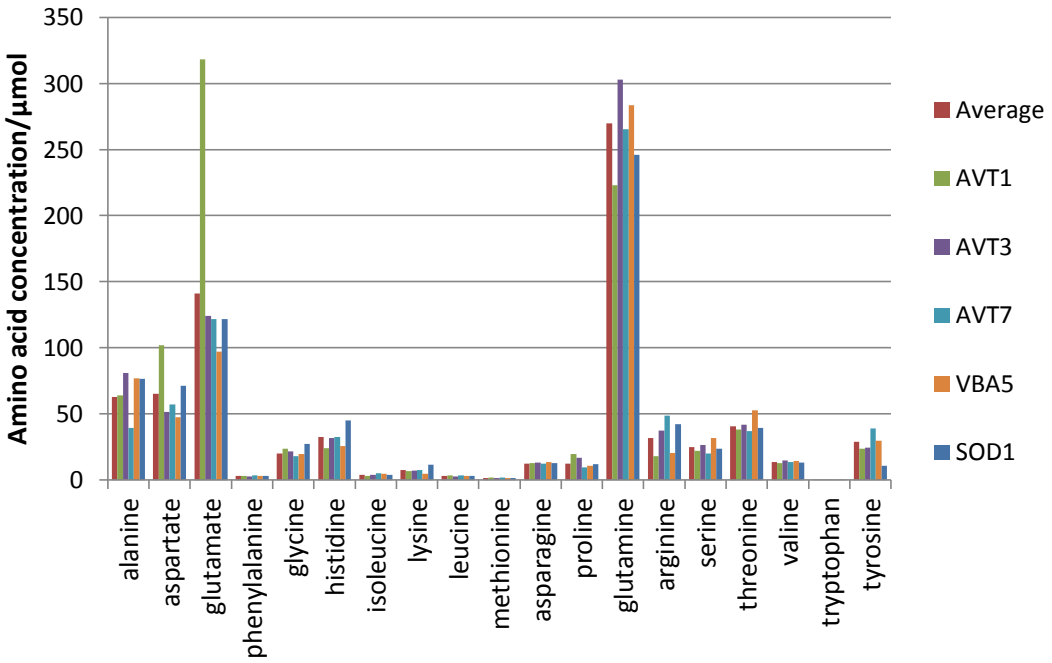

Figure 3.16: Amino acid profiles of yeast deletion strains indicating free amino acid concentrations in cell extracts detected by Mass Spectrometry. Deletion strains with Mahalanobis Distance values above 30.

It was expected that deletion of a particular amino acid transporter would result in increased storage of the types of amino acids generally transported by it; although this data suggests this not to be the case. AVT1 transports neutral amino acids but deletion results in a significant increase in glutamate storage, a negatively charged amino acid. Tyrosine is a neutral amino acid with polar side chains, which appears to be found in lower than average concentrations in *VBA5* deletion strain, VBA5 being a basic amino acid transporter. The *SOD1* deletion strain shows significantly decreased levels of tyrosine but increased storage of lysine, a basic amino acid.

To determine whether there was a common phenotype affecting amino acid levels between the strains that could be attributed to gene deletion, data for all strains was compared for single amino acids. It was hypothesised that leucine concentrations in deletion strains may deviate from the average, particularly in the *SOD1* deletion strain, due to previous evidence showing leucine to have an important role in amino acid signalling and transport (Prohl et al., 2001), and its identification as a regulator of amino acid signalling in the presence of mutant SOD1 (Bastow, 2013). However, a common profile between the deletion strains is not observed, with most not having a

significant Mahalanobis Distance value or specific phenotype. To further investigate the link between SOD1 and amino acid metabolism, Figure 3.16 below shows the amino acids whose concentrations deviated most from the average in the *SOD1* deletion strain.

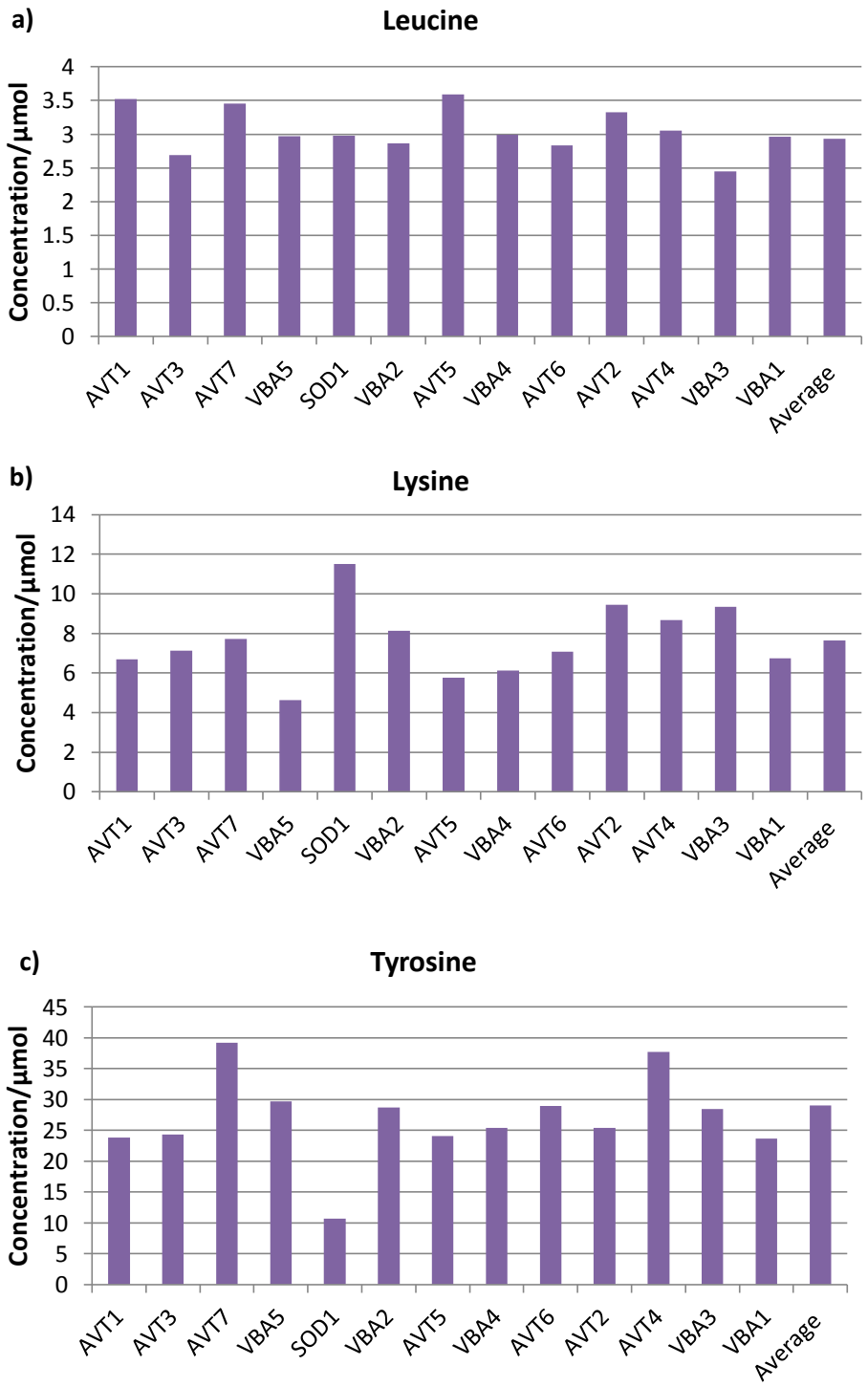

Figure 3.17: Lysine and tyrosine amino acid metabolism may be disrupted in a *SOD1* deletion strain. Mass Spectrometry data of free amino acid concentrations in cell extracts was compared by amino acid, with deletion strains' Mahalanobis Distance values in descending

order from left to right. **a)** Leucine profiles appear variable but relatively close to the average in all strains. **b)** Lysine concentration is elevated in the *SOD1* deletion strain. **c)** Tyrosine concentration is decreased in the *SOD1* deletion strain.

The results show that, as expected, amino acid levels are deregulated by deletion of amino acid transporters however, amino acid levels are also perturbed by deletion of *SOD1*, supporting the idea that SOD1 is linked to amino acid transport.

3.8 Discussion

3.8.1 Effects of GFP fusion on truncated Sod1p stability and toxicity.

Seetharaman et al. (2009) suggested that fALS-associated SOD1 mutations prevent proper maturation of the mutant protein by disrupting interaction of CCS, responsible for copper ion insertion, disulphide bond formation and structural stability of the protein. However, it appears that the presence of a structural component in Sod1p fragments is likely not related to toxicity, since the SOD1 metal binding loop is located between residues 49-84 (Rakhit and Chakrabartty, 2006) (in the human protein, but structurally very similar to the yeast orthologue), so is present in its entirety in Sod1p$^{1-84}$, Sod1p$^{1-115}$ and Sod1p$^{1-125}$. A disulphide bond responsible for stability of the protein is formed between residues 57 and 146 so is not present in any of the truncated proteins, while the electrostatic loop between residues 122-149 is only partly present in Sod1p$^{1-125}$. The fact that Sod1p$^{1-125}$-GFP is only able to form a functional and stable protein as a result of GFP fusion (Figure 3.8) while Sod1p$^{1-115}$-GFP is most toxic of all tested (Figure 3.3, Figure 3.6), suggests length of Sod1p is the determining factor in whether a wild type SOD1 protein is able to function or exhibit toxicity, and the difference between these two is determined by only 10 amino acids. Nevertheless, further investigation into the presence of the electrostatic loop in wild type Sod1p toxicity should be performed, perhaps by creating varying truncations between residues 122 and 149 or equivalent in the yeast protein.

Wright et al. (2013) also showed that structural instability of SOD1 dimers increased their tendency to form aggregates. Fusion of GFP lengthens the protein fragment, so it may be the case that longer Sod1p fragments cause more toxicity than shorter fragments as they are able to aggregate or accumulate within the cell and disrupt

functioning. It has been shown that these longer SOD1-GFP fusion proteins do not form mitochondrial aggregates (Figure 3.10) but aggregates may form in other areas of the cell or accumulation of soluble oligomers may cause toxicity. In the case of Sod1p$^{1-125}$-GFP which is not toxic, the added length of GFP appears to stabilize the protein which is responsible for its acquired SOD activity.

3.8.2 SOD1 may play a role in regulation of amino acid transport.

Sturtz and Culotta (2001) reported that deletion of *SOD1* from yeast lead to the appearance of metabolic defects, including disrupted methionine and lysine biosynthesis. Further evidence has shown SOD1 mutants catalyze oxidative damage of human glutamate transporter GLT1, causing inactivation of the transporter and subsequent neuronal degeneration (Trotti et al., 1999). Addition of an antioxidant was able to reactivate GLT1, suggesting a role of SOD1 in regulation of amino acid transport. The growth differences observed in transporter deletion strains (Figure 3.13) could be interpreted in one of two ways; firstly, it could be that in a transporter deletion strain where no growth defects were observed, the target of toxic Sod1p required to cause toxicity was deleted from the genome preventing interaction between the two and as a result, the cell does not exhibit growth defects. On the other hand, growth defects as a result of toxic Sod1p expression may suggests those transporters are necessary for the cell to function properly in the presence of Sod1p$^{1-115}$-GFP and could be providing protection to the cell. If the latter is true, an explanation for this effect could be that expression of the Sod1p fragment disrupts amino acid transport in the cell causing toxicity, and the deleted transporter is necessary to regulate transport of trapped amino acids, implicating a role for vacuolar amino acid transport in SOD1-mediated toxicity; the relation between SOD1 and amino acid transport is also supported by the Mass Spectrometry data showing perturbed amino acid levels in the *SOD1* deletion strain (Figure 3.17). Questions arising from this are whether the longer truncated SOD1 proteins are able to directly interact with vacuolar amino acid transporters to cause dysfunction, or whether its effect on amino acid transport is regulated via a signalling pathway.

Chapter 4

Exploring the effects of over-expression of human ALS-associated mutant and wild type *SOD1* on *C. elegans*

4.1 Introduction

4.1.1. *C. elegans* life cycle.

The nematode worm *C. elegans* is widely used in modelling of human neurodegenerative diseases. *C. elegans* exists either as a hermaphrodite, able to reproduce asexually or as a male, which are much less common in nature. These organisms have a relatively short lifespan and when grown at optimal conditions of 20°C with plentiful food supply, the adult lifespan is approximately 2-3 weeks. In *C. elegans* development from egg to reproductively functional adult typically takes 3-4 days and progresses through four larval stages, L1 to L4, before reaching adulthood (Figure 4.1). The growth of *C. elegans* is strongly affected by environmental changes; their optimal growth temperature is 20°C, but lowering the temperature to 15°C delays its life cycle and gives rise to worms with a larger body size while increasing temperature to 25°C accelerates their life cycle and leads to a smaller body size. (Devaney, 2005). Under stress conditions such as nutrient starvation, higher than 27°C temperatures or other limitations, *C. elegans* L2 larvae may enter an alternative, stress resistant, long-lived 'dauer' state, induced by neuroendocrine signalling through the dauer pheromone (Hu., 2007; Prahlad and Morimoto, 2009). Worms may remain in this form without the need to eat for up to four month and if optimal conditions are restored during this time, the dauer can return to normal L3 stage and progress into adulthood.

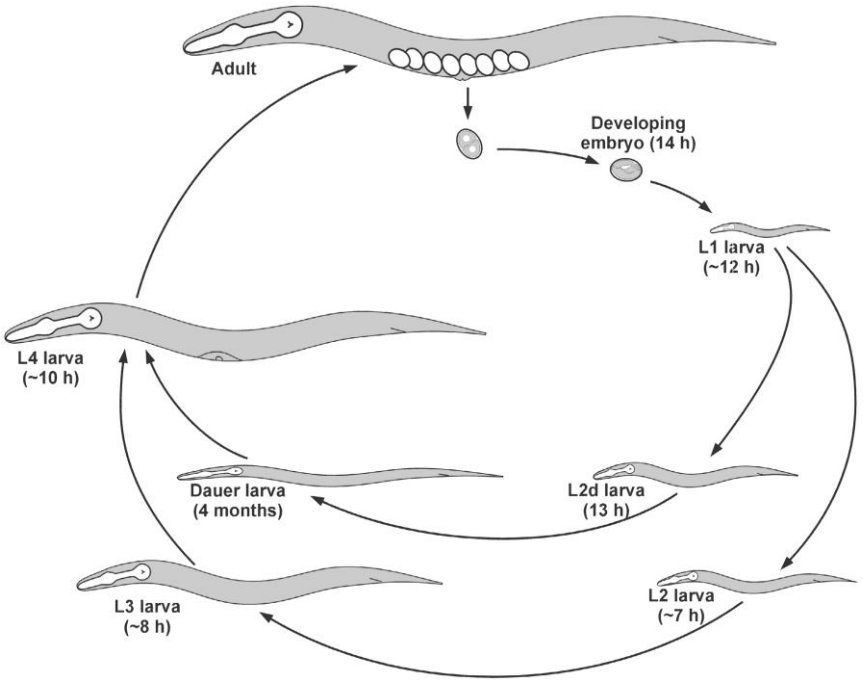

Figure 4.1: *C. elegans* hermaphrodite life cycle. Image from (Strange, 2003).

4.1.2. *C. elegans* as an experimental model.

Metabolic pathways are conserved between *C. elegans* and mammals, in addition to the similarities between their nervous systems; the *C. elegans* nervous system has been thoroughly studied, and complete mapping of their anatomy shows their nervous systems are composed of 302 neurones, which use nearly all the same neurotransmitters as the mammalian nervous system. Full sequencing of the *C. elegans* genome allowed extensive rational genetic manipulation of worms, with many gene deletion and mutant strains now available (Kuwahara et al., 2008; Therrien and Parker, 2014). Around 80% of *C. elegans* genes have orthologues in humans (Lai et al., 2000; Shaye and Greenwald, 2011).

C. elegans provides an excellent model organism to study neurodegenerative diseases for a number of reasons. Firstly, genetic manipulation is easily achieved and many altered strains are already available in addition to the ease in which RNA interference (RNAi) can be performed in worms. RNAi exploits double stranded RNA expressed in the bacterial food source of worms and can be used to regulate and silence gene expression in *C. elegans*. Furthermore, the translucent body of *C. elegans* allows *in vivo* visualisation of anatomy and neurones in a live organism, which is particularly useful when studying the progression of neurodegeneration (Li et al., 2013).

C. elegans has been used in modelling many human neurodegenerative disorders in recent years, including Alzheimer's, Huntington's and Parkinson's diseases. For example, evidence obtained in *C. elegans* has confirmed a role of Huntington's disease-associated mutant polyglutamine (polyQ) expansion as a cause of toxicity in multiple neurodegenerative disorders. Morley, Brignull and Morimoto (2002) tested this using fluorescently-tagged polyQ proteins to observe protein aggregate formation in *C. elegans*, reporting that such aggregate formation and proteotoxicity was slowed in long-lived worms but exacerbated by ageing, showing ageing regulates protein homeostasis.

Alzheimer's disease, characterised by amyloid beta (Aβ) toxicity leading to neuronal accumulation of tau protein, has also been modelled using *C. elegans*. Such studies have led to the discovery that over-expression of tau in neurones causes neuronal dysfunction comparable to that observed in brains with human patients with Alzheimer's disease or frontotemporal dementia (Stoothoff and Johnson., 2005; Wolozin et al., 2011). Link (1995) also modelled β-amyloidosis by producing Aβ in muscle cells of *C. elegans* and later studies by the Link group showed movement defects, a growth deficit and premature death as a result of Aβ expression. However, other changes mirroring those observed in the brains of Alzheimer's disease patients were observed in *C. elegans* cells, including increased expression of heat shock and pro-apoptotic proteins and evidence of mitochondrial dysfunction (Link et al., 2003; Boyd-Kimball et al., 2006; Wolozin et al., 2011).

C. elegans is also an attractive model for studying motor neurone diseases such as ALS. For example, multiple studies have been able to replicate the neuronal degeneration and paralysis observed in the ALS condition, in transgenic *C. elegans* expressing mutant human Sod1p (Gidalevitz et al., 2009; Li et al., 2014; Wang et al., 2009; Witan et al., 2008). Li et al. (2013) found that expression of mutant *SOD1* in *C. elegans* motor neurons caused age-dependent motor defects and impaired axon guidance in addition to aggregation of mutant SOD1, thereby indicating protein aggregation plays an important role in mutant SOD1-mediated neurodegeneration and toxicity. Li et al. (2013) also noted that over 80% of mutant *SOD1*-expressing worms became paralyzed by day 12 of the study, while other studies have shown that mutant *SOD1* expression also causes impaired response to oxidative stress (Oeda et al., 2001). When expressing

mutant *SOD1* throughout the nervous system rather than just motor neurones, Wang et al. (2009) still reported motor defects, accompanied by dysfunctional neuronal transmission. Expression of *SOD1* mutants in *C. elegans* body wall muscles however showed variability in the tendency of these proteins to aggregate (Gidalevitz et al., 2009) suggesting that while aggregation occurs most prominently in motor neurones, SOD1 mutants can also form protein aggregates in other areas of the body in *C. elegans*.

In the results presented in the following study, the effects of fALS-associated G85R *SOD1* mutant or wild type *SOD1* over-expression in transgenic *C. elegans* strains were investigated. The G85R *SOD1* mutation results in amino acid substitution of arginine instead of glycine at residue 85 in the Sod1p primary sequence. This mutation leaves the protein highly susceptible to inactivation and also alters metal binding properties leading to loss of SOD function *in vivo* (Nishida et al., 1994). Previous studies from the Wang laboratory that created these transgenic strains have shown that G85R mutant worms exhibited severe motility defects accompanied by insoluble protein aggregates in addition to soluble G85R proteins (Wang et al., 2009). In the following study, the conditions described by Wang et al. (2009) were replicated to observe the effects on *C. elegans* lifespan and determine whether the motor defects reported in the study are reliable.

4.2 Over-expression of G85R mutant and wild type SOD1 reduces the lifespan of *C. elegans*

Integrated transgenic strains encoding human SOD1-YFP and human SOD1 mutant G85R-YFP (Materials and Methods 2.2.3) were first bleached to remove contamination (Materials and Methods 2.6.1) then the surviving eggs were grown on standard NGM. A plentiful supply of live OP50 bacteria was provided for at least three generations to ensure the strains were well fed. L4 larval stage individuals from these strains, along with well fed wild type N2 strain were transferred onto fresh OP50-seeded NGM media treated with progeny growth inhibitor, 5-fluoro-2'-deoxyuridine (FUDR). The larvae were incubated at 25°C for the course of the experiment, with their survival being monitored every 2-3 days. L4 stage worms mature to egg-producing adults

within one day, so the day following transfer indicated day 1 of the lifespan experiment.

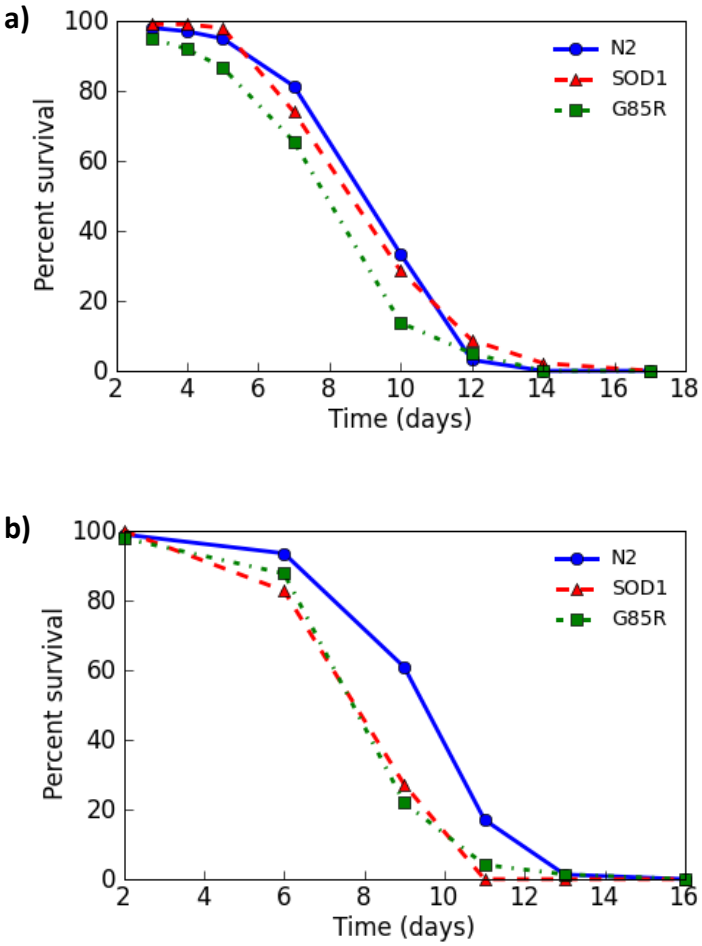

Figure 4.2: Adult lifespan of *C. elegans* is slightly reduced by expression of *SOD1* G85R mutant when grown at 25°C. a) and **b)** represent two repeats of the same experiment. Both experiments begun with 100 L4 larval stage worms, which were grown on standard solid NGM media with live OP50 bacteria and FUDR treatment at 25°C for the course of the experiment. Raw data was analysed using Online Application for Survival Analysis (OASIS) software (Yang et al., 2011).

During this experiment, worms were scored as dead if they did not move at all when prodded with a worm pick and appeared to have died a natural death, but were censored from the experiment if they showed any sign of unnatural death or were lost during the experiment. Common reasons for censoring included internally hatched larvae often causing death, complete or partial intestinal protrusion from the vulva or worms being lost down the edge of the agar.

The null hypothesis is that worm lifespan would not be affected by expression of fALS-associated G85R mutant or over-expression of SOD1. Experiment one showed the mean lifespan for N2, SOD1-overexpressing and G85R strains were 10.36, 9.03 and 9.11 days respectively. P-values (Table 4.1) for SOD1 vs G85R were larger than the critical value, 0.05, so the null hypothesis was not rejected for these datasets indicating there was little significant difference in lifespan between SOD1-overexpressing and G85R strains. However, N2 vs SOD1 and N2 vs G85R P-values were both smaller than the critical value, rejecting the null hypothesis and suggesting there is a significant difference in lifespan between control and transgenic strains. In experiment two, the mean lifespan for N2, SOD1-overexpressing and G85R strains were 10.02, 9.97 and 8.94 days respectively. This time, P-values of N2 vs SOD1 indicated they were not statistically different, but the lifespan of G85R strain was significantly different to both N2 and SOD1 over-expressing strains.

Table 4.1: Statistical analysis of lifespans in *C. elegans* strains.

	Experiment 1		**Experiment 2**	
Condition	**Chi^2**	**P-value**	**Chi^2**	**P-value**
N2 *vs* SOD1	23.68	0.0000011	0.01	0.9147
N2 *vs* G85R	21.99	0.0000027	8.88	0.0029
SOD1 *vs* N2	23.68	0.0000011	0.01	0.9147
SOD1 *vs.* G85R	0.04	0.8397	6.51	0.0107
G85R *vs.* N2	21.99	0.0000027	8.88	0.0029
G85R *vs* SOD1	0.04	0.8397	6.51	0.0107

Statistical analysis of the data (using OASIS software) from both experiments showed that expression of SOD1 G85R mutant did consistently cause a reduction in *C. elegans*

lifespan; conversely, over-expression of SOD1 showed variable effects on lifespan, exhibiting statistically significant lifespan reduction only in Experiment 1.

A potentially important point to note is that the inhibition of progeny growth by FUDR is mediated through ingestion. For each experiment, five NGM plates containing 20 worms each were used for each strain and on plates containing G85R worms, more young progeny appeared to hatch consistently than on plates containing *SOD1*-overexpressing or N2 worms. Although proper quantification of this phenomenon will need to be carried out in the future to investigate its reliability and validity in G85R-expressing worms, this preliminary observation has two important implications. Firstly, the hatching of progeny indicates a physical difference in the G85R worms compared to the controls perhaps reflecting that their ability to feed is impaired resulting in a reduced intake of FUDR, leading in turn to reduced inhibition of progeny development. Secondly, reduced feeding and dosage of FUDR may also impact on lifespan of these worms as some evidence indicates FUDR may increase worm lifespan (Rooney et al., 2014; Aitlhadj and Stürzenbaum, 2010).

4.3 Investigating the impact of leucine supplementation on SOD1-mediated motor defects in *C. elegans*

4.3.1 Over-expression of SOD1 G85R mutant hinders *C. elegans* motility but can be improved by leucine supplementation.

During the lifespan experiments (Section 4.2), it was noticed that mutant worms appeared to adopt an interesting phenotype in which their movement ability was reduced compared to other strains (detailed further in Results 4.3.2). To test this observation, motility experiments were performed by growing 30 worms per strain on NGM medium and scoring their movement into one of three categories, A, B or C. A-scored worms exhibited normal motility, B-scored worms slightly reduced motility and C-scored worms showing little movement except for head or tail (Materials and Methods 2.6.3). Following results from Bastow (2013) that showed leucine supplementation was able to rescue growth defects exhibited by yeast expressing fALS-associated *SOD1* mutants, varying concentrations (0mM, 1mM, 2mM and 5mM) of leucine supplement were also added to the *C. elegans* medium to investigate

whether this would improve their motility. All experiments in this section were carried out using NGM medium seeded with heat-killed OP50 bacteria to prevent metabolism of the supplemented leucine by the bacteria, and treated with FUDR to inhibit progeny growth.

When grown at 20°C, G85R worms clearly showed the highest incidence of B-scoring with no leucine supplement, indicating slight motor defects. The number of worms with slight motor defects in the G85R strain began to increase after day 5 in all conditions; however the 2mM leucine condition appeared to reduce the occurrence of defects (Figure 4.3c). Severe motor defects were difficult to interpret due to the low number of C-scored worms, however the data obtained showed no worms with severe motor defects occurring over the course of the experiment when supplemented with 1mM leucine (Figure 4.4b). In the SOD1 over-expressing strain, the number of worms with slight motor defects was greater than the control by day 7 in all leucine supplemented conditions, and leucine supplementation also did not reduce the occurrence of severe motor defects. Interestingly, higher concentrations of leucine also appeared to marginally increase the number of motor defective worms occurring in the N2 strain. These results suggest that when grown at 20°C, supplementation with low concentrations of leucine can improve motor defects in the G85R worms, but may worsen the condition in SOD1 over-expressing and N2 worms.

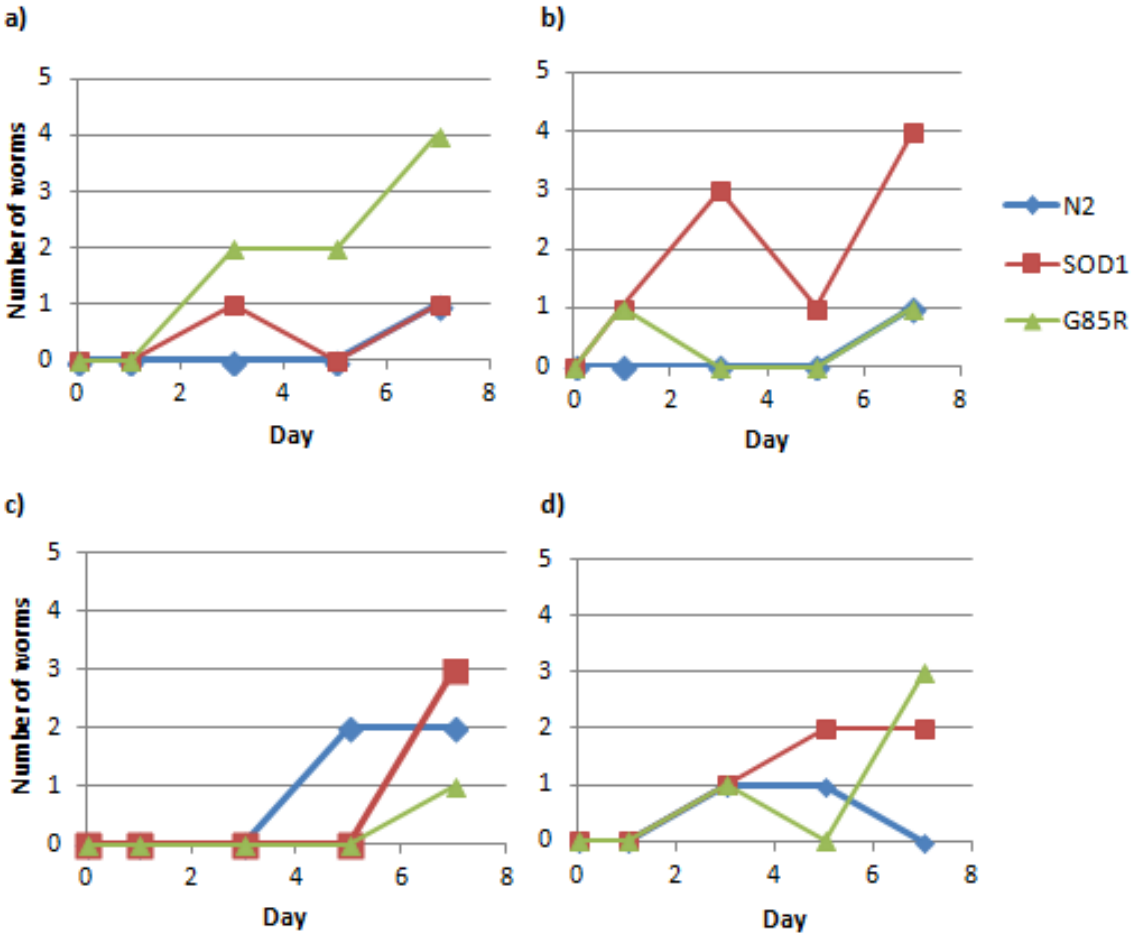

Figure 4.3: Frequency of *C. elegans* with slight motor defects on media supplemented with increasing leucine concentrations when grown at 20°C. a) shows B-scored worms grown on NGM medium with no leucine supplement, **b)** with 1mM leucine supplemented, **c)** 2mM leucine supplement and **d)** 5mM leucine supplement.

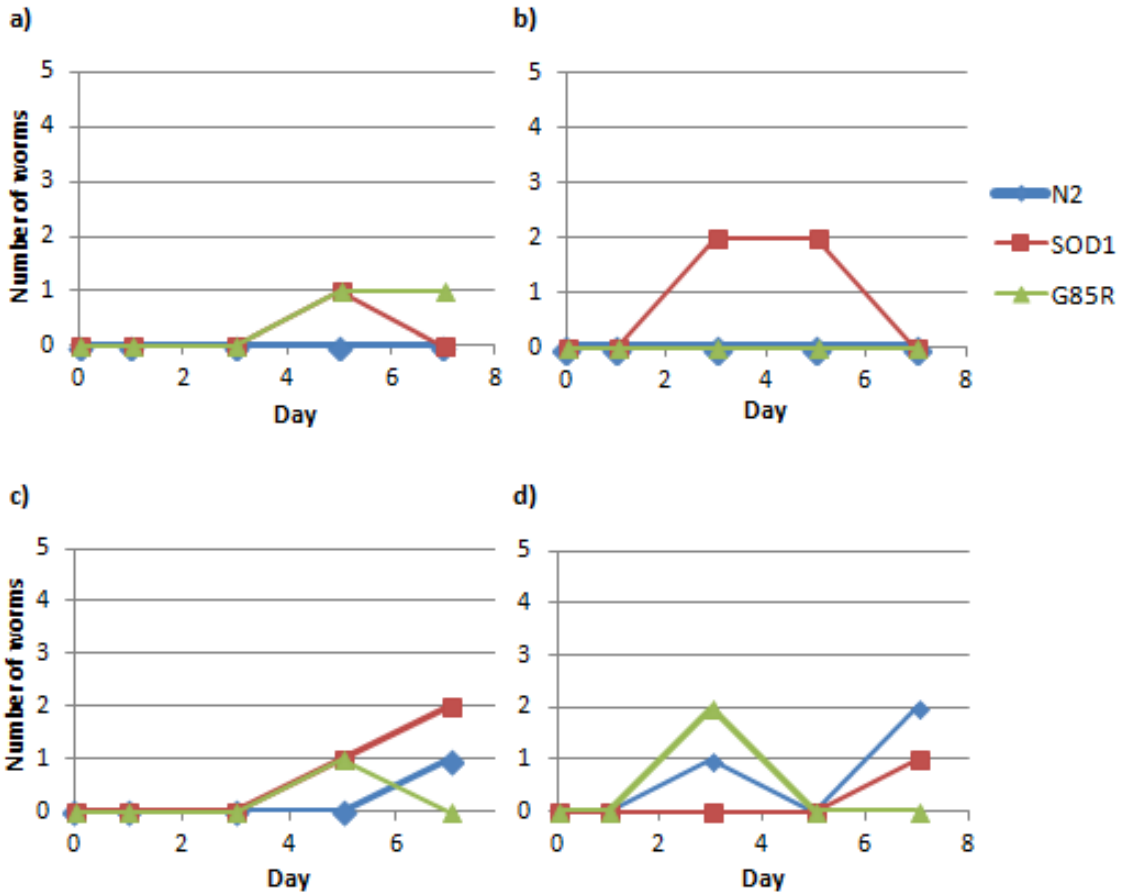

Figure 4.4: Frequency of *C. elegans* with severe motor defects on media supplemented with increasing leucine concentrations when grown at 20°C. Experiment **a)** shows C-scored worms grown on NGM medium with no leucine supplement, **b)** with 1mM leucine supplemented, **c)** 2mM leucine supplement and **d)** 5mM leucine supplement.

When grown at 25°C, leucine addition resulted in little improvement to motility of G85R worms, except at 2mM leucine where occurrence of B-scored worms appeared to slow by day 5 compared to other concentrations, despite reaching the same number of motor defective individuals by day 7 as the non-supplemented condition (Figure 4.5c). The 5mM leucine condition showed the greatest incidence of G85R worms with slight motor defects. SOD1 over-expressing worms also showed most improvement in the presence of 2mM leucine, with lower overall incidence of B-scored worms than the N2 strain. Again, few C-scored worms occurred within the tested time period, but the results indicate 1mM and 2mM leucine concentrations slightly slow the development of severe motor defects in SOD1 over-expressing worms and this may also be the case for G85R worms. However, G85R worms showed higher numbers of severe motor defective worms in all leucine supplemented conditions by day 7 compared to no

leucine supplement (Figure 4.6), suggesting that leucine addition is less able to rescue motor defects in worms grown at 25°C.

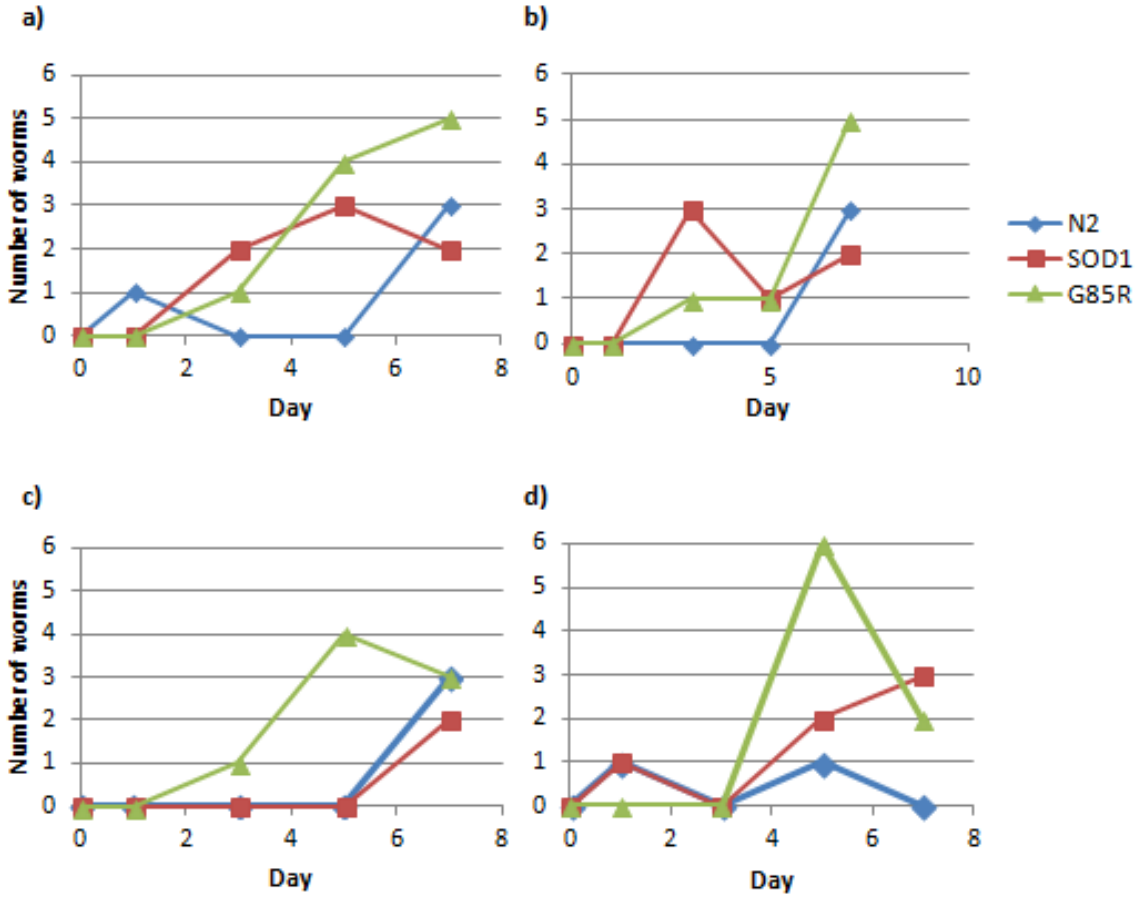

Figure 4.5: Frequency of *C. elegans* with slight motor defects on media supplemented with increasing leucine concentrations when grown at 25°C. Experiment **a)** shows B-scored worms grown on NGM medium with no leucine supplement, **b)** with 1mM leucine supplemented, **c)** 2mM leucine supplement and **d)** 5mM leucine supplement.

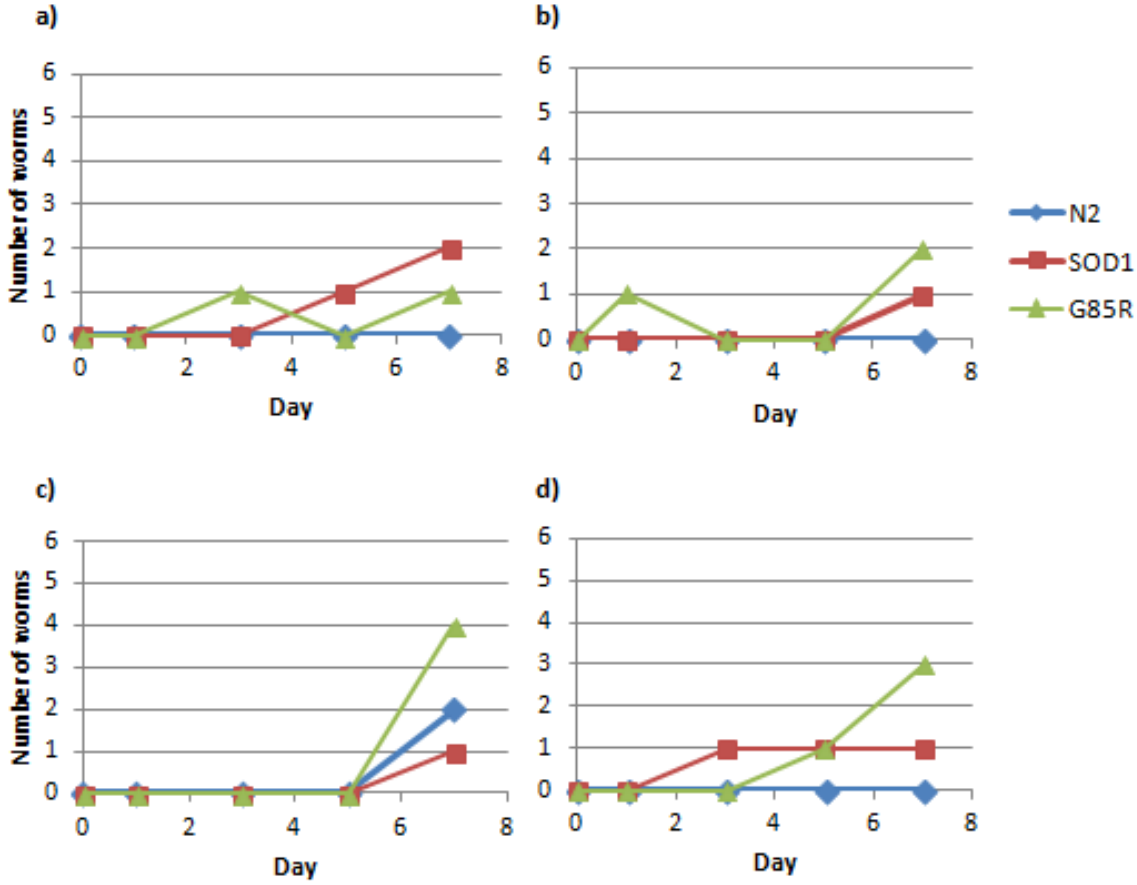

Figure 4.6: Frequency of *C. elegans* with severe motor defects media supplemented with increasing leucine concentrations when grown at 25°C. Experiment **a)** shows C-scored worms grown on NGM medium with no leucine supplement, **b)** with 1mM leucine supplemented, **c)** 2mM leucine supplement and **d)** 5mM leucine supplement.

A longer observation period and larger sample size is necessary to properly investigate the ability of leucine supplementation to rescue motor defects and these preliminary results give encouragement to do so.

4.3.2 Leucine supplementation improves thrashing ability in worms expressing ALS-associated SOD1 mutants.

SOD1 G85R-expressing worms exhibited a notable phenotype, illustrated in Figure 4.7.b. This was also observed by Prof. Alan Morgan (University of Liverpool) whose group also investigated the effects of human SOD1 G85R mutant expression on *C. elegans* movement in parallel to the research presented here. The mutant worms had a tendency to curl up instead of moving freely forward, with reduced movement ability when prodded often only moving their head. The Morgan group also quantified this motor defect, by performing thrashing assays in which N2, wild type SOD1 over-

expressing and G85R mutant strains were placed in liquid media and the number of tail thrashes by each worm monitored within one minute time periods. They showed that SOD1 over-expressing worms gave partially reduced thrashing frequencies in comparison to N2 worms, but G85R mutants had severely impaired thrashing ability compared to both strains (A. Morgan, personal communication; Figure 4.8).

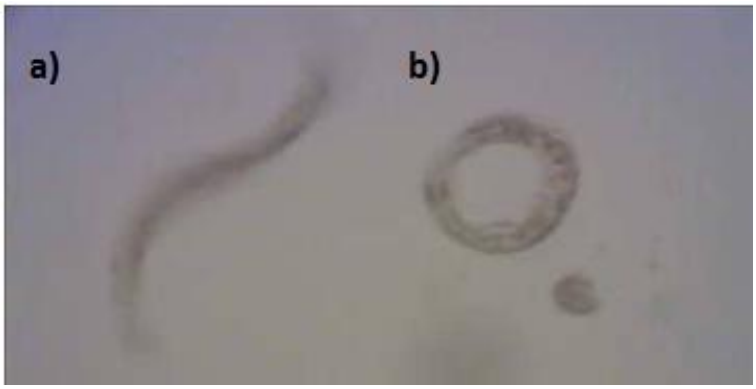

Figure 4.7: Motility defective phenotype exhibited by mutant SOD1 *C. elegans*. Specimens over-expressing **a)** wild type hSOD1 and **b)** G85R hSOD1 mutant. Image obtained from Prof. Alan Morgan (University of Liverpool).

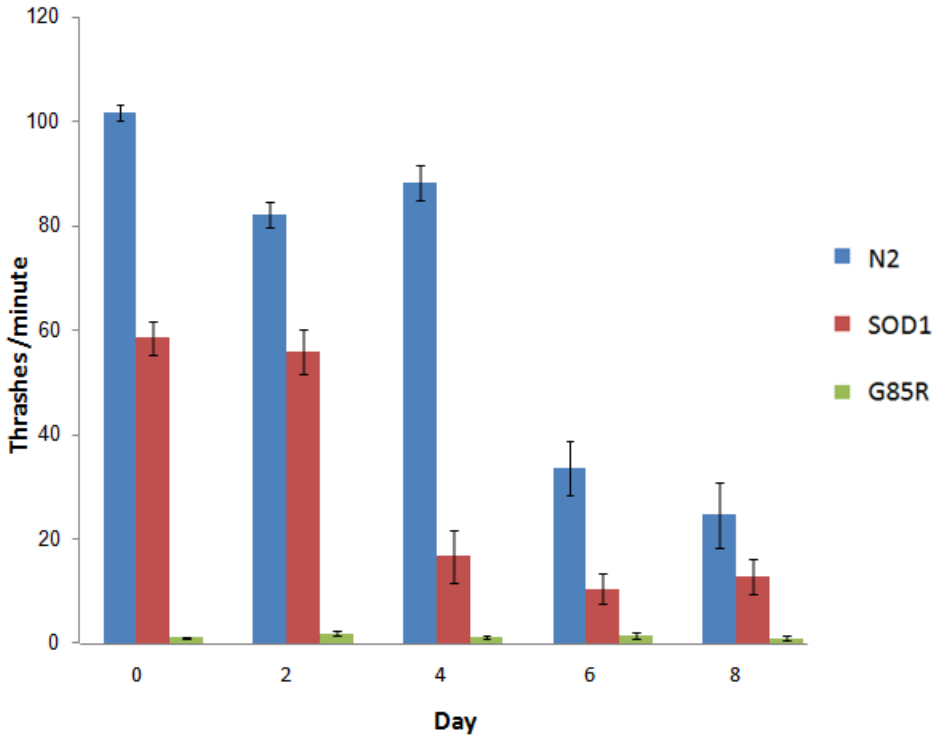

Figure 4.8: Thrashing ability is severely impaired in G85R hSOD1 mutant worms. Number of tail thrashes performed by worms in liquid medium was recorded at one minute intervals for each strain. G85R mutant worms showed greatly reduced thrashing ability compared to the wild type N2 strain. Data obtained from Prof. Alan Morgan (University of Liverpool).

The effects of leucine supplementation on thrashing ability were also explored. When supplemented with 1mg/ml, 2mg/ml, 5mg/ml or 10mg/ml of leucine, it was discovered that for all strains including N2, thrashing was increased most when a concentration of 2mg/ml leucine was added to the liquid media (Figure 4.9). Addition of 10mg/ml leucine restored thrashing frequency to that of the untreated condition in both N2 and G85R strains, suggesting an optimal concentration of leucine is able to improve thrashing ability, but higher concentrations will not provide any further increase. Despite some improvement, the thrashing ability of G85R mutant worms remained very low even in the presence of the optimal leucine supplement.

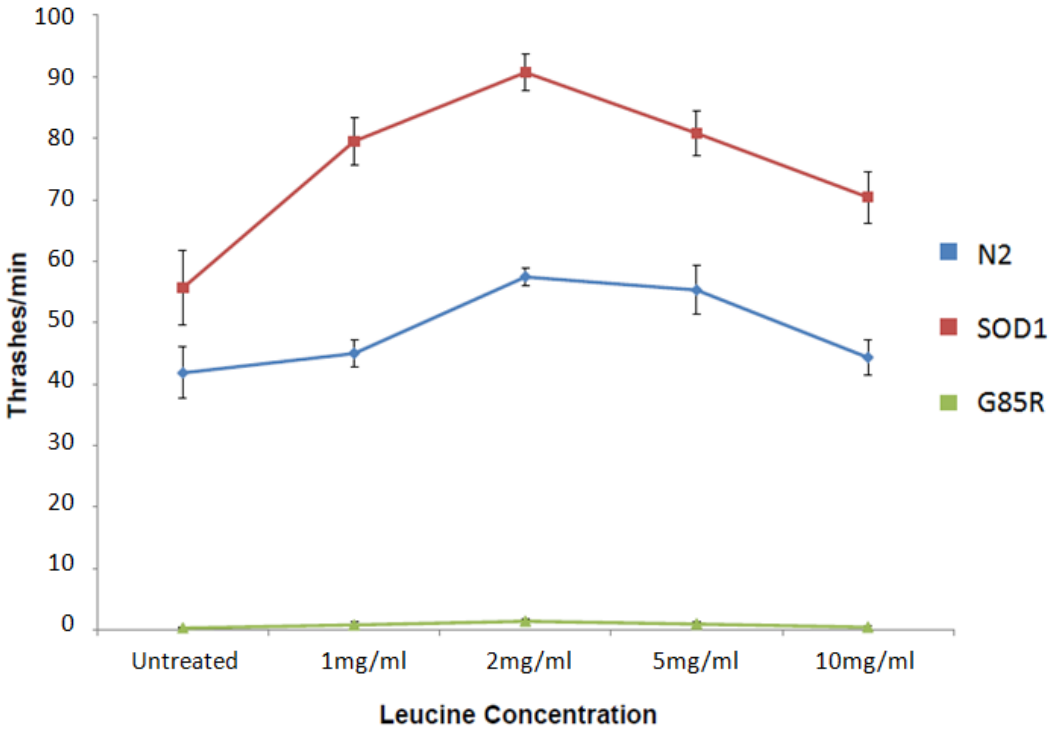

Figure 4.9: Optimal leucine supplementation improves thrashing ability. Thrashing frequency of N2 and SOD1 over-expressing worms is most improved by addition of 2mg/ml concentration of leucine. G85R mutant worms also show slight improvement at this concentration. Data obtained from Prof. Alan Morgan (University of Liverpool).

4.4 Mutant SOD1 expression in *C. elegans* causes vulval defects

4.4.1 SOD1 G85R mutants show increased occurrence of protruding vulvae.

Whilst motility experiments were being performed, the occurrence of vulval differences in the tested strains became apparent. The number of worms exhibiting

protruding vulvae (a phenomenon in which the intestine of the worm begins to protrude through the vulva) were monitored and recorded for each strain and motility category at 20°C and 25°C incubation, alongside the motility experiment i.e. using the same growth conditions and amino acid supplemented conditions. Once the worms exhibiting this phenotype died, they were excluded from the experiment. Due to the relatively low incidence of B and C-scored worms, and proportionately low numbers of worms exhibiting protruding vulvae, the data would be difficult to draw conclusions from so only protruding vulvae shown in A-scored, fully motile worms is presented here.

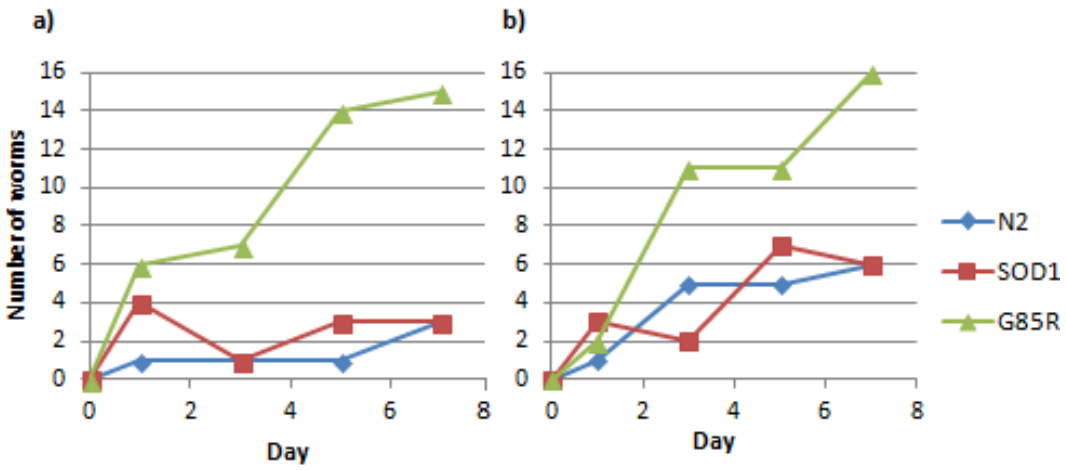

Figure 4.10: Frequency of vulval defects in *C. elegans* over-expressing wild type and G85R mutant h*SOD1*. Experiment **a)** shows A-scored worms grown at 20°C and **b)** shows A-scored worms grown at 25°C, both on standard NGM media. SOD1 indicates over-expression of wild type hSOD1.

When grown on standard NGM with no leucine supplement, G85R-expressing worms showed significantly more protruding vulvae than other strains, indicating mutant SOD1 is likely causing vulval defects, although the same effect is not observed when over-expressing wild type SOD1 suggesting a mutant SOD1-specific defect.

4.4.2 Leucine supplementation reduces the occurrence of vulval defects in worms expressing SOD1 G85R mutant.

The occurrence of protruding vulvae in each strain were also monitored in the presence of leucine supplements, to investigate whether leucine addition could

improve vulval defects in the same way it appeared to rescue movement ability in Section 4.3.

At 20°C incubation, 2mM leucine supplement appeared to alleviate vulval defects to the greatest extent (Figure 4.11b) but at 25°C, 5mM leucine showed the most prominent improvement (Figure 4.11f). Conversely, in the SOD1 over-expressing strain at 20°C, occurrence of protruding vulvae was relatively low in all leucine concentrations except 1mM concentration in which the incidence of protruding vulvae was higher than in either N2 or G85R mutant strains by day 5. At 25°C incubation, SOD1 over-expressing worms exhibited the lowest frequency of protruding vulvae at all leucine concentrations, being equal to or lower than that of N2 worms. These findings indicate that SOD1-G85R mutant expression shows some correlation to the formation of vulval defects in worms, but that these defects can be improved by leucine supplementation. However, wild type SOD1 over-expression generally does not cause vulval defects.

The results also showed that compared to other leucine concentrations and the control, A-scored N2 worms growing at 25°C on 1mM supplemented leucine (Figure 4.11d) medium had a very high incidence of protruding vulvae. Since the medium used in these experiments was seeded with dead OP50 bacteria and was prone to contamination and growth with live bacteria, worms on these plates required transference to fresh medium every few days. It is possible that this is an anomalous result caused by these particular worms being somewhat stressed or damaged by the frequent movement, affecting their degree of vulval protrusion.

Another observation was that in the G85R strain grown at 20°C, five worms were censored on day 1 of the experiment due to death caused by internal hatching of larvae (4 incidences in 1mM leucine condition, 1 in 2mM condition). Internal hatching of larvae may indicate further vulval or egg laying defects, or a response to stress.

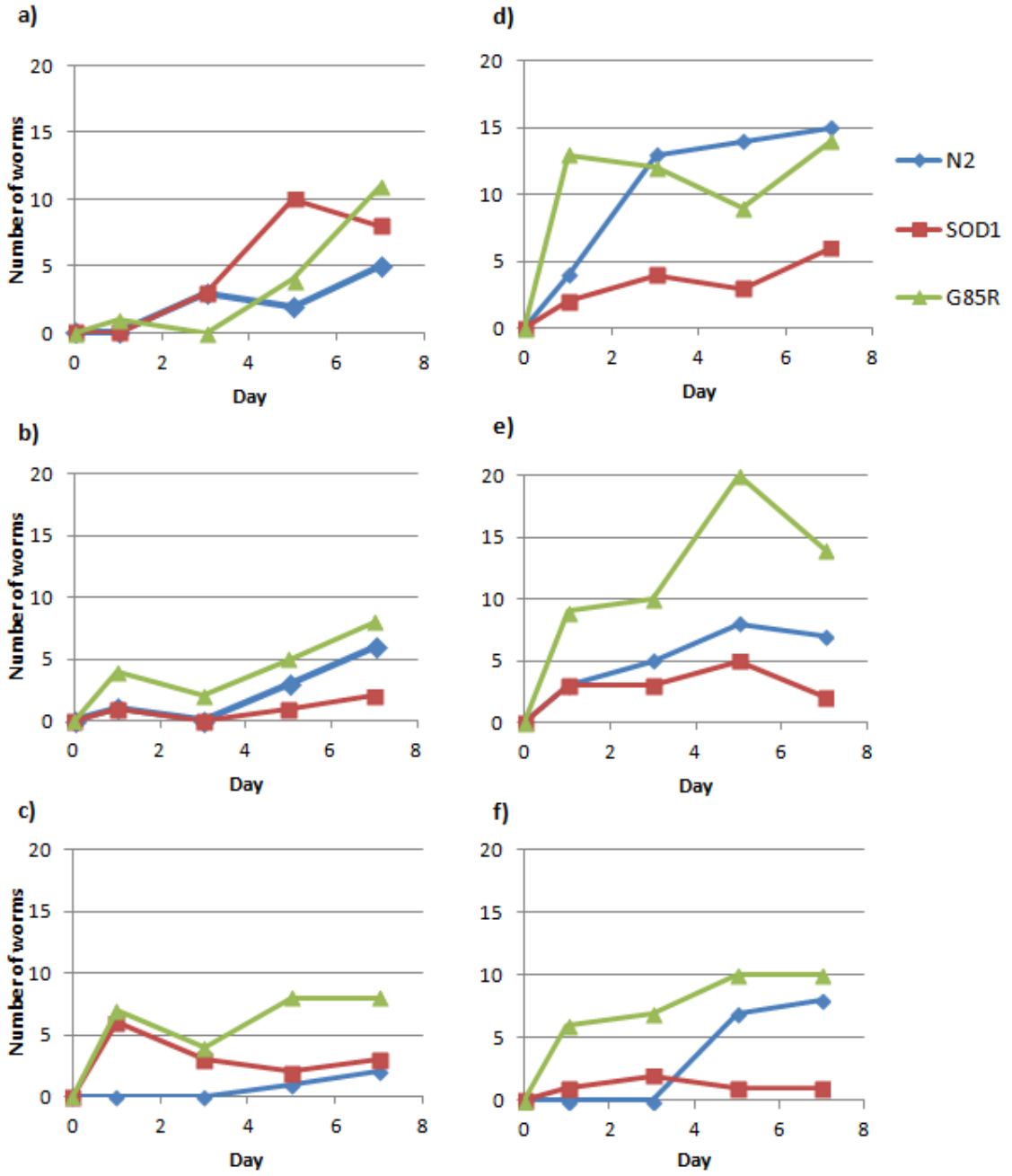

Figure 4.11: Frequency of vulval defects in *C. elegans* strains grown on leucine-supplemented media. Experiments **a) to c)** show A-scored worms grown at 20°C on NGM media supplemented with: **a)** 1mM leucine, **b)** 2mM leucine, **c)** 5mM leucine; Experiments **d) to f)** show A-scored worms grown at 25°C on NGM media supplemented with: **d)** 1mM leucine, **e)** 2mM leucine and **f)** 5mM leucine.

4.5 Discussion

4.5.1 Leucine is able to improve functional defects caused by mutant SOD1 expression.

In a study by Wang et al. (2009), it was reported that expression of mutant human SOD1 G85R protein caused paralysis of *C. elegans*. The evidence presented in this chapter supports this finding, showing motor defects in the G85R strain and to a lesser extent in the SOD1 over-expressing strain, although the motor defective phenotype (Figure 4.7b) was only exhibited in the G85R strain suggesting a paralyzing effect specific to the mutant protein. Furthermore, lifespan was significantly reduced in G85R mutant worms (Table 4.1). It was also discovered in this project that upon addition of leucine to G85R worms, their motor defects showed signs of improvement, in some cases motility was restored to that of the N2 strain. However, this was not supported by thrashing data from the Morgan group. In a similar trend to the motor defects, it was found that vulval defects are exhibited in G85R worms but less so in the SOD1 over-expressing strain, and can be improved by leucine supplementation; these findings support evidence by Bastow (2013) that leucine supplementation could also rescue growth defects in yeast caused by expression of SOD1 mutants. Leucine is well known as a regulator of metabolic signalling, particularly in the TOR pathway nutrient sensing pathway (Lynch, 2001). Its apparent role in improving mutant Sod1p-mediated defects in *C. elegans* as described here suggests mutant SOD1 may be exerting toxicity through a pathway related to metabolic or amino acid signalling.

4.5.2 The role of SOD1 G85R mutant in *C. elegans* reproductive defects and stress response.

During the motility experiments, it was noted that a number of G85R mutant worms appeared to have died with internally hatched larvae, a phenomenon that did not occur in either SOD1 over-expressing or N2 strains. Trent, Tsung and Horvitz (1983) described types of egg laying mutants that showed internal hatching of larvae, and categorised them into three phenotypes: muscle defective mutants that also exhibit paralysis, vulvaless mutants and dauer-constitutive mutants that form dauers under normal, non stress conditions. Considering the incidence of protruding vulvae in G85R worms, it would be a plausible suggestion that mutant SOD1 may also cause egg laying

defects in *C. elegans*. On the other hand, Chen and Caswell-Chen (2003) suggested that internal hatching of larvae (or intra-uterine hatching) is also a constitutive stress response in which the hermaphrodite mother retains eggs when under starvation conditions in order for progeny to use its body as a food source and allow them to transition to dauer stage and aid their survival, in a process termed 'matricide'. In the study, it was reported that this process was reversible by addition of food, provided the progeny had not fatally damaged the mother. Mosser, Matic and Leroy (2011) similarly suggest that internal hatching may be a way of protecting young larvae from unfavourable environments. Considering G85R worms were the only strain to exhibit this phenotype and growth conditions were not unfavourable, it may suggest expression of the mutant hSOD1 protein causes stress to the worms resulting in the egg-retention stress response. A logical interpretation may be that oxidative damage as a result of disrupted SOD functioning may be causing stress in mutant worms, however previous evidence has concluded that mitochondrial oxidative stress is not a determining factor in the occurrence of *C. elegans* matricide (Pestov, Shakhparonov and Kornienko, 2011). This may imply that if mutant SOD1 is indeed causing stress-induced *C. elegans* egg retention and matricide, it may be by an additional mechanism that is a result of mutant SOD1 gain of function. More thorough investigation would be required to assess whether mutant SOD1 is a causative factor in internal hatching of larvae.

Chapter 5

Final Discussion

5.1 Developing a model of SOD1-mediated toxicity

In recent years, it has been proposed that fALS-associated SOD1 mutants exhibit toxic effects through a gain of function, not simply loss of SOD activity (Gurney et al., 1994; Wang et al., 2005). In the yeast system described in chapter 3 of this project, the results portrayed how some truncated SOD1 proteins that had no SOD activity in NBT assays caused growth defects in cells expressing them, showing a greater degree of growth defects than cells expressing no *SOD1* whatsoever (Figure 3.3); this supports the idea that a gain of function is responsible for toxicity by truncated SOD1 proteins by the same mechanism as mutant Sod1p. In contrast, the longest protein fragment Sod1p$^{1-125}$ when fused to GFP did show SOD activity and was also no longer toxic to cells (Figure 3.8; Figure 3.6), the opposite to the effects observed in active SOD1 mutants such as G37R, which retain SOD activity but still exert toxicity (Lobsiger et al., 2007); when not fused to GFP, Sod1p$^{1-125}$ lost its SOD activity but exhibited the greatest toxic effect of all the truncated proteins (Figure 3.5; Figure 3.3). This evidence suggests that truncated wild type SOD1 proteins do not cause toxicity by the same mechanism as mutant SOD1 proteins and implies fragmentation of the protein is not the sole cause of toxicity, contrary to the hypothesis proposed by Ghadge et al. (2006). This is further supported by the finding that expression of truncated SOD1 proteins in yeast does not cause a significant reduction in viability as determined by statistical analysis (Figure 3.9) even in those shown to impair cell growth, whereas expression of human SOD1 G85R mutant in transgenic *C. elegans* does cause a reduction in lifespan (Figure 4.2). Nevertheless, both yeast and worm models presented developmental or functional defects independent of their effects on survival, in yeast this being portrayed by growth impairment and in worms, vulval defects and apparent motor dysfunction.

5.2 ALS models show varying mechanisms of toxicity

One of the aims of this project was to elucidate whether truncated wild type SOD1 proteins would exhibit the same toxic effects as mutant versions of the protein, and in this manner, determine whether the degradation of mutant Sod1p into peptide fragments was causing the pathological changes observed in ALS organisms.

Ghadge et al. (2006) reported truncated SOD1 expression in chick embryo spinal cord neural cells formed cytoplasmic aggregates and caused cells death, the same mechanism by which mutant SOD1 exerted toxicity. In this project, it has been shown that longer truncated SOD1 proteins cause cellular defects in yeast, resulting in significantly slowed growth; this was mirrored in the worm model, which exhibited motor and vulval defects in mutant worms that were not exhibited to the same extent by over-expression of wild type SOD1. However, defects caused by truncated Sod1p did not reduce viability of yeast, whereas mutant SOD1 expression did reduce lifespan of worms. It is unclear if despite reducing lifespan in worms, the affected motor neurones are actually killed prematurely as a result of mutant SOD1 expression. Indeed, Wang et al. (2009) reported toxic mutant SOD1 expression to cause motor defects but did not cause early death of motor neurones. A similar finding has been demonstrated in *Drosophila* (Watson et al., 2008). As such, this may suggest a similar mechanism occurring in both truncated SOD1-mediated toxicity in yeast and mutant SOD1-mediated toxicity in worms, characterised by defective cellular functioning but not premature death.

Furthermore, expression of truncated Sod1p in yeast did not lead to formation of mitochondrial aggregates, while expression of both truncated and mutant Sod1p in chick embryo spinal cords was shown to form cytoplasmic aggregates (Ghadge et al., 2006). Animal models have demonstrated increased localisation of mutant Sod1p to mitochondria (Vehviläinen et al., 2014) and *C. elegans* models exhibit accumulation of both soluble mutant SOD1 oligomers and insoluble aggregates in motor neurones (Wang et al., 2009). The fact that a toxic effect is observed on cells even with inconsistent or no aggregation may indicate insoluble aggregate formation is not a cause of toxicity.

5.3 Soluble mutant SOD1 proteins may disrupt mitochondrial function

Localisation studies looking at fluorescently-tagged truncated SOD1 proteins indicated that the fragments do not specifically localise to mitochondria or form aggregates (Figure 3.10). However, significant evidence suggests that toxicity is not necessarily caused by aggregate formation. Ayers et al. (2014) showed that SOD1 D101N, I113T and L144F mutants caused rapidly progressing diseased states despite having low

tendencies to form aggregates, while further studies have suggested misfolded soluble Sod1p mutants are more toxic than mutants that form insoluble aggregates (Brotherton et al., 2012; Karch et al., 2009; Weichert et al., 2014; Zetterström et al., 2007). Much recent evidence has alluded to the association of mutant Sod1p with mitochondria; antibodies specific for misfolded Sod1p showed mutant Sod1p association with mitochondrial in spinal cords of rodents (Brotherton et al., 2012; Velde et al., 2008), and spinal cords of ALS mice were found to have high levels of misfolded soluble mutant Sod1p, the conformation of which would allow translocation into mitochondria (Zetterström et al., 2007). Furthermore, Wang et al. (2005) discovered that some SOD1 mutants expressed in mice showed association with spinal cord motor neurones but not distal fibres, suggesting mutant SOD1 could exert neuronal toxicity without directly interacting with the axon. It is possible that this may also be the case for truncated SOD1 proteins, which may be exerting mitochondrial toxicity through indirect interaction and may also be soluble proteins, hence why aggregate formation is not observed. However, the results showed that expression of mutant and truncated forms of Sod1p does not impair mitochondrial respiratory metabolism (Figure 3.14), suggesting mitochondrial toxicity may not be the main mechanism by which these proteins cause defective cell growth. Further work on this area could focus on investigating organelle-specific localisation of soluble truncated SOD1 proteins in yeast to determine whether it is causing mitochondrial toxicity.

5.4 The Wnt signalling pathway plays a role in SOD1-mediated toxicity

The Wnt signalling pathway is highly evolutionarily conserved in animals and remains similar even between fruit flies and humans (Inoki et al., 2006). It has roles in the regulation of a wide range of signalling pathways and is involved in organogenesis, cell fate determination and stem cell renewal in animals. Activation of the Wnt pathway begins through a Wnt protein binding to transmembrane Frizzled (Fz) receptors then signal transduction to cytosolic Dishevelled (Dsh) protein (Logan and Nusse, 2004); after activation by ligands, the Wnt signal branches into three major signalling cascades, the Wnt/β-catenin dependent (canonical) pathway or Wnt/β-catenin independent (non-canonical) Planar Cell Polarity and Wnt/Ca2+ pathways. In the

Wnt/β-catenin dependent pathway, accumulation of β-catenin acts as a co-activator of transcription factors in the nucleus.

Wnt signalling is known to play an essential role in embryonic and cell development and disruption of the pathway has been discovered to cause birth defects, most notably spina bifida; defective signalling is also implicated in development of many types of cancer in addition to skeletal defects (Logan and Nusse, 2004). More recent evidence has established a link between decreased Wnt signalling and neurodegenerative diseases including Alzheimer's and Parkinson's (Inestrosa and Arenas, 2010; L'Episcopo et al., 2011). Further research into ALS mice indicates altered expression of Wnt signalling molecules within motor neurones (Chen et al., 2012; Li et al., 2013; Wang et al., 2013), while Pinto et al. (2013) portrayed how an ALS model consisting of NSC-34 motor neurone-like mouse hybrid cells expressing human G93A SOD1 mutation showed inhibited Wnt/β-catenin dependent transcription but upregulation of BMP/Smad-dependent transcription. Upregulation of the Wnt signalling pathway has also shown a protective function in multiple Alzheimer's disease models (Alvarez et al., 2004; Cerpa et al., 2010; De Ferrari et al., 2003; Purro et al., 2012). In vitro studies showed chemical upregulation of the Wnt pathway by lithium chloride lead to an increase in β-catenin and increased neuronal survival in an Alzheimer's disease model (Alvarez et al., 2004; De Ferrari et al., 2003).

Both canonical and non-canonical Wnt pathways also exist in *C. elegans* although there are some notable differences; in particular, the functioning of β-catenin is shared between three homologues in worms, BAR-1, WRM-1 and HMP-2 (Korswagen et al., 2000; Natarajan et al., 2001). Evidence suggests that the canonical pathway in worms using β-catenin homologue BAR-1 functions similarly to the canonical pathway in other animals, however pathways using β-catenin homologue WRM-1 function non-canonically, but differ from non-canonical pathways in other animals, while further evidence has implicated the canonical Wnt/BAR-1 pathway in *C. elegans* vulval development. Three types of vulval precursor cells (VPCs) are responsible for development of the *C. elegans* vulva. Vulval development occurs through these main stages that are regulated by various genes; the first stage is creation of VPCs, followed by fate determination of the VPCs and their proper development and differentiation into these fated cells, and finally vulval morphogenesis (Eisenmann, 2005). The

discovery that two of the genes involved in fate determination of VPCs, bar-1 and mom-3/mig-14, also have roles in the Wnt signalling pathway lead to the conclusion that the Wnt pathway may be involved in *C. elegans* vulval development (Eisenmann and Kim, 2000). Vulval development mutant phenotypes often exhibit characteristics of hermaphrodites that are unable to lay eggs or show defects such as protruding vulvae or vulval eversion (Sternberg, 2005). When expressing SOD1 G85R mutant in *C. elegans*, it was observed that a number died from internal hatching of larvae in addition to vulval defects; Results 4.5.2 briefly discussed the possible implications of this egg retention, including egg-laying defects and stress-induced egg retention. However, these mutant worms remained fertile and most were able to lay eggs. One hypothesis was that mutant worms may be physiologically defective and exhibit vulval and egg laying defects due to disrupted development of VPCs in forming the egg laying system. BAR-1 is known to be involved in specification of vulval precursor cell fates in *C. elegans* by regulation of LIN-39, which is first required during L1 larval stage specification of cells into VPCs rather than F fate cells which are no longer able to form part of the vulva (Eisenmann et al., 1998). Partial reduction of LIN-39 activity by mutation allows some of the ventral epidermal Pn.p cells to develop into VPCs but exhibit specification defects. Disrupted Wnt/BAR-1 signalling by mutant SOD1 could potentially disrupt vulval cell specification by deregulation of LIN-39. Trent, Tsung and Horvitz (1983) reported that the egg laying system is made up of 18 vulval cells, 16 neurones and 16 vulval and uterine muscle cells. Of the 16 developed vulval and uterine muscle cells involved in hermaphrodite egg laying, removal of all 8 uterine muscles does not cause a significant defect in egg laying, neither does removal of the four vm1 vulval muscles (Schafer, 2005); however, removal of the four vm2 vulval muscles stops egg laying completely, suggesting these muscles are required for contraction and opening of the vulva to facilitate egg laying. G85R worms do not show severe egg laying defects, but it may be that development of vulval or uterine muscles are affected by mutant SOD1 expression through disruption of BAR-1 signalling in the Wnt pathway.

An alternative hypothesis was that mutant worms were retaining eggs in response to stress; it was previously noted that the G85R mutant strain showed more progeny hatching and developing than other strains, suggesting reduced feeding and reduced

uptake of FUDR progeny growth inhibitor. Evidence has shown that vulval induction, which occurs in L3 stage larvae, can be repressed by starvation conditions and is mediated by SRA-13 through the RAS/MAPK pathway (Battu et al., 2003). This suggests a potential alternative reason for the internal hatching of larvae observed in G85R worms, which may have not have fully developed vulvae during larval stages as a result of decreased feeding ability, leading to egg retention and internal hatching. Thorough quantification of egg bloated and defective egg laying worms in a mutant SOD1 strain would need to be performed to draw any definitive conclusions.

The Wnt pathway also functions to regulate mTOR nutrient sensing and protein synthesis pathway (mTOR pathway detailed in Chapter 1). Activation of the Wnt signalling pathway leads to inhibition of GSK3 which in turn is then unable to phosphorylate TSC2. Active TSC2 is then able to activate the mTOR nutrient sensing and signalling pathway ultimately leading to protein synthesis and cell growth. An interaction between fALS-associated SOD1 mutants and the TOR pathways has already been established in yeast by Bastow (2013) and also in mice (Morimoto et al., 2007). The results discussed in Chapter 4 illustrate the occurrence of protruding vulva and egg-laying defective mutants in *C. elegans* expressing fALS-associated SOD1 G85R mutant, which supports the growing body of evidence portraying disruption of the Wnt pathway as a mechanism of mutant SOD1-mediated toxicity. Furthermore, not only motility defects but also vulval defects in G85R worms can be improved by supplementation of leucine, a potent activator of the TOR pathway (Results 4.3; Results 4.4); this implies impaired nutrient sensing or amino acid uptake regulated by the TOR signalling pathway, a downstream effect of Wnt signalling disruption. As TOR signalling is responsible for regulating protein synthesis and cell growth, disruption of the Wnt pathway and downstream effects on TOR signalling may also explain the decrease in lifespan observed in G85R worms. However, the Wnt pathway only exists in animals, indicating there is an alternative mechanism of SOD1-mediated toxicity occurring in yeast.

5.5 Truncated and mutant SOD1 deregulate amino acid signalling

A recent study investigating ALS in mice found that SOD1 G93A mutants showed abnormal blood plasma amino acid profiles and that and treatment with an inhibitor of

glutamine synthetase, an enzyme involved in amino acid metabolism, was able to normalise these abnormalities and increase lifespan of mutant mice (Bame et al., 2014). It was suggested that this deregulation of amino acid levels may provide insight into the biochemical basis of ALS. In chapter 3, the role of yeast vacuolar amino acid transporters in SOD1-mediated toxicity was investigated. It was shown by Mass Spectrometry data that free amino acid levels were perturbed in amino acid transporter deletion strain as expected, but also in a *SOD1* deletion strain (Results 3.7.4), suggesting SOD1 may be involved in amino acid regulation. It was also demonstrated that truncated SOD1 proteins appear to have a synthetic effect on vacuolar amino acid transporters, exhibiting growth defects in some amino acid transporter deletion strain (Figure 3.13). From these results, it was suggested that truncated Sod1p may be interacting with the transporters and causing toxicity by blocking amino acid transport; this could also contribute to the disrupted TOR signalling described by Bastow (2013) when expressing SOD1 mutants. In addition to this, although growth defects were clearly demonstrated, there was no significant reduction in the viability of yeast expressing truncated Sod1p. This suggests amino acid transport is not completely inhibited by truncated Sod1p expression but rather blocked or defective, or the cells would likely exhibit premature death. Bastow (2013) reported that supplementation of leucine was able to significantly improve growth defects observed in yeast expressing SOD1 mutants, concluding mutant SOD1 was causing toxicity through defective leucine biosynthesis. However, the finding was not replicable in this project when G85R mutant worms were supplemented with increasing concentrations of leucine. Although optimal concentrations of leucine appeared to improve motor function and vulval defects, defects were not reduced to the level of the N2 control worms. Furthermore, leucine was readily available in the media even without supplementation, suggesting firstly that amino acid uptake into cells may be impaired and also that leucine supplementation is not able to eradicate the toxicity induced by mutant SOD1 and that there is an addition mechanism of toxicity at work; in worms, this may be the disrupted Wnt pathway, deregulating TOR signalling as a downstream effect. It is also possible that by a similar mechanism to that observed in yeast, the animal equivalent of a vacuole, the lysosome, may be affected by mutant Sod1p specifically by interfering with vacuolar/lysosomal amino acid influx or efflux and disrupting the nutrient composition of other areas of the cell.

This disruption would also deregulate TOR nutrient sensing, where supplementation of leucine may improve the observed defects in worms by upregulating TOR signalling rather than curing the toxicity.

5.6 Conclusions and future work

Yeast vacuole transporter model.

Following these results, a yeast model is proposed which suggests that the digestion of mutant Sod1p into peptide fragments disrupts TOR signalling leading to reduced ability of the cell to sense nutrient availability, thus it takes up more tyrosine and less lysine than required (Results 3.4) and amino acid auxotrophies are exhibited. It is also possible that mutant Sod1p disrupts lysine biosynthesis within the cell leading to this auxotrophy. The model also proposes that mutant Sod1p interferes with vacuolar amino acid transport, leading to amino acid trapping in compartments of the cell, potentially inhibiting accurate nutrient sensing by TOR and exacerbating the problem of deregulated amino acid uptake and utilization (Figure 5.1).

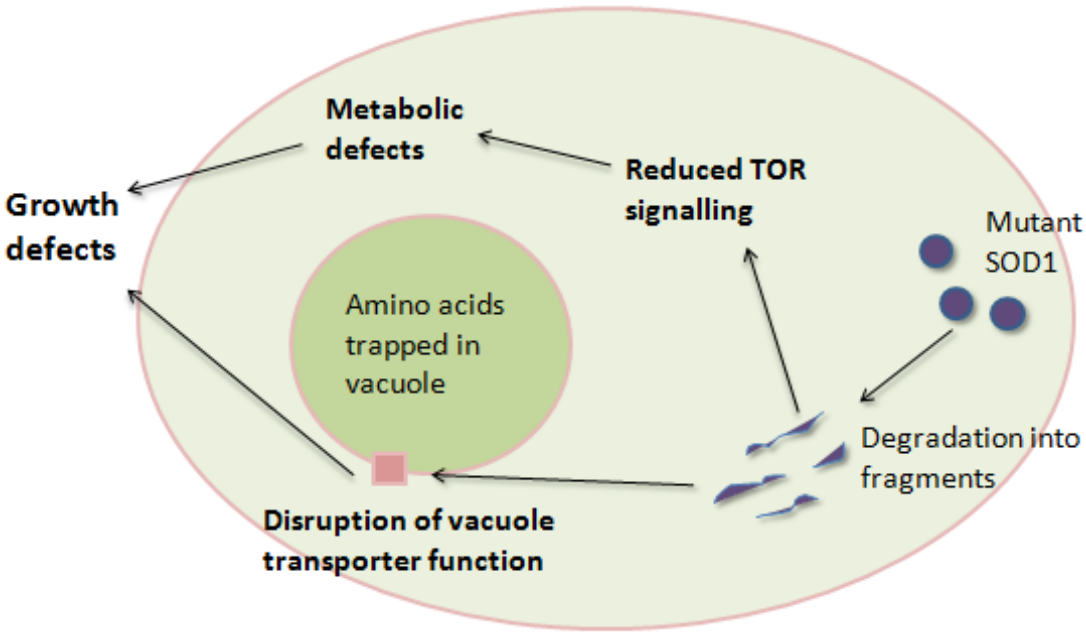

Figure 5.1: Yeast model of mutant SOD1-mediated toxicity.

Worm Wnt pathway model.

The second model proposes that in *C. elegans*, mutant Sod1p exerts its toxic effect through disruption of the canonical Wnt/BAR-1 signalling pathway leading to vulval

development defects and also impaired TOR signalling. Lysosomal amino acid transport may also be disrupted. As with the yeast model, impaired TOR signalling may lead to amino acid auxotrophies and growth defects that can be improved by upregulation of the TOR pathway by leucine addition.

Future work.

Following on from the findings presented in this project, better insight into the hypothesised mechanisms could be provided through these additional experiments:

- Wang et al. (2009) discovered that GFP fused SOD1 mutants showed altered activity in *C. elegans* compared to their non-fused counterparts, and the same was also shown in this project when expressing truncated SOD1 proteins in yeast. Future work should include expression of non-YFP fused SOD1 mutant and wild type proteins in *C. elegans* to determine how this affects their toxic effects.
- Perform lifespan and motility assays using genetically out-crossed SOD1 G85R and wild type SOD1 strains that have the same genetic background as the N2 controls.
- Truncated Sod1p fragments should be expressed in worms to see if they also cause the same defects as SOD1 mutants, and whether they cause motor neurone death as observed in chick embryo neural cells by Ghadge et al. (2006).
- Chemical upregulation of the Wnt signalling pathway in *C. elegans* using lithium chloride could be used to determine whether it reduces toxic effects on the organism, including motility or vulval defects.

Further research question include:

- Does mutant SOD1 cause motor defects in C. elegans through death or dysfunction of motor neurones?
- Does leucine supplementation increase mutant *C. elegans* lifespan?
- Is matricide a result of stress or egg-laying vulval defects caused by mutant SOD1 expression?

References

Aitlhadj, L., Stürzenbaum , S. R. 2010. *The use of FUdR can cause prolonged longevity in mutant nematodes*. Mechanisms of Ageing and Development. 131(5): 364-365.

Amyotrophic Lateral Sclerosis (ALS) Fact Sheet. 2013 [cited 2013 October]. National Institute of Neurological Disorders and Stroke Available from: http://www.ninds.nih.gov/disorders/amyotrophiclateralsclerosis/detail_ALS.htm.

Alvarez, A.R., Godoy, J.A., Mullendorff, K., Olivares, G.H., Bronfman, M., Inestrosa, N.C. 2004. *Wnt-3a overcomes β-amyloid toxicity in rat hippocampal neurons*. Experimental Cell Research. 297(1): 186-196.

Ash, P.E., Zhang, Y.J., Roberts, C.M., Saldi, T., Hutter, H., Buratti, E., Petrucelli, L., Link, C.D. 2010. *Neurotoxic effects of TDP-43 overexpression in C. elegans*. Human Molecular Genetics. 19(16): 3206-3218.

Askwith, C., Kaplan, J. 1998. *Iron and copper transport in yeast and its relevance to human disease*. Trends in Biochemical Sciences. 23(4): 135-138.

Avruch, J., Long, X., Ortiz-Vega, S., Rapley, J., Papageorgiou, A., Dai, N. 2009. *Amino acid regulation of TOR complex 1*. American Journal of Physiology - Endocrinology and Metabolism. 296(4): 592-602.

Ayers, J., Lelie, H., Workman, A., Prudencio, M., Brown, H., Fromholt, S., Valentine, J., Whitelegge, J., Borchelt, D. 2014. *Distinctive features of the D101N and D101G variants of superoxide dismutase 1; two mutations that produce rapidly progressing motor neuron disease*. Journal of Neurochemistry. 128(2): 305-314.

Baars, T.L., Petri, S., Peters, C., Mayer, A. 2007. *Role of the V-ATPase in regulation of the vacuolar fission-fusion equilibrium*. Molecular Biology of the Cell. 18(10): 3873–3882.

Bame, M., Grier, R.E., Needleman, R., Brusilow, W.S.A. 2014. *Amino Acids as biomarkers in the SOD1G93A mouse model of ALS.* Biochimica et Biophysica Acta. 1842(1): 79-87.

Bastow, E.L., Gourlay, C.W., Tuite, M.F. 2011. *Using yeast models to probe the molecular basis of amyotrophic lateral sclerosis*. Biochemical Society Transactions. 39(5): 1482-1487.

Bastow, E.L. 2013. *Developing a yeast model of amyotrophic lateral sclerosis (ALS),* in School of Biosciences. PhD Thesis, University of Kent: Canterbury.

Battu, G., Hoier, E.F., Hajnal, A. 2003. *The C. elegans G-protein-coupled receptor SRA-13 inhibits RAS/MAPK signalling during olfaction and vulval development*. Development. 130: 2567-2577.

Bleackley, M.R., MacGillivray, R.T.A. 2011. *Transition metal homeostasis: from yeast to human disease*. BioMetals. 24(5): 785-809.

Bossy-Wetzel, E., Petrilli, A., Knott, A.B. 2008. *Mutant huntingtin and mitochondrial dysfunction*. Trends in Neurosciences. 31(12): 609–616.

Boyd-Kimball, D., Poon, H.F., Lynn, B.C., Pierce, W.M., Klein, J.B., Ferguson, J., Link, C. D., Butterfield, D.A. 2006. *Proteomic identification of proteins specifically oxidized in Caenorhabditis elegans expressing human Abeta(1-42): implications for Alzheimer's disease*. Neurobiology of Aging. 27(9): 1239-1249.

Brasil, A.A., Belati, A., Mannarino, S.C., Panek, A.D., Eleutherio, E.C., Pereira, M.D. 2013. *The involvement of GSH in the activation of human Sod1 linked to FALS in chronologically aged yeast cells*. FEMS Yeast Research. 13(5): 433-440.

Braun, R.J. 2012. *Mitochondrion-mediated cell death: dissecting yeast apoptosis for a better understanding of neurodegeneration*. Frontiers in Oncology. 2: 182.

Brotherton, T.E., Li, Y., Cooper, D., Gearing,, M., Julien J.-P., Rothstein, J.D., et al. 2012. *Localization of a toxic form of superoxide dismutase 1 protein to pathologically affected tissues in familial ALS.* Proceedings of the National Academy of Sciences of the United States of America. 109(14): 5505–5510.

Campesan, S., Green, E.W., Breda, C., Sathyasaikumar, K.V., Muchowski, P.J., Schwarcz, R., et al. 2011. *The kynurenine pathway modulates neurodegeneration in a Drosophila model of Huntington's disease*. Current Biology. 21(11): 961–966.

Cerpa, W., Farias, G.G., Godoy, J.A., Fuenzalida, M., Bonansco, C., Inestrosa, N.C. 2010. *Wnt-5a occludes Abeta oligomer-induced depression of glutamatergic transmission in hippocampal neurons*. Molecular Neurodegeneration. 5: 3.

Chang, E.C., Kosman, D.J. 1990. *O2-dependent methionine auxotrophy in Cu,Zn superoxide dismutase-deficient mutants of Saccharomyces cerevisiae*. Journal of Bacteriology. 172(4): 1840-1845.

Chen, J., Caswell-Chen, E.P. 2003. *Why Caenorhabditis elegans adults sacrifice their bodies to progeny*. Nematology. 5(4): 641-645.

Chen, Y., Guan, Y., Zhang, Z., Liu, H., Wang, S., Yu, L., Wang, X. 2012. *Wnt signaling pathway is involved in the pathogenesis of amyotrophic lateral sclerosis in adult transgenic mice*. Neurological Research. 34(4): 390-399.

Chen, H., Qian, K., Du, Z., Cao, J., Petersen, A., Liu, H., et al. 2014. *Modeling ALS with iPSCs reveals that mutant SOD1 misregulates neurofilament balance in motor neurons*. Cell Stem Cell. 14(6): 796-809.

Cheng, W.C., Leach, K.M., Hardwick, J.M. 2008. *Mitochondrial death pathways in yeast and mammalian cells.* Biochimica et Biophysica Acta. 1783: 1272–1279.

Cherry, J.M., Hong, E.L., Amundsen, C., Balakrishnan, R., Binkley, G., Chan, E.T., Christie, K.R., Costanzo, M.C., Dwight, S.S., Engel, S.R., Fisk, D.G. et al. 2012. *Saccharomyces Genome Database: the genomics resource of budding yeast.* Nucleic Acids Research. Jan;40(Database issue):D700-5.

Cobine, P.A., Pierrel, F., Bestwick, M.L., Winge, D.R. 2006. *Mitochondrial matrix copper complex used in metallation of cytochrome oxidase and superoxide dismutase*. Journal of Biological Chemistry. 281(48): 36552-36559.

Correia, S.C., Santos, R.X., Perry, G., Zhu, X., Moreira, P.I., Smith, M.A. 2012. *Mitochondrial importance in Alzheimer's, Huntington's and Parkinson's diseases*. Advances in Experimental Medicine and Biology. 724: 205–221.

Corson, L.B., Folmer, J., Strain, J.J, Culotta, V.C., Cleveland, D.W. 1999. *Oxidative stress and iron are implicated in fragmenting vacuoles of Saccharomyces cerevisiae lacking Cu,Zn-superoxide dismutase*. The Journal of Biological Chemistry. 274(39): 27590-27596.

Cozzolino, M., Pesaresi, M.G., Amori, I., Crosio, C., Ferri, A., Nencini, M., Carrì, M.T. 2009. *Oligomerization of mutant SOD1 in mitochondria of motoneuronal cells drives mitochondrial damage and cell toxicity*. Antioxidants and Redox Signaling. 11(7): 1547-1558.

De Ferrari, G.V., Chacón, M.A., Barría, M.I., Garrido, J.L., Godoy, J.A., Olivares, G., Reyes, A.E., Alvarez, A., Bronfman, M., Inestrosa, N.C. 2003. *Activation of Wnt signaling rescues neurodegeneration and behavioral impairments induced by β-amyloid fibrils*. Molecular Psychiatry. 8: 195-208.

Devaney, E. 2006. *Thermoregulation in the life cycle of nematodes. International* Journal for Parasitology. 36(6):641-649.

Eisenmann, D.M., Maloof, J.N., Simske, J.S., Kenyon, C., Kim, S.K. 1998. *The beta-catenin homolog BAR-1 and LET-60 Ras coordinately regulate the Hox gene lin-39 during Caenorhabditis elegans vulval development*. Development. 125: 3667-3680.

Eisenmann, D.M., Kim, S.K. 2000. *Protruding Vulva Mutants Identify Novel Loci and Wnt Signaling Factors That Function During Caenorhabditis elegans Vulva Development.* Genetics Society of America. 156(3): 1097-1116.

Eisenmann, D. M. (June 25, 2005) *Wnt signaling* WormBook, ed. The C. elegans Research Community, WormBook. doi/10.1895/wormbook.1.7.1, http://www.wormbook.org.

Ellis, C.D., Wang, F., MacDiarmid, C.W., Clark, S., Lyons, T., Eide, D.J. 2004. *Zinc and the Msc2 zinc transporter protein are required for endoplasmic reticulum function*. Journal of Cell Biology. 166(3): 325-335.

Feany, M.B., Bender, W.W. 2000. *A Drosophila model of Parkinson's disease*. Nature. 404(6776): 394-398.

Ferri, A., Fiorenzo, P., Nencini, M., Cozzolino, M., Pesaresi, M.G., Valle, C., et al. 2010. *Glutaredoxin 2 prevents aggregation of mutant SOD1 in mitochondria and abolishes its toxicity*. Human Molecular Genetics. 19(22): 4529–4542.

Furukawa, Y., Torres, A.S., O'Halloran, T.V. 2004. *Oxygen-induced maturation of SOD1: a key role for disulfide formation by the copper chaperone CCS*. The EMBO Journal. 23: 2872-2881.

Ghadge, G.D., Wang, L., Sharma, K., Monti, A.L., Stevens, F.J., Roos, R.P. 2006. *Truncated wild-type SOD1 and FALS-linked mutant SOD1 cause neural cell death in the chick embryo spinal cord*. Neurobiology of Disease. 21(1): 194-205.

Gidalevitz T., Krupinski T., Garcia S., Morimoto R. I. 2009. *Destabilizing protein polymorphisms in the genetic background direct phenotypic expression of mutant SOD1 toxicity.* PLoS Genetics. 5(3): e1000399.

Giorgini, F., Moller, T., Kwan, W., Zwilling, D., Wacker, J.L., Hong, S., et al. 2008. *Histone deacetylase inhibition modulates kynurenine pathway activation in yeast, microglia, and mice expressing a mutant huntingtin fragment*. The Journal of Biological Chemistry. 283(12): 7390–7400.

Gurney, M.E., Pu, H., Chiu, A.Y., Dal Canto, M.C., Polchow, C.Y., Alexander, D.D., et al. 1994. *Motor neuron degeneration in mice that express a human Cu, Zn superoxide dismutase mutation*. Science 264(5166): 1772–1775.

Hartwell, L.H. 2004. *Yeast and cancer*. Bioscience Reports. 24(4-5): 523-544.

Hu, P.J. (August 08, 2007) *Dauer*. WormBook, ed. The C. elegans Research Community, WormBook, DOI: 10.1895/wormbook.1.144.1.

Inestrosa, N.C., Arenas, E. 2010. *Emerging roles of Wnts in the adult nervous system.* Nature Reviews Neuroscience. 11(2): 77-86.

Inoki, K., Ouyang, H., Zhu, T., Lindvall, C., Wang, Y., Zhang, X., Yang, Q., Bennet, B. 2006. *TSC2 integrates Wnt and energy signals via a coordinated phosphorylation by AMPK and GSK3 to regulate cell growth*. Cell. 126(5): 955-968.

Johnston, J.A., Dalton, M.J., Gurney, M.E., Kopito, R.R. 2000. *Formation of high molecular weight complexes of mutant Cu,Zn-superoxide dismutase in a mouse model*

for familial amyotrophic lateral sclerosis. Proceedings of the National Academy of Sciences of the Unites States of America. 97(23): 12571–12576.

Jones, E.W., Zubenko, G.S., Parker, R.R. 1982. *PEP4 gene function is required for expression of several vacuolar hydrolases in Saccharomyces cerevisiae*. Genetics. 102 (4): 665–77.

Jonsson, P.A., Graffmo, K.S., Brännström, T., Nilsson, P., Andersen, P.M., Marklund, S.L. 2006. *Motor neuron disease in mice expressing the wild type-like d90a mutant superoxide dismutase-1*. Journal of Neuropathology and Experimental Neurology. 65(12): 1126–1136.

Karch, C.M., Prudencio, M., Winkler, D.D., Hart, P.J., Borchelt, D.R. 2009. *Role of mutant SOD1 disulfide oxidation and aggregation in the pathogenesis of familial ALS*. Proceedings of the National Academy of Sciences of the United States of America. 106(19): 7774–7779.

Kawamata, H., Manfredi, G. 2010. *Import, maturation, and function of SOD1 and its copper chaperone CCS in the mitochondrial intermembrane space*. Antioxidants and Redox Signalling. 13(9): 1375-1384.

Korswagen, H.C., Herman, M.A., Clevers, H.C. 2000. *Distinct β-catenins mediate adhesion and signalling functions in C. elegans*. Nature. 406(6795): 527–532.

Kuwahara, T., Koyama, A., Koyama, S., Yoshina, S., Ren, C., Kato, T., Mitani, S., Iwatsubo, T. 2008. *A systematic RNAi screen reveals involvement of endocytic pathway in neuronal dysfunction in α-synuclein transgenic C. elegans*. Human Molecular Genetics. 17(19): 2997-3009.

Kwon, E-S., Jeong, J-H., Roe, J-H. 2006. *Inactivation of Homocitrate Synthase Causes Lysine Auxotrophy in Copper/Zinc-containing Superoxide Dismutase-deficient Yeast Schizosaccharomyces pombe*. Journal of Biological Chemistry. 281(3): 1345-1351.

Lai, C. H., Chou, C. Y., Ch'ang, L. Y., Liu, C. S., and Lin, W. 2000. *Identification of novel human genes evolutionarily conserved in Caenorhabditis elegans by comparative proteomics*. Genome Research. 10(5): 703–713.

Lakso M., Vartiainen S., Moilanen A. M., Sirviö J., Thomas J. H., Nass R., et al. 2003. *Dopaminergic neuronal loss and motor deficits in Caenorhabditis elegans overexpressing human alpha-synuclein*. Journal of Neurochemistry. 86(1): 165–172.

Lamb, A.L., Torres, A.S., O'Halloran, T.V., Rozenzweig, A.C. 2001. *Heterodimeric structure of superoxide dismutase in complex with its metallochaperone*. Nature Structural Biology. 8: 751-755.

L'Episcopo, F., Tirolo, C., Caniglia, S., Testa, N., Morale, M.C., Serapide, M.F., Pluchino, S., Marchetti, B. 2011. *Targeting Wnt signaling at the neuroimmune interface for*

dopaminergic neuroprotection/repair in Parkinson's disease. Journal of Molecular Cell Biology. 6(1): 13-26.

Li, J., Huang, K., Le, W. 2013. *Establishing a novel C. elegans model to investigate the role of autophagy in amyotrophic lateral sclerosis*. Acta Pharmacologica Sinica. 34(5): 644-650.

Li J., Li T., Zhang X., Tang Y., Yang J., Le W. 2014. *Human superoxide dismutase 1 overexpression in motor neurons of Caenorhabditis elegans causes axon guidance defect and neurodegeneration*. Neurobiology of Aging. 35(4): 837–846.

Link, C.D. 1995. *Expression of human beta-amyloid peptide in transgenic Caenorhabditis elegans*. Proceedings of the National Academy of Sciences of the United States of America. 92(20): 9368-9372.

Link, C.D., Taft, A., Kapulkin, V., Duke, K., Kim, S., Fei, Q., Wood, D.E., Sahagan, B.G. 2003. *Gene expression analysis in a transgenic Caenorhabditis elegans Alzheimer's disease mode*l. Neurobiology of Aging. 24(3): 397-413.

Lobsiger, C.S., Boillée, S., Cleveland, D.W. 2007. *Toxicity from different SOD1 mutants dysregulates the complement system and the neuronal regenerative response in ALS motor neurons*. Proceedings of the National Academy of Sciences of the United States of America. 104(18): 7319-7326.

Logan, C.Y., Nusse, R. 2004. *The Wnt signaling pathway in development and disease.* Annual Review of Cell and Developmental Biology. 20: 781-810.

Longo, V.D., Gralla, E.B., Valentine, J.S. 1996. *Superoxide dismutase activity is essential for stationary phase survival in Saccharomyces cerevisiae.* Journal of Biological Chemistry. 271(21): 12275-12280.

Longo, V.D., Ellerby, L.M., Bredesen, D.E., Valentine, J.S., Gralla, E.B. 1997. *Human Bcl-2 reverses survival defects in yeast lacking superoxide dismutase and delays death of wild-type yeast*. Journal of Cell Biology. 137(7): 1581-1588.

Lynch, C.J. 2001. *Role of leucine in the regulation of mTOR by amino acids: revelations from structure-activity studies.* Journal of Nutrition. 131(3): 861-865.

Magrané, J., Hervias, I., Henning, M.S., Damiano, M., Kawamata, H., Manfredi, G. 2009. *Mutant SOD1 in neuronal mitochondria causes toxicity and mitochondrial dynamics abnormalities.* Human Molecular Genetics. 18(23): 4552-4564.

Mannarino, S.C., Vilela, L.F., Brasil, A.A., Aranha, J.N., Moradas-Ferreira, P., Pereira, M.D., Costa, V., Eleutherio, E.C. 2011. *Requirement of glutathione for Sod1 activation during lifespan extension*. Yeast. 28(1): 19-25.

Mascarenhas, C., Edwards-Ingram, L.C., Zeef, L., Shenton, D., Ashe, M.P., Grant, C.M. 2008. *Gcn4 is required for the response to peroxide stress in the yeast Saccharomyces cerevisiae*. Molecular Biology of the Cell. 19(7): 2995-3007.

Masliah, E., Rockenstein, E., Veinbergs, I., et al. 2000. *Dopaminergic loss and inclusion body formation in alpha-synuclein mice: implications for neurodegenerative disorders.* Science. 287(5456): 1265–1269.

McGoldrick, P., Joyce, P.I., Fisher, E.M.C., Greensmith, L. 2013. *Rodent models of amyotrophic lateral sclerosis*. Biochimica et Biophysica Acta. 1832(9): 1421-1436.

Michaillat, L., et al. 2012. *Cell-free reconstitution of vacuole membrane fragmentation reveals regulation of vacuole size and number by TORC1*. Molecular Biology of the Cell. 23(5): 881-895.

Morimoto, N., Magai, M., Ohta, Y., Miyazaki, K., Kurata, T., Morimoto, M., Murakami, T., Takehisa, Y., Ikeda, Y., Kamiya, T., Abe, K. 2007. *Increased autophagy in transgenic mice with a G93A mutant SOD1 gene*. Brain Research. 1167: 112-117.

Morley, J.F., Brignull, H.R., Weyers, J.J., Morimoto, R.I. 2002. *The threshold for polyglutamine-expansion protein aggregation and cellular toxicity is dynamic and influenced by aging in Caenorhabditis elegans*. Proceedings of the National Academy of Sciences of the United States of America. 99(16): 10417-10422.

Mosser, T., Matic, I., Leroy, M. 2011. *Bacterium-induced internal egg hatching frequency is predictive of life span in Caenorhabditis elegans populations*. Applied and Environmental Microbiology. 77(22): 8189-8192.

Natajaran, K., Meyer, M.R., Jackson, B.M., Slade, D., Roberts, C., Hinnebusch, A.G., Marton, M.J. 2001. *Transcriptional profiling shows that Gcn4p Is a master regulator of gene expression during amino acid starvation in yeast.* Molecular and Cellular Biology. 21(13): 4347-4368.

Nelson, N., Perzov, N., Cohen, A., Hagai, K., Padler, V., Nelson, H. 2000. *The cellular biology of proton-motive force generation by V-ATPases*. Journal of Experimental Biology. 203(1): 89-95.

Nishida, C.R., Gralla, E.B., Valentine, J.S. 1994. *Characterization of three yeast copper-zinc superoxide dismutase mutants analogous to those coded for in familial amyotrophic lateral sclerosis*. Proceedings of the National Academy of Sciences of the United States of America. 99: 9906-9910.

Noor, R., Mittal, S., Iqbal, J. 2002. *Superoxide dismutase--applications and relevance to human diseases*. Medical Science Monitor. 8(9): 210-215.

Oeda, T., Shimohama, S., Kitagawa, N., Kohno, R., Imura, T., Shibasaki, H., et al. 2001. *Oxidative stress causes abnormal accumulation of familial amyotrophic lateral*

sclerosis-related mutant SOD1 in transgenic Caenorhabditis elegans. Human Molecular Genetics. 10(19): 2013–2023.

Pao, S.S., Paulsen, I.T., Saier, M.H. Jr. 1998. *Major facilitator superfamily*. Microbiology and Molecular Biology Reviews. 62(1): 1-34.

Pedrini, S., Sau, D., Guareschi, S., Bogush, M., Brown, R.H.J., Naniche, N., Kia, A., Trotti, D., Pasinelli, P. 2010. *ALS-linked mutant SOD1 damages mitochondria by promoting conformational changes in Bcl-2*. Human Molecular Genetics. 19: 2974–2986.

Pestov, N.B., Shakhparonov, M.I., Kornienko, T.V. 2011. [*Matricide in Caenorhabditis elegans as an example of programmed death of whole animal organism: role of mitochondrial oxidative stress*]. Bioorganicheskaia Khimiia. 37(5): 705-710.

Pinto, C., Cárdenas, P., Osses, N., Henríquez, J.P. 2013. *Characterization of Wnt/β-catenin and BMP/Smad signaling pathways in an in vitro model of amyotrophic lateral sclerosis*. Frontiers in Cellular Neuroscience. 7: 239.

Prahlad, V., Morimoto, R.I. 2009. *Integrating the stress response: lessons for neurodegenerative diseases from C. elegans*. Trends in Cell Biology. 19(2): 52-61.

Pramatarova, A., Goto, J., Nanba, E., Nakashima, K., Takahashi, K., Takagi, A., Figlewicz, D.A., Rouleau, G.A. 1994. *A two basepair deletion in the SOD 1 gene causes familial amyotrophic lateral sclerosis*. Human Molecular Genetics. 3(11): 2061-2062.

Prohl, C., Pelzer, W., Diekert, K., Kmita, H., Bedekovics, T., Kispal, G., Lill, R. 2001. *The yeast mitochondrial carrier Leu5p and Its human homologue Graves' disease protein are required for accumulation of coenzyme A in the matrix*. Molecular and Cellular Biology. 21(4): 1089-1097.

Puig, S., Thiele, D.J. 2002. *Molecular mechanisms of copper uptake and distribution*. Current Opinion in Chemical Biology. 6(2): 171-180.

Purro , S.A., Dickins, E.M., Salinas, P.C. 2012. *The secreted Wnt antagonist Dickkopf-1 is required for amyloid β-mediated synaptic loss*. The Journal of Neuroscience. 32(10): 3492-3498.

Rakhit, R., Chakrabartty, A. 2006. *Structure, folding, and misfolding of Cu,Zn superoxide dismutase in amyotrophic lateral sclerosis*. Biochimica et Biophysica Acta. 1762(11-12): 1025-1037.

Rooney, JP., Luz, A.L., González-Hunt, C.P., Bodhicharla, R., Ryde, I.T., Anbalagan, C., Meyer, J.N. 2014. *Effects of 5'-fluoro-2-deoxyuridine on mitochondrial biology in Caenorhabditis elegans*. Experimental Gerontology. 56: 69-76.

Ross, C.A., Tabrizi, S.J. 2011. *Huntington's disease: from molecular pathogenesis to clinical treatment*. The Lancet Neurology. 10(1): 83–98.

Schafer, W. R. (December 14, 2005) *Egg-laying*. WormBook, ed. The C. elegans Research Community, WormBook. doi/10.1895/wormbook.1.38.1, http://www.wormbook.org.

Seetharaman, S. V., Prudencio, M., Karch, C., Holloway, S.P., Borchelt, D.R., Hart, P.J. 2009. *Immature copper-zinc superoxide dismutase and familial amyotrophic lateral sclerosis*. Experimental Biology and Medicine. 234(10): 1140-1154.

Seetharaman, S.V., Winkler, D.D., Taylor, A.B., Cao, X., Whitson, L.J., Doucette, P.A., Valentine, J.S., Schirf, V., Demeler, B., Carroll, M.C., Culotta, V.C., Hart, P.J. 2011. *Disrupted zinc-binding sites in structures of pathogenic SOD1 variants D124V and H80R*. Biochemistry. 49(27): 5714-5725.

Sekito, T., Fujiki, Y., Ohsumi, Y., Kakinuma, Y. 2008. *Novel families of vacuolar amino acid transporters*. IUBMB Life. 60(8): 519-525.

Shaye, D. D., Greenwald, I. 2011. *OrthoList: a compendium of C. elegans genes with human orthologs*. PLoS ONE 6:e20085.

Shimazu, M., Sekito, T., Akiyama, K., Ohsumi, Y., Kakinuma, Y. 2005. *A family of basic amino acid transporters of the vacuolar membrane from Saccharomyces cerevisiae*. The Journal of Biological Chemistry. 280: 4851-4857.

Solans, A., Zambrano, A., Rodriguez, M., Barrientos, A.2006. *Cytotoxicity of a mutant huntingtin fragment in yeast involves early alterations in mitochondrial OXPHOS complexes II and III*. Human Molecular Genetics. 15(20): 3063-3081.

Staschke, K.A., Dey, S., Zaborske, J.M., Palam, L.R.. McClintick, J.N., Pan, T., Edenberg, H.J., Wek, R.C. 2010. *Integration of general amino acid control and target of rapamycin (TOR) regulatory pathways in nitrogen assimilation in yeast*. Journal of Biological Chemistry. 285(22): 16893-16911.

Sternberg, P.W. (June, 25 2005) *Vulval development* WormBook, ed. The C. elegans Research Community, WormBook. doi/10.1895/wormbook.1.6.1, http://www.wormbook.org.

Stevens, J.C., Chia, R. 2010. *Modification of superoxide dismutase 1 (SOD1) properties by a GFP tag – Implications for research into amyotrophic lateral sclerosis (ALS).* PLOS One. 5: e9541.

Stoothoff, W.H., Johnson, G.V. 2005. *Tau phosphorylation: physiological and pathological consequences*. Biochimica et Biophysica Acta. 1739(2-3): 280-297.

Strange, K., 2003. *From genes to integrative physiology: ion channel and transporter biology in Caenorhabditis elegans*. American Physiological Society. 83(2): 337-415.

Sturtz, L.A., Diekert, K., Jensen, L.T., Lill, R., Culotta, V.C. 2001. *A fraction of yeast Cu,Zn-superoxide dismutase and its metallochaperone, CCS, localize to the intermembrane space of mitochondria*. Journal of Biological Chemistry. 276(41): 38084-38089.

Su, L.J, Auluck, P.K, Outeiro, T.F et al. 2010. *Compounds from an unbiased chemical screen reverse both ER-to-Golgi trafficking defects and mitochondrial dysfunction in Parkinson's disease models*. Disease Model Mechanisms. 3(3-4): 194–208.

Tenreiro, S., Outeiro, T.F. 2010. *Simple is good: yeast models of neurodegeneration*. Federation of European Microbiological Societies Yeast Research. 10(8): 970-979.

Therrien, M., Parker, J.A. 2014. *Worming forward: amyotrophic lateral sclerosis toxicity mechanisms and genetic interactions in Caenorhabditis elegans*. Frontiers in Genetics. 5:85.

Trent, C., Tsung, N., Horvitz, H.R. 1983. *Egg-laying defective mutants of the nematode Caenorhabditis elegans*. Genetics Society of America. 104: 619-647.

Trotti, D., Rolfs, A., Danbolt, N.C., Brown Jr, R.H., Hediger, M.A. 1999. *SOD1 mutants linked to amyotrophic lateral sclerosis selectively inactivate a glial glutamate transporter*. Nature Neuroscience. 2: 427-433.

Uchida, A., Sasaguri, H., Kimura, N., Tajiri, M., Ohkubo, T., Ono, F., Sakaue, F., Kanai, K., Hirai, T., Sano, T., Shibuya, K., Kobayashi, M., et al. 2012. *Non-human primate model of amyotrophic lateral sclerosis with cytoplasmic mislocalization of TDP-43.* Brain, 135(Pt 3): pp. 833–846.

Vehviläinen, P., Koistinaho, J., Gundars, G. 2014. *Mechanisms of mutant SOD1 induced mitochondrial toxicity in amyotrophic lateral sclerosis*. Frontiers in Cellular Neuroscience. 8: 126.

Velde, C.V., Miller T.M., Cashman, N.R., Cleveland, D.W. 2008. *Selective association of misfolded ALS-linked mutant SOD1 with the cytoplasmic face of mitochondria*. Proceedings of the National Academy of Sciences of the United States of America. 105(10): 4022–4027.

Wang, J., Xu, G., Borchelt, D.R. 2002. *High molecular weight complexes of mutant superoxide dismutase 1: age-dependent and tissue-specific accumulation.* Neurobiology of Disease. 9(2): 139–148.

Wang, J., Slunt, H., Gonzales, V., Fromholt, D., Coonfield, M., Copeland, N.G., Jenkins, N.A., Borchelt, D.R. 2003. *Copper-binding-site-null SOD1 causes ALS in transgenic mice: aggregates of non-native SOD1 delineate a common feature*. Human Molecular Genetics. 12(21): 2753-2764.

Wang, J., Xu, G., Li, H., Gonzalez, V., Fromholt, D., Karch, C., Copeland, N.G., Jenkins, N.A., Borchelt, D.R. 2005. *Somatodendritic accumulation of misfolded SOD1-L126Z in motor neurons mediates degeneration: αB-crystallin modulates aggregation*. Human Molecular Genetics. 14(16): 2335-2347.

Wang, J., Farr, G.W., Hall, D.H., Li, F., Furtak, K., Dreier, L., et al. 2009. *An ALS-linked mutant SOD1 produces a locomotor defect associated with aggregation and synaptic dysfunction when expressed in neurons of Caenorhabditis elegans*. PLoS Genetics. 5(1):e1000350.

Wang, S., Guan, Y., Chen, Y., Li, X., Zhang, C., Yu, L., Zhou, F., Wang, X. 2013. *Role of Wnt1 and Fzd1 in the spinal cord pathogenesis of amyotrophic lateral sclerosis-transgenic mice.* Biotechnology Letters. 35(8): 1199-1207.

Watson, M.R., Lagow, R.D., Xu, K., Zhang, B., Bonini, N.M. 2008. *A Drosophila model for amyotrophic lateral sclerosis reveals motor neuron damage by human SOD1*. The Journal of Biological Chemistry. 283(36): 24972-24981.

Weichert, A., Besemer, A.S., Liebl, M., Hellmann, N., Koziollek-Drechsler, I., Ip P., et al. 2014. *Wild-type Cu/Zn superoxide dismutase stabilizes mutant variants by heterodimerization*. Neurobiology of Disease. 62: 479–488.

Weisiger, R.A., Fridovich, I. 1973. *Mitochondrial superoxide dismutase site of synthesis and intramitochondrial localization*. The Journal of Biological Chemistry. 248(13): 4793–4796.

Witan H., Kern A., Koziollek-Drechsler I., Wade R., Behl C., Clement A. M. (2008). *Heterodimer formation of wild-type and amyotrophic lateral sclerosis-causing mutant Cu/Zn-superoxide dismutase induces toxicity independent of protein aggregation.* Human Molecular Genetics. 17(10): 1373–1385.

Wolozin, B., Gabel, C., Ferree, A., Guillily, M. 2011. *Watching worms whither: modeling neurodegeneration in C. elegans*. Progress in Molecular Biology and Translational Science. 100: 499-514.

Wong, P.C., Pardo, C.A., Borchelt, D.R., Lee, M.K., Copeland, N.G., Jenkins, N.A., Sisodia, S.S., Cleveland, D.W., Price, D.L. 1995. *An adverse property of a familial ALS-linked SOD1 mutation causes motor neuron disease characterized by vacuolar degeneration of mitochondria*. Neuron. 14(6): 1105-1116.

Wright, G.S.A., Antonyuk, S.V., Kershaw, N.M., Strange, R.W., Hasnain, S.S. 2013. *Ligand binding and aggregation of pathogenic SOD1*. Nature Communications. 4: 1758.

Yang, J-S., Nam, H-J., Seo, M., Han, S.K., Choi, Y., et al. 2011. *OASIS: Online application for the survival analysis of lifespan assays performed in aging research*. PLoS ONE. 6(8): e23525.

Young, G.B., Jack, D.L., Smith, D.W., Saier, M.H. Jr. 1999. *The amino acid/auxin:proton symport permease family*. Biochimica et Biophysica Acta. 1415(2): 306-322.

Zetterström, P., Stewart, H.G., Bergemalm, D., Jonsson, P.A., Graffmo, K.S., Andersen, P.M., et al. 2007. *Soluble misfolded subfractions of mutant superoxide dismutase-1s are enriched in spinal cords throughout life in murine ALS models*. Proceedings of the National Academy of Sciences of the United States of America. 104(35): 14157–14162.

Zetterström, P., Graffmo, K.S., Andersen, P.M., Brännström, T., Marklund, S.L. 2013. *Composition of soluble misfolded superoxide dismutase-1 in murine models of amyotrophic lateral sclerosis*. Neuromolecular Medicine. 15(1): 147–158.

Zu, J.S., Deng, H.X., Lo, T.P., Mitsumoto, H., Ahmed, M.S., Hung, W.Y., Cai, Z.J., Tainer, J.A., Siddique, T. 1997. *Exon 5 encoded domain is not required for the toxic function of mutant SOD1 but essential for the dismutase activity: identification and characterization of two new SOD1 mutations associated with familial amyotrophic lateral sclerosis*. Neurogenetics. 1(1): 65-71.

Zwilling, D., Huang, S.Y., Sathyasaikumar, K.V., Notarangelo, F.M., Guidetti, P., Wu, H. Q., et al. 2011. *Kynurenine 3-monooxygenase inhibition in blood ameliorates neurodegeneration*. Cell. 145(6): 863–874.